LOW FRICTION HYBRID NANOCOMPOSITE MATERIAL FOR BRAKE PAD APPLICATION

Submitted in fulfilment of the requirements for the degree of **Master in Engineering: Mechanical Engineering:** in the Faculty of Engineering and the Built Environment at the **Durban University of Technology.**

Oluwatoyin Joseph GBADEYAN

Approved for final submission:

Supervisor: _____ **Date:** _____

Prof. Krishnan Kanny

Co-supervisor: _____ **Date:** _____

Dr. T.P. Mohan

January 2017

ABSTRACT

Despite the huge improvements made in the development of vehicle brake pad materials, problems such long stopping distances, noise pollution, and heat dissipation still continue to persist. In this regard, a novel polymer-based hybrid nanocomposite brake pad (HC) has been developed. Here, a combination of carbon-based materials, including those at a nanoscale, was used to produce the brake pad. The coefficient of friction, wear rate, noise level, and interfacial temperature was investigated and compared with that of a commercial brake pad material (CR). It was found that the brake pad performance varied with the formulation of each pad. Hybrid nanocomposite brake pads material exhibited superior performance in most tests when compared to the commercial brake pad. They exhibited a 65% lower wear rate, 55% lower noise level, 90% shorter stopping distance, and 71 % lower interfacial temperature than the commercial brake pad (CR).

Furthermore, mechanical properties such as hardness, compressive strength, shear strength, and impact resistance were also evaluated. The material exhibited a 376% higher shear strength, 100% improved compressive strength, 77% greater modulus and 100% higher impact strength than the commercial brake pad. The hardness of both brake pads material was statistically comparable. Additionally, the thermal stability, degradation, water and oil absorption behaviour were measured. It was found that HC brake pad material exhibited a 100% lower water absorption and 80% oil absorption rate. The brake pads also exhibited a thermal stability within the brake pad standard maximum working temperature of 300 -400 ^{0}C.

The superior performance of hybrid nanocomposite brake pad material observed was due to synergism between the carbon-carbon additives and uniform dispersion of carbon fiber as shown in Figure 4.16. Scanning electron microscopy study was subsequently performed on fracture and worn surfaces of the brake pads. The micrographs show changes in the structural formation after the incorporation of carbon based fillers. It also shows the smooth structure and uniform dispersion of the carbon fiber. The smooth surface of the worn brake pad is an indicative of a harder structure. No ploughing or score marks were evident. Hence, it was deduced that the reinforced

had superior mechanical and tribological properties. These improved properties are suggestive of materials that may be successfully used for brake pad application.

DECLARATION

I declare that the dissertation herein submitted to the Department of Mechanical Engineering, Durban University of Technology for the award of Master's Degree in Engineering (Mechanical) is my work and has not been previously submitted for a degree at any other University or Higher Institution of Education.

JOURNAL PAPERS SUBMITTED ARISING FROM THIS STUDY

Gbadeyan O. J, Kanny K., Mohan T.P (2016). Influence of the Multi-walled carbon nanotube and short carbon fiber composition on tribological properties of epoxy composites. *Tribology- materials, Surface &Interfaces*. pp. 1-7, 2017.

Gbadeyan O. J & Kanny K., 2016. Braking performance of polymer-based hybrid nanocomposite brake pad. *Submitted to Journal of the Brazilian Society of Mechanical Science and Engineering*. Manuscript number BMSE-D-16-01098 (Under review)

Gbadeyan O. J, Kanny K., Mohan T.P (2017). Tribological, mechanical and microstructural of multi-walled carbon nanotubes/short carbon fiber epoxy composites. Submitted to Journal of tribology. Manuscript number TRIB-17-1107 (Revision Under review)

ABSTRACTS ACCEPTED ARISING FROM THIS STUDY

Gbadeyan O. J, Kanny K., Mohan T.P. 2015. Wear and friction of epoxy resin filled with short carbon fiber 2015. Abstract accepted. In: *the Second International Conference on Composites, Biocomposite, and Nanocomposite (ICCBN)*, Durban University of Technology, Durban, South Africa, 28 - 30 October 2015.

Gbadeyan O. J, Kanny K., Mohan T.P. 2016. Braking performance of polymer-based low friction hybrid nanocomposite brake pad Wear and friction of epoxy resin filled with short carbon fiber 2015. Abstract accepted. In: *the first Indo-South African research workshop on nanocomposite materials and their application*s, Durban. 7 – 9 July 2016.

DEDICATION

This thesis is dedicated to the Almighty God, the master of all knowledge for seeing me through this program. I also dedicate the completion of this research work to my late mother, Mrs. Comfort Gbadeyan. Your last wishes inspired me in the pursuit of excellence and in the desire to acquire more knowledge.

ACKNOWLEDGEMENTS

I return all glory, honor, and adoration to God Almighty for the grace and mercy received for the completion of this study. Your help has always been there for me. My profound gratitude goes to my supervisor, Prof. K. Kanny, for his supervision, support, and guidance throughout the program. Your consistent encouragement, constructive criticism, and insightful guidance during the course of this program are most appreciated. The technical support of my co-supervisor; Dr. T. P. Mohan, is well appreciated. My immeasurable thanks go to Durban University of Technology, for the remission of fees and the scholarship provider in the course the program.

The financial support of South Africa Council for Scientific and Industrial Research (CSIR) is also gratefully appreciated. I wish to appreciate the entire staff Department of Mechanical Engineering, Most especial outgoing Head of the Department, Mr. Thurbon Graham Arthur, You are the best. I also thank Pastor& Pastor (Mrs.) Adejimi, for introducing me to Durban University of Technology education system. My gratitude goes to my friend and brother, Mr. Olusanya John Olumide for his motivation and encouragement at all time. A big shout-out to all my colleagues at Composite Research group – Mr Festus Mwangi, Mr Avinash Ramsooroop, Mr Sifiso Nkosi, Mr Kenneth Okeke, Ms Sathie Chetty, Mr Prajan Ramdeen, Mr Muforo Moyo, Mr. Ajay Rane, Dr Mohan Pandurangan, Dr Vimla Paul, for impressive support and words of encouragement towards the success of this program.

My acknowledgment will not be complete without a sincere appreciation to my lovely wife, a treasure of priceless value, Mrs. Omonike Ige-Gbadeyan and my adorable daughter Ayomide Bethel Gbadeyan for been there throughout this program. Your support, motivation, and sacrifice contributed immensely towards the completion of this research work. I am indeed indebted to you both. Finally, I like to appreciate all my siblings and my parents, most especially, Mrs. Olujumoke Gbadeyan-Godwin, Mrs. Adenike Babalola, Mr. Anthony Gbadeyan and Mr. Adebayo Gbadeyan, Mrs. lucy Olaifa, and Rev. & Mrs. Ige. This is the evidence that your prayers were never in vain. Your consistent calls and encouragement were the ointments that grease my hands throughout this dissertation.

TABLE OF CONTENTS

List of Figures

List of Tables

ABBREVIATIONS

ASTM - American Society for Testing and Materials

DGEBA - diglycidyl ether of bisphenol-A

ER- Epoxy resin

CABP- Commercial asbestos brake pad

CFRFM- Carbon fiber reinforced friction material

CMBP- Conventional brake pad

CNTs- Carbon nanotube

CoF- Coefficient of friction

CR- Commercial brake pad

Cu- Copper

GN- Graphite nanopowder

HB- Hardness Brinel

Hv- Hardness value

IOL-Independent online

IR-Infrared

LRT- Light Rail Transit

MWCNTs- Multi-walled carbon nanotube

PRASA- Passenger Rail Agency of South Africa

PVC- Polyvinyl chloride

RPM- Revolution per minute

SAE- Society of Automobile Engineers

SCF- Short carbon fiber

SEM - Scanning electron microscope

TA -Thermal analysis

DSC - Differential scanning calorimetry

TG - Thermogravimetry

UTM-MTS- Universal Testing Machine- Material testing machine.

Chapter One: Introduction

1.1 Background and context of the study

Improvements in technology, such as those relating to transportation that has taken place since the beginning of the industrial revolution have been linked to growing economic opportunities. Since transportation is the cornerstone of every economy, it stands to reason that growth in the economy must be drawn from the development of the transportation sector. The use of ports from 16th to the 18th century of concomitant with the expansion of international trade. This fostered the early development of inter-country trade. However, they were constrained by inadequate inland access.

To alleviate these challenges, two stages were adopted, which are water and land transportation. The water transportation was the first stage to be implemented to transport heavy good. This development provided quick growth of rudimentary and the constrained inland distribution. Consequently, this led to the advent of the industrial revolution in the late 18th and early 19th centuries [1]. However, nations not only depend on transportation to compete globally but also to help build the domestic economy within the countries. In the 19th century, land transportation was suggested to be the second stage of the industrial revolution. This was linked to the development and implementation of the rail system to enable flexibility and effectiveness of inland transportation. Railway development led to the increase of economic and social opportunities.

The 20th century witnessed rapid development of road transportation systems such as highway system and automobile manufacturing. This permitted individual transportation and commercial market with the reliable door-to-door delivery of goods [1]. However, among this land transportation system, railway vehicles were found to be the most efficient as they carried a larger number of passenger, as well as heavy loads over long distances [2]. Concomitantly, engineers and scientists strived to improve railway transportation reliability and efficiency. The transport innovations, such as the expansion of high-speed railway systems led to the developed of the modern wagon [4].

This innovative improvement resulted in a notable decrease in travel time and higher capacity to convey heavy loads from one place to another. Conversely, as the train's payload and speed increased, the need for more powerful braking system became necessary. The basic function of a braking system was to slow down the vehicle's speed. This function was performed by converting train kinetic energy into heat energy, which dissipates into the environment. To ensure safe and efficient braking, numerous brake systems were developed. Production, design, and operation of this braking system were, however, developed based on various factors. These factors include speed, traffic condition, structure and characteristics of the vehicle.

According to Cruceanu [5], several studies were conducted to develop an effective braking system for rail vehicles. It was therefore argued that the compressed air braking system offered the most acceptable characteristics. Consequently, this system was commonly used and to this day remains the fundamental and essential system for rail vehicles. This system also works using the basic principle similar to the highway vehicle's braking system that performed its function shown in Figure 1.1.

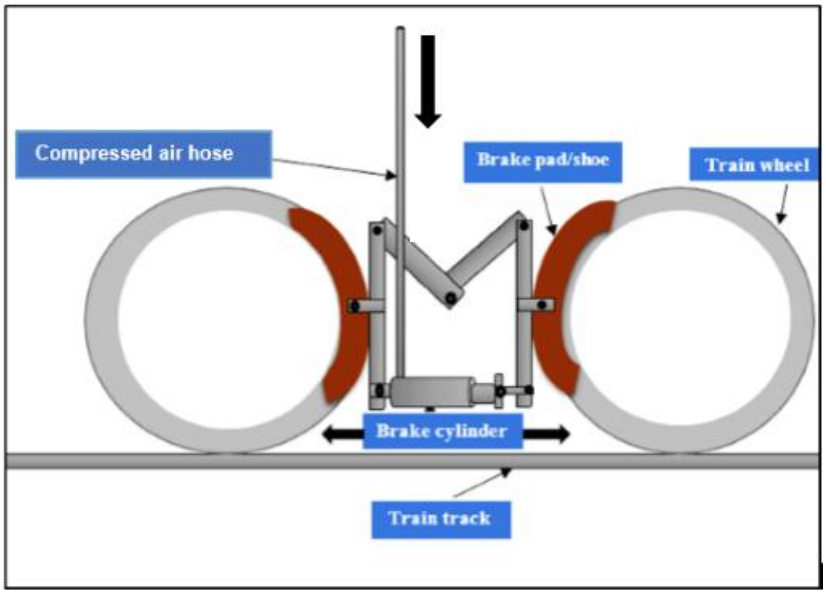

Figure 1.1: Representation of the locomotive brake system

Figure 1.1 shows the air brake's mode of operation. Pressurized air that comes from the air compressor pushes on a piston in a cylinder. The piston forces brake pad on

the wheels through a mechanical linkage, resulting in friction that reduces train's speed [2].

Regardless of the quality performance of this braking system, choosing the correct set of brake pads for commuting has generated various problems. This include the development of a higher braking force, maintenance of a stable friction coefficient, dissipating higher volume of heat energy in a shorter period of time, and better wear resistance, resulting in a more complex braking requirement for brake pad.

This complexity resulted from different phenomena which manifest during braking. These include but not limited to mechanical fade, pneumatic pressure, and thermal stresses on the brake pads surface and the wheel. In view of this complexity, brake pad with properties that can reliably improve braking performance in rail industry became a necessity [3-7]. The discovery of the high strength, heat and chemical resistance properties of asbestos led to its introduction as brake pad material with enhanced braking performance [8]. However, asbestos was later discovered to contain toxic fibers, which are hazardous to humans [9].

During the production of the brake pad, tiny asbestos fibers released into the air were often inhaled by the worker. In addition, during asbestos pad functioning, debris were often released into the environment. This exposed people in the community and at the workplace to the tiny fiber of the asbestos causing lung cancer. This asbestos exposure has affected millions of lives. According to the Mesothelioma Center in South Africa, more than 2,700 citizens lost their lives to lung related diseases caused by asbestos exposure between 1987 and 2000 [9]. As a result of the associated health hazards, in 2010, a global ban was placed on the use of asbestos, which eventually led to the closure of companies manufacturing brake pads using the asbestos [10].

Subsequently, metallic and semi-metallic materials that were used to replace asbestos have generated several challenges, which include, inadequate braking power, excessive noise while functioning, poor heat dissipation capacity, stopping at a very long distance and durability. These led to train brake failure that has often resulted in the loss of lives and goods. The incidents caused by train brake failures between 2010 and 2016 claimed more than 50,000 lives, left millions injured, and goods worth billions of dollars have been wasted globally. In South Africa only, more than 1000 lives were

lost. More than 3000 people were injured, and 1200 people cases were critically due to this effect [11].

South Africa railway operator, Passenger Rail Agency of South Africa (PRASA) was reported to have lost millions of rands to train facility damage, as a result of an accident caused by brake failure between 2000 and 2015 [12]. Similarly, the IOLNew/South African reported that in 2010, Rovos rail operator suffered R15 million for damage incurred after an accident caused by brake failure killed three people [13]. These incidents showed the importance of railway vehicles braking systems and the need for essential knowledge and understanding of the existing brake pad problems. Hence, to improve rail transportation safety, dependability, and effectiveness, there is a need for a more efficient brake pad. Considering the complexity of railway braking requirements, more effective, quicker and safer, brake pad needs to meet the specific requirement for slowing down the vehicle [14].

These include sufficient braking force to stop the vehicle in a shorter distance, low noise while functioning, better heat dissipation capability, durability and must be environmentally friendly. Hence, this present study developed a polymer-based brake pad that offers better braking force that can stop the vehicle at a shorter distance, dissipates a larger amount of energy within a shorter time, is durable, and environmentally friendly.

1.2 Aim of the Study and Research Objectives

The aim of this study is to develop an efficient brake pad material using a polymer-based low friction hybrid nanocomposite.

1.3 Research Objectives

The objectives of this study to produce brake pad material that exhibits:

1.3.1. Improved mechanical properties such as hardness, compressive modulus, shear, impact and compressive strength, which often influence braking force.

1.3.2. Lower wear rate, lower noise and stable coefficient of friction.

1.3.3. Shorter stopping distance and good heat dissipating capacity.

1.3.4. Durable and environmentally friendly

1.4 Research Hypothesis

The new polymer-based low friction hybrid nanocomposite is a suitable alternative brake pad to existing brake pads as it effectively offers better braking performance, is durable and environmentally friendly.

1.5 Structure of the Thesis

The thesis will be divided into five chapters. Chapter 1 introduces the problems and its settling in the rail industry. It shows the importance of the problems and the significant of the solutions. In this regards, *Chapter 2* presents an overview of the solution that other contributed in solving the problems. Subsequently, the introduction and review of low friction hybrid nanocomposite material for brake pad application follow. Then, *Chapter 3* describes the methodology in each phase of this research. It presents the data of the mechanical test such as Impact strength, shear strength, compressive strength, hardness and young modulus. It also gives data on braking performance test, such as wear, stopping distance, interfacial temperature; the coefficient of friction and thermal stability of the hybrid nanocomposite brake pads application.

Afterward, Chapter 4 presents results gather from this study. These include mechanical test results such as compressive strength, Young's modulus, shear strength, and hardness. Thermal properties such as weight loss (thermogravimetric) and heat flow (Differential scanning calorimetry) results were also reported. Wear rate and coefficient of friction, interfacial temperature, and stopping distance, noise level, worn surface of the composite material of the brake pad sample will be presented in this chapter. Tables, images, and graphs will support the analytical results. Overall, this chapter provides discussion on polymer based low friction nanocomposite material brake pads and existing materials used for brake pad by comparing the tribological property, mechanical property, and the thermal property, braking performance value measured on the existing materials used for brake pad application.

Chapter 5 presents conclusions drawn from the study. It will also identify any limitations and consider future directions for this research, and *Chapter 6* gives references used for this study.

Chapter Two: Literature review

2.1 Introduction

In this chapter, the material used for brake pad application is reviewed and is structured into two sections. Section one discusses the evolution of brake systems and the performance of the current braking system. It also reviews the typical properties of the components and their combination for the brake pad production. In section two, the properties and functions of the materials for the production of brake pads are described. This help in understanding the development of the new friction material as an alternative material to current brake pad materials. Subsequently, the different quality standards (American Society for Testing and Materials ASTM) follows. This forms the base of the theory in the development of brake pad.

It is envisaged that understanding the relationship between performance properties of the brake pad and braking performance help in characterizing low friction hybrid nanocomposite as a potential material for the brake pad application. In this regard, the chapter concludes with an evaluation of the thermal, chemical; physical mechanical and tribological properties brake pad, and the technique used in determining brake pad performance.

2.2 Overview and history of brake pads

Brake pads are part of the integral components of vehicle braking system, which help in the smooth retardation and keep the vehicle stationary when parked. The efficiency of brakes, to some extent, depend on the proper composition and quality of brake pad used [15]. This suggests that good set of brake pads are required for safe, reliable and effective braking. In this case, material or combination of material for brake pad should possess better engineering and environmental requirement. Nagesh *et al.* [16], defined brake pad as a heterogeneous material, containing various components that enhance braking performance under different conditions and temperatures (high or low). Ideally, these components should enhance the durability, increase strength, rigidity and reduce the noise of the brake pads during its functioning. Correspondingly, they are supposed to be environmentally friendly.

Kim *et al*, Ikpambese *et al*., and Imaekhai and Paul [4, 15, 17] highlighted that the type of materials, combination ratio, fabrication techniques, and mixing procedures of these

materials determine final products (brake pad) properties. This implied that all these factors must be put into consideration and well controlled when producing brake pad.

According to Kim *et al,* brake pads are expected to meet a set of environmental and engineering requirements [18]. These properties termed engineering requirements include but not limited to tribological, mechanical and thermal. In the like manner, having a good understanding of the brake pad functionality is vital because it is an essential part of a vehicle connected to the safety of living beings. In view of this, material or a combination of materials used for brake pad application needs to be thoroughly investigated and tested before use. This finding has generated an intensive investigation of different material composition, their properties, and performance should be ensured.

According to Jang *et al* and Rivera *et al* [19, 20], vehicle manufacturers found it easier to modify the brake pad than the modifying brake system. Additionally, the innovative improvements on vehicles call for a more efficient braking force. This innovation led to brake pad evolution, which still continues to date.

Prior to the advent of modern brake pads in 1898, Elmer Ambrose developed a brake pad made of metallic discs in a large disc integral hub wheel [8], This utilized electromagnets and springs on small press discs to impart a frictional force between the pad and the rotating discs of the vehicle. This was, however, found to generate excess heat and noise hence its use was discontinued.

In 1902, Lancaster designed a non-electric spot disc lined with copper material. According to automobile history [8, 21], non-electric copper lining material had the challenge of excessive noise due to the contact between the copper and the metallic rotor. In 1907, Herbert Frood invented the use of asbestos in the making of brake pads. This had the advantages of heat dissipation, durability and stopping performance. This strengths increased the use of asbestos in brake pad making [8, 21]. In spite of these advantages, asbestos had an inherent problem of environmental and health hazards, which caused lung disease [8, 22]. Consequently, this led to the reduction and ultimately a ban on its use [10, 21, 23].

In pursuit of health and environmentally friendly brake pad with good performance, organic plastic material was introduced in the1950s [24, 25]. These organic brake pads

made of plastic fiber had the advantages of environmental friendliness and offered good braking performance. However, organic brake pad exhibited a poor thermal stability and wear fast hence generated dust particles [24, 25]. In the 1970s, metallic brake pads were made. Apart from having an economic advantage and durability, Greg [26] stated that metallic brake pad had good braking performance. The abrasion of the rotor and excessive noise pollution, however, caused the elimination of metallic materials as brake pads [25, 26].

In the pursuit of the acceptable brake pad, semi-metallic brake pad was invented in the 1980s [19, 20, 27]. As outlined by Hartman, Steve, Sixty, and Diffen [27-29] [30], these materials had better mechanical properties and braking performance. Similarly, it possesses good friction coefficient for consistent stopping. Nevertheless, they abrade the rotors and generate high noise. Further search for more acceptable brake pad led to the hybridization of metallic and ceramic materials around the 1990s in what is today known as semi-metallic brake pads. This offers good braking performance and durability over a wide range of driving conditions, including better heat dissipation, low wear rate and stable friction coefficient in function. As outlined by various authors [26, 28, 29], these materials were expensive, cause damage to the rotor and needed to be warmed up to a certain temperature before it can perform its function.

In view of the limitations of the above-mentioned brake pad materials, organic sintered brake pad was developed in the early 2000s. Organic sintered brake pads are high-density materials which exhibited high friction coefficient across the full range of operating temperatures with high braking performance. Several authors [31-33], outlined that over time, these brake pads were discovered to be expensive, noisy, wear quickly and have poor strength. This type of brake pad also exhibited poor thermal conductivity due to mass porosity.

In recent years, various hybrid composite materials have been studied. It was found that a combination of nanoparticle fillers, fibers, and resins provides ideal properties required for the brake pad application [34-39]. Researchers [17, 37, 40] have combined these materials for brake pad application. This fabricated composite pad offered better mechanical and tribological properties, yet have some deficiencies. Brake pads history indicates that the performance of a brake pad depends on the functionality of the brake pad constituent. Therefore, it is imperative to evaluate the

composition and functionalities of the materials used for brake pad application. In doing this, knowledge about the materials selection method is essential hence the next section reviews the selection of materials.

2.3. Brake pad material selection

Material selection is one of the fundamental processes for brake pad production. Maleque et al[41]. highlighted that selecting the optimum combination of material for brake system was not an easy task but a gradual process which involves different stages in decision making. Nicholson et al.[42], asserted that material selection for brake pad not only depended on material functions but also on the cost, availability, and processability. However, Jang et al. and Kennedy et al. [43, 44], argued that the selection of material was essentially based on the appropriate properties required for braking performance. Herbert et al. probably selected asbestos for brake pad production due it strength, good resistance to heat, chemical, and fire [23, 45].

As earlier highlighted by Lawrence and Paul [4], material composition for brake pad are typically classified into three categories namely: metallic, semi-metallic and non-asbestos (NAO). Numerous studies have been conducted on the combination of nanocomposites and several types of fiber, such as metallic, glass, ceramic and carbon fiber composites for brake application [16, 34-39, 46]. The aforementioned fibers are commonly used as various reinforcement and filling constituents to produce NAO brake pads [4, 36]. Sanjeev *et al* [47]*.* affirmed that the numerous pads produced in the past two decades were from NAO, each with their unique formulation claiming to be better than other, however, performing the same task [4].

In view of this, Imaekhai *et al.,* Österle *et al.,* Chan *et al* and Nagesh *et al.*[4, 16, 48, 49], therefore stressed that proper selection of materials with appropriate properties does not depend on the fundamental understanding of the material alone but also on the required amount of constituents. They argued that material selection was largely based on experimental trial and error as well as experience. Sequel to this, Malegue [41], concluded that selection of ideal material combination and development was not a simple task but a gradual process involving different material selection stages. Continuing, Malegue [41] introduced two methods for material selection. These were

the cost per unit property of a material and digital logic methods. It is worth noticing that the two methods as represented in (Figure 2.1) complement each other.

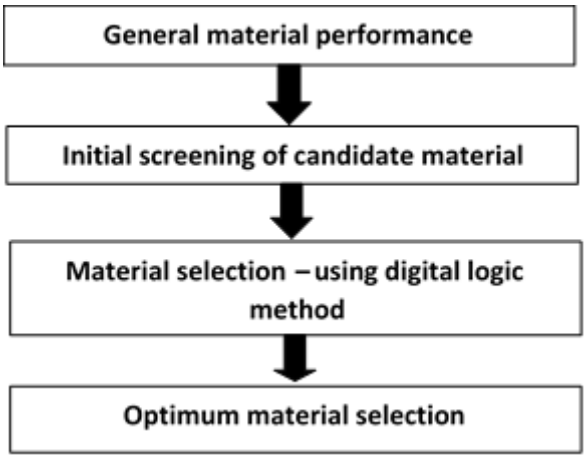

Figure 2.1: Flow chart of material selection modified [41].

As shown in Figure 2.1, this procedure of material selection was limited to ingredient property per unit cost, and their effect on final selection, which may only be adopted for a product with lesser performance requirement. Farag et al. [50] argued that material and process selection for brake pad production is different from exact science, where a single correct solution solves problems but a process where some factors need to be considered. These factors include material necessitating compromises and take-offs, conflicting benefits and limitation, In this case: unique satisfactory solutions are required. Some specified mechanisms (materials) produced by separate manufacturers may have similar functions and maybe, on the contrary, resulting from different production procedures. In view of this, it is imperative to discuss brake pad materials functionality.

2.4 Brake pad material functionality.

The synergistic function of materials selected influence the resultant properties, allowing the brake pad to exhibit properties that they do not fundamentally possess. This helps the brake pad to accomplish functions such as a stable coefficient of friction, resistant to wear rate, thermal stability, good mechanical strength and low noise level. Considering all this, material functionality is very important in determining brake pad performance.

According to Blau *et al.* [6], friction component performed different function in the brake pad formulation. This implied that the type of ingredients or combination of ingredients selected influenced final properties, which in turn impact performance. For instance, Du-quit *et al.* [51] investigated the tribological properties (wear and friction) of carbon fiber reinforced for brake pad (CFRFM), evaluated with glass fiber reinforced and asbestos fiber-reinforced composite. They asserted that carbon fiber reinforced offered better tribological performance due to the carbon fiber resistance to heat, wear resistance and better properties.

Similarly, Ikpambese *et al.* [17] studied the properties of asbestos-free brake pad produced from palm kernel fiber, aluminum oxide, graphite, calcium carbonate and epoxy resin matrix (binder) hybrid composite. They affirmed that the brake pad produced for the above-mentioned material exhibited lower wear rate (3.64mg/m) due to excellent adhesion between the additives, which resulted in low shrinkage, resistance to moisture and good dimensional stability [4, 17, 52].

On the properties and effects of the materials on brake pad performance, Darius *et al.* [53], observed that ceramic and low carbon steel fibers were most suitable for the brake pad. This probably may be because of their good thermal stability and high hardness values. In this regard, they developed and evaluate brake pad constituted with different types of ceramic and organic fibers with Light Rail Transit (LRT) commercial brake pad. They concluded that the composite brake pads developed were better than LRT as they exhibited less weight loss and wear rate. They attributed the performance to thermal stability and wear resistance of the ceramic fiber in the composition.

Ho *et al.* [54], postulated that the brake pads made from metallic materials are associated with cracks/voids due to poor compatibility. Hence, suggested the lesser amount of metallic fiber for the brake pad. Similarly, studies [22, 55] discovered that the brake pad containing metal or metal fiber had a negative effect of abrading wheel/rotor and makes excessive noise during braking. This finding resulted in limited use of metallic material for the brake pad.

According to Nagesh et al and Blau *et al.* [6], a different amount of constituents in brake pad formulation determines it final performance properties. Keeping this in mind, Rathod *et al.* [56], developed brake pad formulation grouped into two by varying weight percentages of aluminum (80-90%) and silicon carbide (10-20%) to determine the strength and wear rate. They affirmed that the formulation with 20% silicon carbide (SiC) exhibited better hardness; however, this brake pad was brittle due to the agglomeration caused by the high-loading of the reinforcement (SiC). On the other hand. Liew *et al.* [57] investigated the effects of sliding speed, nominal contact pressure, and sliding distance on the coefficient of friction (CoF), temperature and wear rate for commercial asbestos brake pad (CABP), and non-asbestos brake pad (NABP). They affirmed that NABP offered a desirable frictional performance and compromising durability. This was attributed to the toughness of the metal fiber and self-sustaining layers formed by the graphite. However, limited studies have been conducted on the brake pad produced from the carbon-based material.

Ahmet *et al.* [58] developed and conducted wear, friction hardness on three different brake pads namely: Pig-iron sintered sabot and composite sabot. The result indicated that the hardness values in different orders, Pig-iron sabot 233 Brinell hardness value (HB), sintered sabot 123.6HB and composite sabot 102 HB. They attributed these high hardness values to the high metallic material concentration. This material formulation, however, exhibited high wear rate and heavy. Composite sabot was considered to be the optimum choice selected for pull vehicle (wagons) due to its lightness, durability, low cost, and availability. These performances were attributed to the graphite, functioning as a solid lubricator that protected the surface and the synergistic functions formed by the composite ingredients.

At times, certain materials are placed in more than one grouping of brake pad composition to perform multiple functions. This has resulted in inevitable overlapping of a specific constituent in the basic brake pad formation. Kennedy *et al*. [44] confirmed that the particle size of material constituted influences pad functionality and advised thorough control. For example, rounded beads of a hard, abrasive material can have a different effect than angular grits on the formation and stability of the friction-induced surface films that control braking performance [6].

Kumar *et al*. [59] investigated the role of nano-sizes copper particles on brake pad tribo-performance. In this regards developed two friction composite by varying the size copper powder. One of the developed micro-composite contained copper particles (Cu) of (400 - 600 µm) and the other contained (50 – 200 µm) Cu. They discovered that the brake pad performance properties, such as density, hardness, thermal diffusivity and conductivity improved with the addition of a small amount (2%) of nano-Cu powder. However, the developed friction composite abrades the wheel.

According to Blau *et al.* [6], analyzing the role of additives in the brake pad can not only be limited to functionality, since their composition, processing and the distribution influences the braking performance. Therefore, it is imperative to compare some typical composition of materials to ascertain how the additives formulation affect braking performance.

2.5 Typical composition of brake pad material

Brake pads normally consist of 5-40 different constituents. These additives were typically categorized into four classes of constituents: friction modifier, abrasive, reinforcement filler and binder [5, 6, 41, 48, 56]. Several studies [6, 56, 60] combined these different additives as sintered metal, carbon-carbon, and organic materials to produce the brake pad. According to Blau et al [6], the categorisation of brake pad is ambiguous because some of these materials perform more than one function. This has often led to the concurrent use of material in basic brake pads. In this regard, some authors report the list of additives used by composition [49, 59, 61] while other, illustrate the kinds of formulation that are specified by using proper composition of commercial additives [16, 20, 49].

Meanwhile, Nicholson *et al.* and Blau *et al.* [6, 42], argued that it is conventional to list brake pad composition in volume percent. In general, it was observed that in most cases, a range of hybrid compositions was reported rather than a single value, even, the percentages of the constituents may not add to a total of 100%. In view of this, it might be concluded that pad manufacturer is doing that to obscure the actual compositions [6].

2.5.1 Friction modifier

The main purpose of friction modifier is to lubricate, control friction to help in controlling interfacial films. Similarly, lubricant often accumulates the friction film to form a layer on the interface (wheel/rotor), which plays a critical role in controlling rotor abrasion and noise during braking [6, 20]. They may be in powder or flake form, natural or synthetic. As reported by Deshmukh *et al*., Kim *et al*., Han *et al*., Cho *et al*., Jang *et al*. [43, 62-65] braking performance such as stopping distance, noise propensity and other related tribological properties strongly depends on a number of solid lubricants included in the brake pad. According to them, the performance of solid lubricant depends on temperature. Decomposition of solid lubricant at an elevated temperature often results in unpredicted friction behavior. This affects the friction films maintenance on contact zone and destabilizes coefficient of friction [66]. Table 2.1 shows the effect of most used solid lubricants in the brake pad.

Table 2.1: Advantage and disadvantage of most used solid lubricant as extracted from reference shown in the table.

Materials	Advantages	Disadvantages	References
Carbon (Graphite)	Commonly used to control tribological properties due to its ability to transfer films, which formed self-sustaining layers. It also exhibited better thermal stability. It also increases cooling rate.	High loading of graphite reduces hardness and increase brake pad overall heat conductivity.	[6, 17, 67, 68].
Molybdenum disulfide	(MoS2) a typical layer-lattice-type lubricant with good friction performance.	Poor wear resistance, and anti-fading properties	[69-71]
Antimony trisulfide	(Sb_2S_3) Improve fade resistance; lubricant to reduce vibrations and to improve friction stability	Increase wear rate, disk thickness variation generation, and potentially carcinogenic substance	[69, 70, 72, 73]

Coke	High coefficient of friction and better adhesion resistance.	low fade resistance and unstable friction	[74]
Friction dust	Commonly consists of processed cashew resin may have a rubber base; used to reduced impulsive combustion or help particle dispersion.	Poor performance at an elevated temperature	[6]
Metal sulphides	ZnS: Modifies and stabilizes coefficient of friction	Very expensive	[66]
Zirconium silicate (ZrSiO4)	High coefficient of friction and friction stability	Increases wear rate	[43]

Studies [20, 66, 70] have shown that the addition of two or more solid lubricants in the brake pad could play a complementary role in reducing fade, wear, creep groan and stabilize friction. In this regard, Cho *et al*. [70] studied the tribological properties of two brake pad containing different solid lubricants. One of the brake pads contains Sb_2S_3 and graphite, and the solid lubricant used for the other was Sb_2S_3 and MoS_2. They discovered that the synergistic functions formed by Sb_2S_3 and graphite improve the friction stability, and the fade resistance. These performances were attributed to the existence of Sb_2O_3 on the sliding interface, which plays as high-temperature solid lubricants. However, Sb_2O_3 is a potentially carcinogenic substance. On the other hand, the friction materials with Sb_2S_3 and MoS_2 exhibited poor wear and fade resistance. This suggested that brake pads friction stability, fade resistance, anti-fade, and wear rates are determined by the type and relative amounts of solid lubricants in the friction materials.

2.5.2 Abrasive materials

The addition of abrasive material is to serve as a cleaning agent to maintain clean contact surfaces by removing the build-up friction firm at the interface. Similarly, the addition abrasive material increases the coefficient of friction of the brake pad and the wear rate of the rotor [4, 6, 20, 68]. Studies [6, 75-77], acknowledged that the selection of abrasive materials in commercial brake pad basically depends on various factor,

including fracture toughness, shape, hardness, size, wear resistance and aggressiveness against the wheel/rotor.

For instance, Ma *et al.* [75] confirmed that abrasives such as $ZrSiO_4$, zirconium oxide (ZrO_2), aluminum oxide (Al_2O_3), and silicon carbide (SiC) had higher Mohs hardness values of around 7–9. The commonly used abrasives include zircon, quartz, alumina, magnesia, zirconia, zeolite, chromate, silicon carbide, and iron oxides [43, 77].These abrasive were used to replace asbestos since they offered related functions [6]. However, Chan *et al*. [48], emphasized that larger amount of abrasives in brake pad effects a greater variation of friction coefficient, which ultimately results in braking torque instability. In this case, a solid lubricant is required to balance braking torques and to stabilize coefficient of friction.

2.5.3 Fillers and reinforcements

Fillers, although not as critical as other components such as reinforcing fibers, play a significant role in improving certain characteristics of a brake pad. Several fillers of a different type, shape, size, amount, and compatibility have been used to influence brake pad performance [4]. However, among this filler, Kumar *et al*. [59] affirmed that the metallic fillers are important constituents because of their multiple functionalities. Aside from improving strength, they play the main role of absorbing frictional heat generated under severe conditions. Nevertheless, a large amount of metallic fiber in brake pad raises thermal conductivity, which affects other performance properties, resulting in the spongy brakes [78]. Also, a carbon-based additive such as carbon fibrer and graphite can be used as a replacement for metallic fiber since they possess better heat energy absorption properties with good cooling rate [6, 43].

According to Friedrich *et al*. and Kim *et al*. [39, 67], fillers are not only used to improve thermal, physical, chemical and mechanical properties but to stabilize brake pad coefficient of friction and promote ingredients cross-linking. This, in turn, helps in increasing brake pad wear resistance. Kumar *et al*. [5], stated that combination of filler is crucial to meet the complex performance norms for enabling brake reliability and safety. Several reinforcement materials have been used to improve performance properties such as tribological, thermal, and mechanical properties. These fillers include metallic, glass, ceramic and carbon fibers. These components provide multiple

functions that influence brake pad performance. Table 2.2 presents the contribution of most used fillers to braking performance.

Table 2.2: Contribution of reinforcement fillers to brake pad performance as extracted from reference shown in the table.

Materials	Description/comment	References
Fe-additives	Help to increase fade temperature and processing. However, high loading of metallic often manipulate brake pad thermal conductivity and affect other performance properties negatively.	[4, 78].
Molybdenum Trioxide	Used to modify thermal expansion and prevent lining cracking lining under high-temperatures conditions, however, exhibit poor wear resistance.	[4, 6].
Cashew Powder	Improves resilience in the binder system, heat absorption and suppress noise. It also used to improve the brake pad coefficient of friction at an elevated temperature.	[4, 6, 20].
Mica	Commonly used to suppress low-frequency brake noise. However, causes interlayer splitting of the friction lining at an elevated temperature.	[4].
Barium Sulfate	It impacts heat stability on brake pad, better melting point but toxic.	[4, 53]
Copper Powder	Helpful for improving brake pad performance properties, but has compatibility deficiency and causes excessive cast iron wear.	[5, 33, 59, 78]
Vermiculite	Help to suppress noise; however, it is a porous material with poor wear resistance and low heat resistance	[4, 53]

Carbon-based fillers (fibers & CNTs)	Carbon fiber offers good tribological properties, combined with high heat resistance (at temperatures above 2800°C) and low density (about 2 g/cm^3) that improves brake pad performance. Carbon nanotubes(CNTs) modifies all performance properties such as hardness, strength, wear resistance, the stable coefficient of friction and thermal stability.	[61, 79-85]
Potassium titanate	It Improves the coefficient of friction stability, fades and wear resistance. However, high content of potassium titanate reduces the friction coefficient, hardness and has the potential of causing lung diseases.	[60, 86, 87]

The multifunctional contribution of reinforcement filler to brake pad can be clearly seen in Table 2.2. This shows that proper combination of a material with more than two required properties for brake pad such as carbon based additives will reduce the number of the additive. It will also reduce processing time and cost.

2.5.4 Binders

The binder is one of the most important ingredients used in the pad to maintain structural wholeness under thermal and mechanical stress [88]. Nagesh *et al* [16] confirm that binder provides good bonding actions to the brake pad various components. Liew *et al* [89], affirmed that the binder resin and reinforcement fiber used in brake pad have a strong effect in determining performance properties such friction and wear. In this case, Imaekhai *et al* [4] stressed that binder should possess a better heat resistance to withstand the excessive generated at elevated temperature, resulting in degradation of binder another constituent. According to Imaekhai *et al* and Blau *et al* [4, 6] phenolic resins and modified resin such as cresol, epoxy, linseed oil, boron, rubber, and PVC is the typical binder used for the brake pad. These binder

materials were used to modify brake pad bonding characteristics and heat resistance at a very high temperature [6].

Among this additive, the phenolic resin, and the modified resin are probably the most commonly used for brake pad binder not only to reduce fade but to also maintain pads structural stability while functioning under extreme conditions. Nagesh *et al* [16], however, asserted that phenolic resin possesses a brittle nature, highly toxic, low impact resistance and decomposes at very low temperature. This discovery led intensive studies on modified resins. Wang *et al* and Bijwe *et al* [35, 52], investigated the effect of modified resin on brake pads performance properties such as thermal, mechanical and tribological properties.

Wang *et al* [41] observed that the brake pad produced from phenolic resin composites modified with different volume ratios of nitrile rubber and boron offered different porosity and flexural strength in inverse proportion. According to them, composites with the ratio of resins being 1:3 showed improved thermal resistance and high friction coefficient at different loads and speeds, however, exhibited poor wear behavior. Bijwe *et al* [41] results show that the characteristics of the brake pad vary with the type of resin, and no resin proved best for all the selected performance parameters. Alkyl benzene modified resin composite proved best in terms of strength, friction, fade, and recovery, but was poorest in wear performance.

The combination and functionalities of the additives used for the brake pad have been discussed, and the review shows that each of this additives property has a strong effect on pad performance.

2.6 Performance properties of brake pads.

The braking performance of brake pads depends on several factors among which; tribological, thermal and mechanical properties are key and necessary. Numerous studies [6, 34, 89] consistently show that additive must possess certain properties before it could be considered for brake pad application. These properties can be sub-divided into five sections, which are; tribological properties, chemical properties, physical properties, mechanical properties and thermal properties.

2.6.1 Tribological properties

Braking performance and durability of a pad requires tribological properties, which include the stable coefficient of friction and negligible wear rate during braking. Aside from material concentration effect, studies [90-93] proved that environmental condition, test facilities, and procedures often affect tribological properties. These factors include but not limited to speed, load, temperature, sliding surface and test facilities also influence tribological properties. The pad should generate wear debris that serves as a lubricant on the counterpart surface. It should also have the ability to reduce transmitted vibration created by wheel load and track irregularities.

According to Dagwa and Ibhadade [94], average wear rate for commercial brake pad is 0.5 micrometer per application, which approximately equivalent to 3 mg material lost per braking [6]. They reported 4.4 mg/application after wear test conducting brake pad made from agricultural waste. This wear rate value was reported to depend on the brake pad continent formulation, heat generated by friction and test procedures.

Anderson as cited in Blau [6], stated that the coefficients of friction (μ) for a set of brake pad span a range of 0.07 to 0.7. However, most vehicles operate within a narrower range of 0.3 - 0.6 μ practically. This value is also similar to the standard value recommended by *Society of Automotive Engineers* (SAE J661 C-Z) for vehicle brake pad [6]. Most of the coefficient of friction value reported not only fell within the values stated above but also influenced by the brake pad composition, the mechanics of the system, test procedures, and environment mentioned earlier [5, 6, 34, 74, 94].

2.6.2 Chemical properties requirements

Chemical properties of material is an important factor in determining brake pad performance. The brake pad should possess a good chemical stability in any condition may it cold or hot. It must be inflammable, not absorbance of water and oil, insoluble in any solvent and should be able to adhere to other material such metal when is under production. The combination of material used for pad production must have good mixability as well as compatibility along with better corrosion resistance [6].

2.6.3 Physical property requirements

The physical properties of a pad included a flat top surface and good dimensional stability. It should possess less or no porosity and be at the center of the back plate. It must also provide optimum deflection compatible to the back plate fastening system. This fastening helped to provide the necessary resistance to the longitudinal and lateral wheel force at all time [6, 17, 95].

2.6.4 Mechanical properties

Brake pads mechanical properties such as compressive strength, young modulus; shear determines its tribological properties and also has a strong influence on the braking system stopping time. Therefore, the pad should provide sufficient compressive and shear strength, stiffness and hardness with a good abrasion resistance to prevent deformation while functioning [6, 96, 97].

2.6.5 Thermal properties

In general, the thermal properties of break pads have been measured using a Differential Scanning Calorimeter. According to previous research, a good brake pad must have a working temperature ranging between 300 and 400^{o}C [35]. Brake pads should also have thermal stability to prevent an increase in wear at a very high temperature. Furthermore, they should exhibit lower thermal expansion and must possess the ability to absorb heat from the wheel and dissipate in seconds [68].

2.7 Low friction hybrid nanocomposite brake pad: Validation 'Fitness for Purpose'.

Fitness for the purpose has been defined as the possible criteria to establish whether or not a product meets expected potentials for better performance [98]. Consequently, studies [6, 38, 99, 100] have conducted several tests in determining proper properties of the materials or combination of additives for the brake pad. According to Blau *et al,* brake pad performance depends on several factors among which; tribological, thermal and mechanical properties are key and obligatory. Density, porosity, and water absorption investigations are also important [5, 17, 58, 68].

In general, brake pad testing method can be classified into two namely: material tests and full-size component tests. Material tests such as shear test, compression, thermal conductivity, hardness are employed during the development of brake materials and

additives. While full-size component test involving extensive on-vehicle study is used to brake pad final qualification for brakes. Among these test methods, Blau *et al.* [6] asserted that full-size component test was advisable because it reduces preliminary material qualification, and research facilitates costs. In this regard, different laborated-scale test machines range from massive inertia dynamometers with electronic controls and sensors to small, rub-shoe machines that can sit on a bench have been developed [6, 17, 55].

These machines were used for brake pad Off-vehicle test methods. They range from simple drag tests at contact pressure and constant speed to complex, multi-stage criterion tests involving pre-set changes in contact speed, pressure, temperature, and repetitive contacts that simulate vehicle braking procedures (e.g., SAE J 1652). Braking performance; however, not only depend on materials and vehicle hardware design but significantly on driver behavior, the vehicle usage and the overall environment in which the vehicle is driving. Considering the possible influence of sleekness in the wheel well, braking control systems and engine braking, no laboratory test can mimic driving condition precisely [6].

To validate material performance, numerous techniques [4, 6, 38, 55, 97] have been employed. These were used to investigate the development of additives components for the brake pad. These were carried out to determine brake pads durability, thermal conductivity, the stable coefficient of friction, vibration, and satisfactory environmental condition while functioning.

Over the decades, either block-on-block or pin-on-disc was commonly used to measure the tribological property (wear and friction), static friction and the effect of temperature on the material selected for the brake pad. Kim *et al*. [34], affirmed that factors such as sliding speed, applied load, and velocity influenced tribological properties. They as well stated that varying this parameter often helps in determining wear rate and coefficient of friction.

Similarly, MTS-UTM has been used to determine the mechanical properties of the raw material and finished product such as composite, metal, textiles, and plastic. This

material testing machine can test material samples for compressive strength, shear strength and also execute bend test alongside with other important laboratory tests. It mainly used to generate the stress-strain diagram, after which computers excel or algorithms are used to calculate yield strength, Young's modulus or total elongation and compressive strength [101-103].

In addition, thermogravimetric and differential scanning calorimetric (TGA/DSC) have been used to investigate material thermal behaviors [104]. This machine is used to measure both weight loss (thermogravimeter) and heat flow (Differential scanning calorimetry) in a material as a function of time and temperature. The information obtained from (TGA/DSC) is used to differentiate endothermic and exothermic measures that have no relationship with weight loss (e.g., melting and crystallization) and that is weight loss associated (e.g., degradation) [105]. The above-mentioned methodology is relevant to this study when determining the thermal behavior of the brake pad. Basically, friction, wear, Young's modulus, thermal behavior, compressive and shear strength determinations are appropriate for this study, particularly when determining the braking performance and the stopping force of low friction hybrid brake pad.

2.8 Summary

The review carried out on the brake pad evolution, selection of material, material functionality, the composition of materials for brake pad and different techniques for determining brake pad suitability and reliability. This review shows the relationship between a proper selection of material and friction material functionality. It also highlighted the effect of composition and amount of additives on brake pad performance. In general, this review suggested proper selection and formulation of components for brake and thorough control of the additives content to ensure better performance.

Chapter Three: Research Design and Methodology

The materials and methods involved in fabricating low friction hybrid nanocomposite for brake pad are discussed in this chapter. Subsequently, the testing of specimens: both quasi-static and dynamic loading, that is, various experimental works and analyses that were conducted, leading to the prediction of hybrid nanocomposite suitability for brake pad application are discussed. The polymeric binder selected for incorporating graphite nanopowder, multi-wall carbon nanotube, and carbon fiber were an epoxy resin.

3.1 Introduction and Background to the research methodology

This study was fundamentally stimulated from observation and inductive reasoning while considering material selection and brake performance of a brake pad. Researchers [5, 6, 17, 39, 52] observed that the braking performance of a brake pad depends on the material selection, composition, and functionalities. Similarly, M.H. Chou et al and K.K. Ikpambese et al [17, 39] observed that the braking performance of brake pad depends on the combined tribological properties, thermal stability, and mechanical properties. It was also observed that the removal of asbestos in brake pad industries gave birth to many safer materials, which include metallic, semi-metallic, ceramic and sintered materials [8, 48].

However, studies [22, 55] mentioned that brake pad contained metal or metal fiber has a negative effect of abrading the wheel and also make excessive noise during the braking. Thus, advised that an alternative material to metallic and semi-metallic material needs to be sourced and investigated. Inductive reasoning proved that the combination of nanoparticle fiber and polymer composite offers similar performance as metallic and asbestos materials [5, 17, 95]. It, therefore, appears that polymer-based low friction hybrid nanocomposite materials could be used as an alternative material for pad production [34-39].

To facilitate the proposed research design and methodology, a step by step methodology was considered suitable. This study will first discuss the development and testing of low friction hybrid nanocomposite materials. These will help in determining the synergistic effect of the combined material and will also enable the researcher to meet the first research objectives described in chapter 1. Thereafter, the

braking performance of the full-size brake pad will be evaluated with existing brake pads, and this will enable the researcher to meet research objectives 2, 3 and 4 of the study. Finally, the recommendation of hybrid nanocomposite brake pad that exhibits better braking performance as compared to current brake pad will enable the researcher to accomplish the aim of this study.

3.2 Development, and testing of low friction hybrid nanocomposite materials.

As asserted by several researchers [5, 17, 58, 68], various investigations needed to be conducted on materials or combination of an ingredient for brake pad development to ascertain fitness for this application. Material testing such as wear, friction, compression, hardness, thermal conductivity, and solvent absorption has been used for determining materials suitability for brake pad application. This material testing helps in selecting the appropriate combination of materials and also increases the reliability of the study. However, development of brake pad material comes before testing. Hence, the next section will discuss the materials and brake pad fabrication.

3.3 Materials

Binder abrasives, friction modifiers, fillers, and reinforcement have been found as the main compositions of a brake pad [4, 6, 36]. This study considered commercial bi-functional epoxy resin, diglycidyl ether of bisphenol-A (DGEBA) sold under the trade name of LR-20 with an unmodified cyclic aliphatic amine-based curing agent; LH-281 hardener a binder. Epoxy resin and hardener used had a density of 1.13g/cm^3 and 1.01g/cm^3 respectively at 25^{0}C. In addition, epoxy resin possesses a viscosity which ranges from 800 to 1100mPas at 25^{0}C and hardener has a viscosity of 650mPas at 25^{0}C. The epoxy resin and hardener have a flashing point (DIN 51758)^{0}C of 130 and 105 respectively. The hardener has a yellow transparent colour and epoxy resin was semi-transparent in colour. The chemical structure shown in Figure 3.2 was for both epoxy resin and hardener.

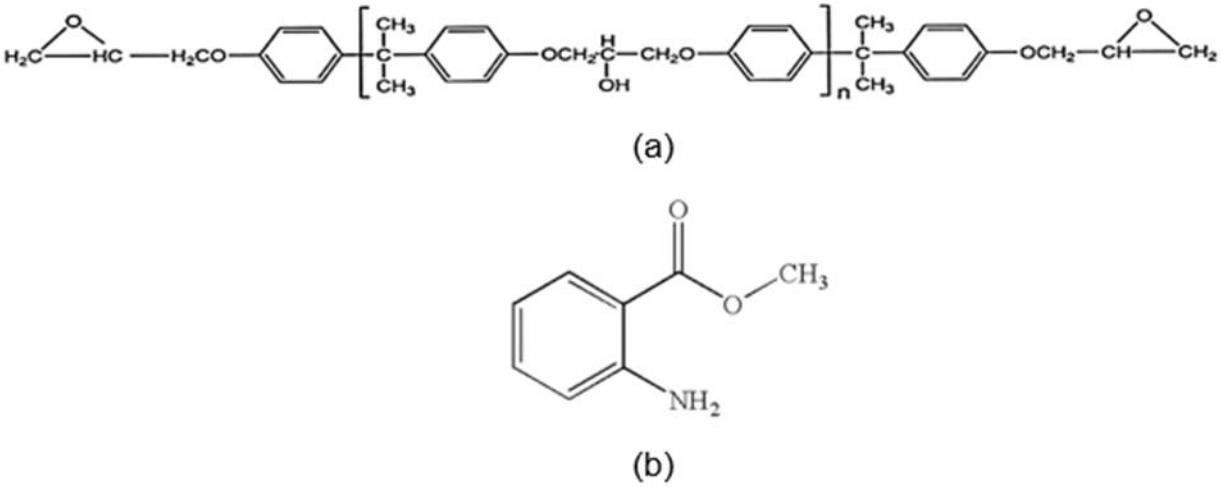

Figure 3.1: Chemical structure of; (a) Epoxy resin, diglycidyl ether of bisphenol-A (DGEBA) and (b) an unmodified cyclic aliphatic amine-based hardener [106].

Multi-wall carbon nanotube and graphite nanopowder were used as friction modifier and filler since they are multifunctional fillers. Both carbon-based fillers were in nanopowder form. The multi-wall carbon nanotube has a real density ranging from 1-2 g/cm^3; its tubes occur in bundles of length ~1 - 20µm. (±1. 5µm) with a diameter of 10-20nm (3-8µm). Multi-wall carbon nanotube is a black additive, normally used to improve thermal conductivity, mechanical and tribological properties of polymer material [107-110]. Similarly, the graphite nanopowder was from hydrophobic natural graphite with 1-2.3 g/cm^3 density, <100nm in size and it an Iron-black to steel-gray in color. It is normally used as an internal lubricator, thermal stability additives also used to control wear and friction of brake pad [111-113].

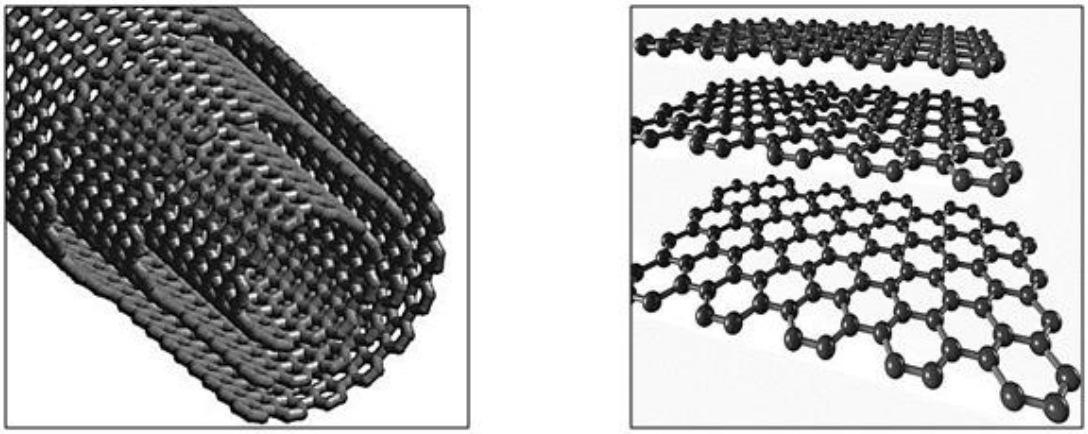

Figure 3.2: Structure of; (a) Multi-wall carbon nanotube[114] and (b) Graphite [115].

In addition, short carbon fiber was used as reinforcement filler since it has been used to improve mechanical strength, thermal stability, creep and wear resistance of polymer materials [93, 116, 117]. The woven carbon fiber with a density of 2.00 g/cm^3 was cut to a length between 5 to 10 mm to ensure better dispersion of fiber in the matrix.

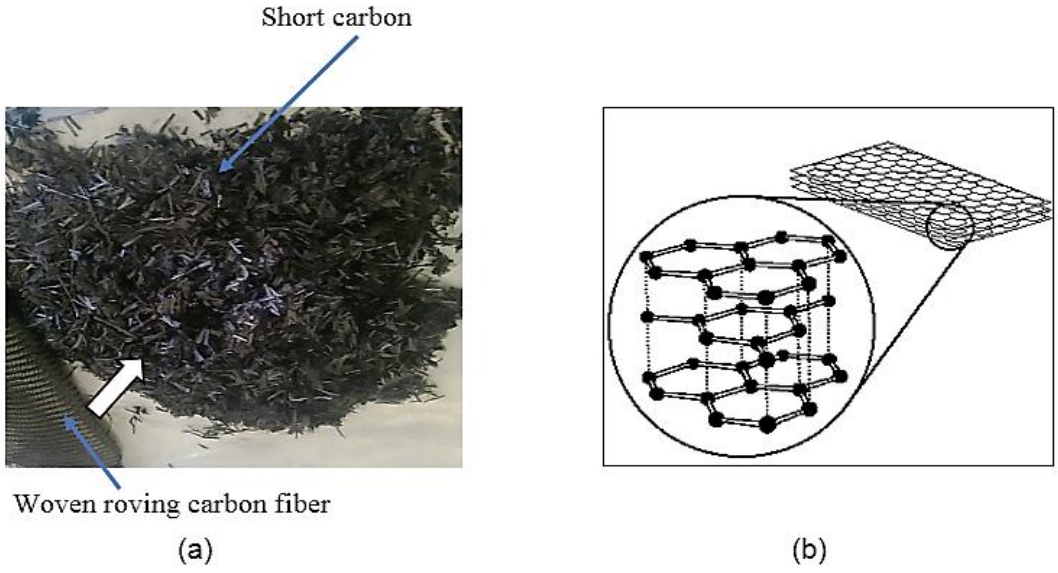

Figure 3.3: Carbon fiber; (a) Demonstrate woven roving carbon fiber cut with the aid of scissors to a length of 5 to 10 mm (b) carbon fiber structures [118].

Epoxy resin (ER) and catalyst (LR 20 and LH218), as well as carbon fiber (SCF), were purchased from AMT composite, Durban South Africa. Multi-walled carbon nanotube (MWCNT's) and graphite nanopowder (GN) (<100 nm) were procured from Capital Lab Supplies, Durban South Africa.

3.4 COMPOSITE FABRICATION

Table 3.1: Hybrid nanocomposite formulation

Constituents	*Hybrid nanocomposite samples (Vol. %)*											
	HC_1	HC_2	HC_3	HC_4	HC_5	HC_6	HC_7	HC_8	HC_9	HC_{10}	HC_{11}	HC_{12}
Epoxy resin	88.9	88.8	88.7	86.9	86.8	86.7	78.9	78.8	78.7	76.9	76.8	76.7
Carbon fiber	10	10	10	10	10	10	20	20	20	20	20	20
MWCNTs	0.1	0.2	0.3	0.1	0.2	0.3	0.1	0.2	0.3	0.1	0.2	0.3
GN	1	1	1	3	3	3	1	1	1	3	3	3

In order to fabricate polymer-based hybrid nanocomposite material, epoxy resin was measured into a beaker and heated up to 70ºC to decrease the viscosity of the resin and to facilitate incorporation of multi-walled carbon nanotubes and graphite nanopowder. Epoxy resin, multi-walled carbon nanotubes, and graphite nanopowder were mixed using a mechanical stirrer at 500 RPM for sixty minutes to obtain a homogeneous solution. It is well known that small contents of additives ranging from 1-5 vol. % have a better effect on composite properties and depleted when the additive content is more [39, 67]. In this regard, additives weight percentage contents were kept low at 0.1-0.3 vol. % for MWCNTs and 1vol. - 3vol. % for graphite powder. The hybrid nanocomposite was naturally cooled to room temperature. Thereafter, epoxy nanocomposite and catalyst were mixed using a ratio of 100-30 vol. %. Then, Short carbon fiber (10vol. %, and 20vol. %) was added to have different formulation as shown in Table 3.4. Afterward, the mix was poured into an open mold to a level of 12mm. Prior to pouring into the mold, wax was applied on the inner surface of the

plastic mold to facilitate composite easy removal after two days. The composite panel was removed and tested after fourteen days to allow for proper curing.

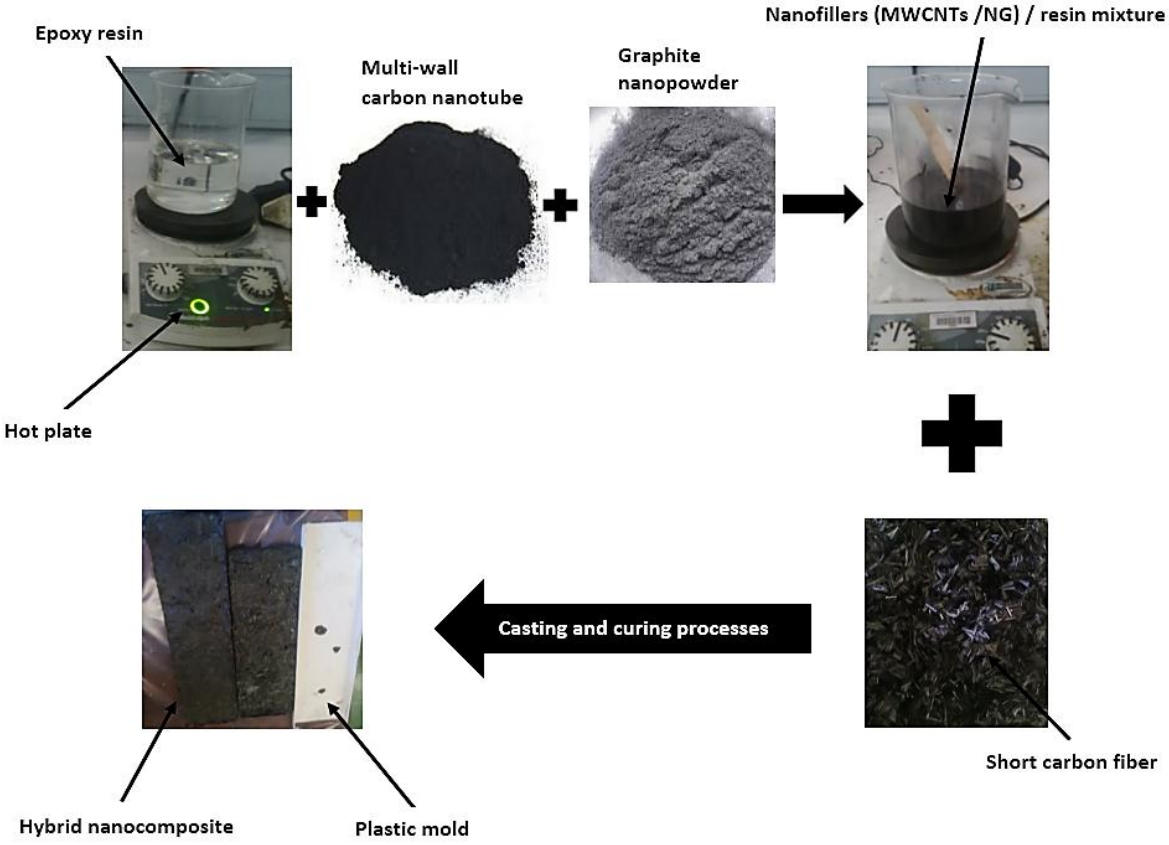

Figure 3.4: Process overview of polymer-based hybrid nanocomposite brake pad.

3.5 Description of techniques and procedures

In this section, various techniques used to characterize hybrid nanocomposite brake pad are discussed. A checklist is given in Table 3.2.

Table 3.2 List of characterization techniques conducted in this study

Technique	Purpose of the test
SEM	Determination of fracture and wear mechanism
TG/DSC	Determination of degradation temperature, heat energy absorption, and thermal stability.
Compressive test	Material strength and stiffness
Compressive modulus	Measure of stiffness of material
Shear test	Determination of shear strength
Impact test	Resistance to shock
Hardness	Measure of hardness
Water absorption	Moisture uptake
Oil absorption	Oil absorption rate
Wear rate	Measure of brake pad durability
Coefficient of friction	Study of coefficient of friction stability
Noise level	Determination of noise level generated during braking.
Interfacial temperature	A measure of frictional heat.
Stopping distance	Study of a quicker braking

.

3.6 THERMAL ANALYSIS

3.6.1 Differential scanning calorimetry (DSC)

Differential scanning calorimetry (DSC) measurement of brake pad samples was conducted on a Thermal Analyser (TA) apparatus (Thermal Universal V 4.5 A). Power-compensation DSC was conducted on brake pad samples. A heating rate of 10 ^{0}C/min was used under a dry nitrogen gas at a flow rate of 100 mL/min from 20 ^{0}C to 600 ^{0}C. The glass transition temperatures (*Tg*) were determined from the midpoint of the onset to the offset curve of the baseline shaft.

3.6.2 Thermo-gravimetric analysis (TGA)

Thermal stability and degradation were determined using a thermogravimetric analysis (TGA). The thermal Analyser (Thermal Universal V 4.5 A) instrument was used to measure thermal stability and degradation. The investigation was conducted under a dry nitrogen gas flow at the rate of 100 mL/min from 20^{0}C to 600^{0}C, at a heating rate of 10 ^{0}C/min.

3.7 MECHANICAL TESTING

It is well known that vehicle braking involves squeezing of the brake pad on the rotor. Considering the way and manner at which pressure and force are applied, better mechanical properties are required for efficient braking. The following quasi-static and dynamic testing methods were used for determining brake pads mechanical properties.

3.7.1 Quasi-static test

3.7.1.1 Compressive

The purpose of the test was to investigate the strength and stiffness of hybrid nanocomposite brake pad. Brake pads compressive properties were determined according to ASTM D 695 tests standard specification [119].

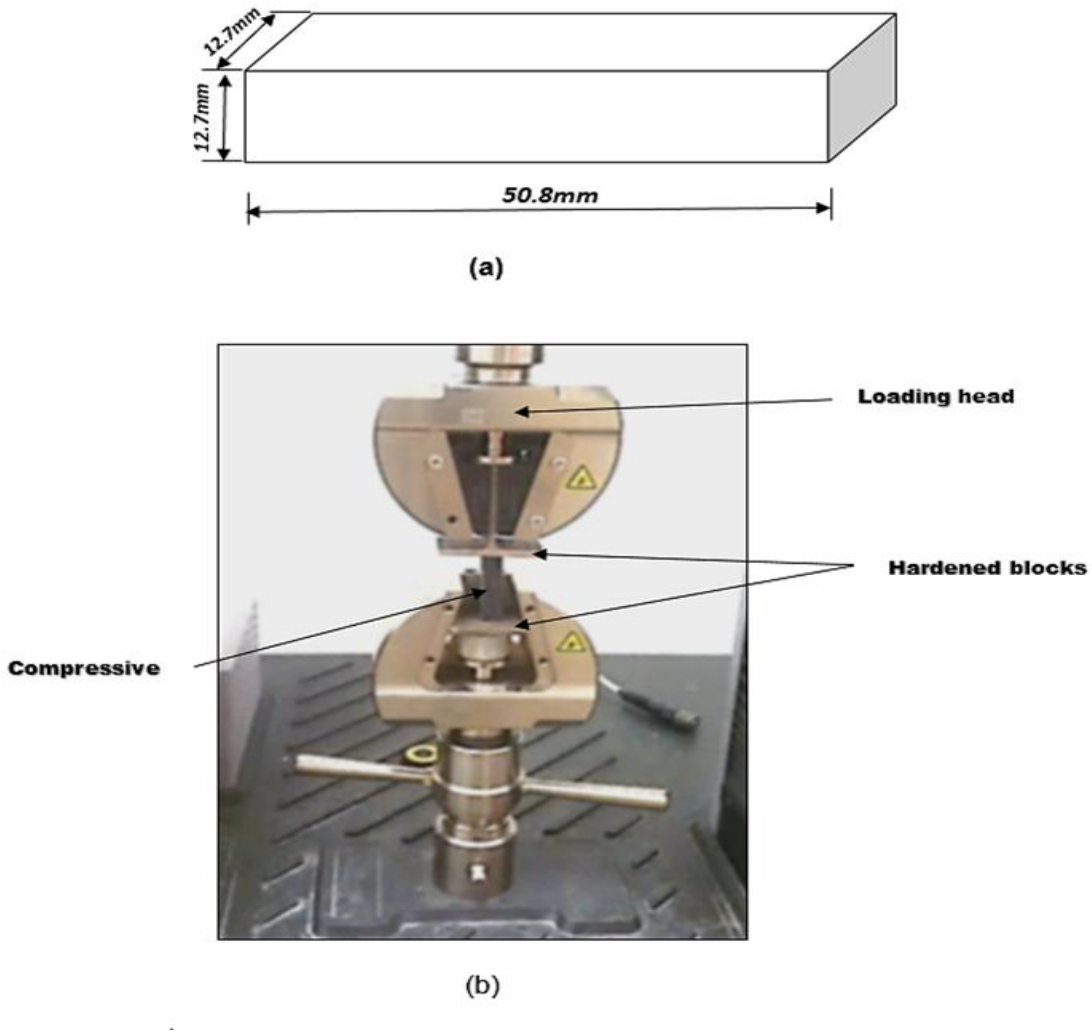

Figure 3.5: Schematic diagram of (a) compression sample and, (b) compressive test with hardened blocks on Lloyd testing machine.

The test was carried out on samples using Lloyd universal testing machine (Model 43) filled with a 30kN load cell. The test rectangular specimen of 12.7 x 12.7 x 50.8 mm in width, thickness and length of dimension as shown in Figure 3.5a was cut from brake pad (polymer hybrid nanocomposite) samples using a diamond cutting machine. Samples sharp edges left by diamond cutting machine were smoothing using sand papers prior to testing. The test specimen gripped straight in between two hardened blocks shown in Figure 3.5b was compressed until failure occurs in gauge section. Five samples were tested at ambient temperature and speed of testing was 1.3± 0.3 mm (0.050±0.010 in.)/min. The mean value of the five samples was used for graphical

illustrations and discussion. Compressive strength, strain, and modulus were calculated using the following equation.

$$\sigma_e = \frac{F^*}{A^0} \quad 3.1$$

$$\varepsilon_e = \frac{(l_0 - l^*)}{l_0} \quad 3.2$$

$$E = \frac{\sigma_2 - \sigma_1}{\varepsilon_2 - \varepsilon_1} \quad 3.3$$

Where;

σ_e: compressive strength

F:* maximum load applied before crushing (N)

A_0 **:** original cross-sectional area of the sample in the gauge length (mm^2)

$\boldsymbol{l}_0$ **:** original gauge length (mm)

$\boldsymbol{l}^*$: specimen length after crushing (mm)

E: compressive modulus (MPa)

σ_1, σ_2: corresponding stress at the specific strain (MPa)

ε_1, ε_2: corresponding stress at the specific stress (MPa)

3.7.1.2 Shear

Shear properties of brake pad samples were determined according to ASTM D 732-02 standard test specification [120]. The test was carried out on samples using Lloyd universal testing machine (Model 43) filled with a 30kN load cell. The test rectangular specimen of 12.7 x 12.7 x 50 mm in width, thickness and length by dimension as shown in Figure 3.6 was cut from brake pad samples using the diamond cutting machine. The test specimen had a parallel upper and lower surface. A hole of 11 mm diameter was drilled through the center of the sample. This hole was made using pillar drilling machine.

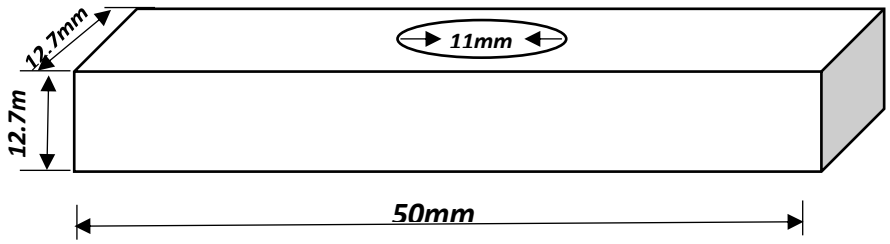

Figure 3.6: Schematic diagram of compression sample

The compression tests were performed by clamping specimen in the shear tool. The shear tool of punch type was in- house fabricated based on ASTM D 732-02 [120]. Figure 3.7 shown cross-sectional views of the shear tool used. It was so constructed that the specimen was rigidly clamped to the stationary and movable block so that it can deflect during the test. The specimen was placed over the pin of the punch and fastened tightly by using of bolt and nut. Then, the tool jig was assembled, and the bolts were tightened. The Shear tool was positioned in Lloyd universal testing machine jaw and fastened tightly as shown in Figure 3.7.

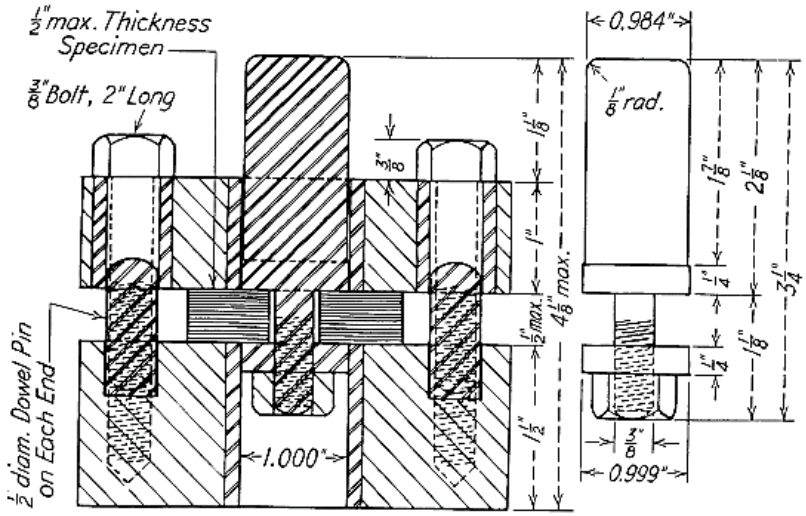

Figure 3.7: Modified shear tool cross-sectional view [120].

Shear tools were so constructed in such a way that the specimen was rigidly clamped to the stationary and movable block so that it can deflect during the test. The specimen was placed over the pin of the punch and fastened tightly to it by the means of bolt and nut. Thereafter, the tool jig was assembled, and the bolts were tightened. It was later placed on the Lloyd universal testing machine and fastened as shown in Figure 3.8.

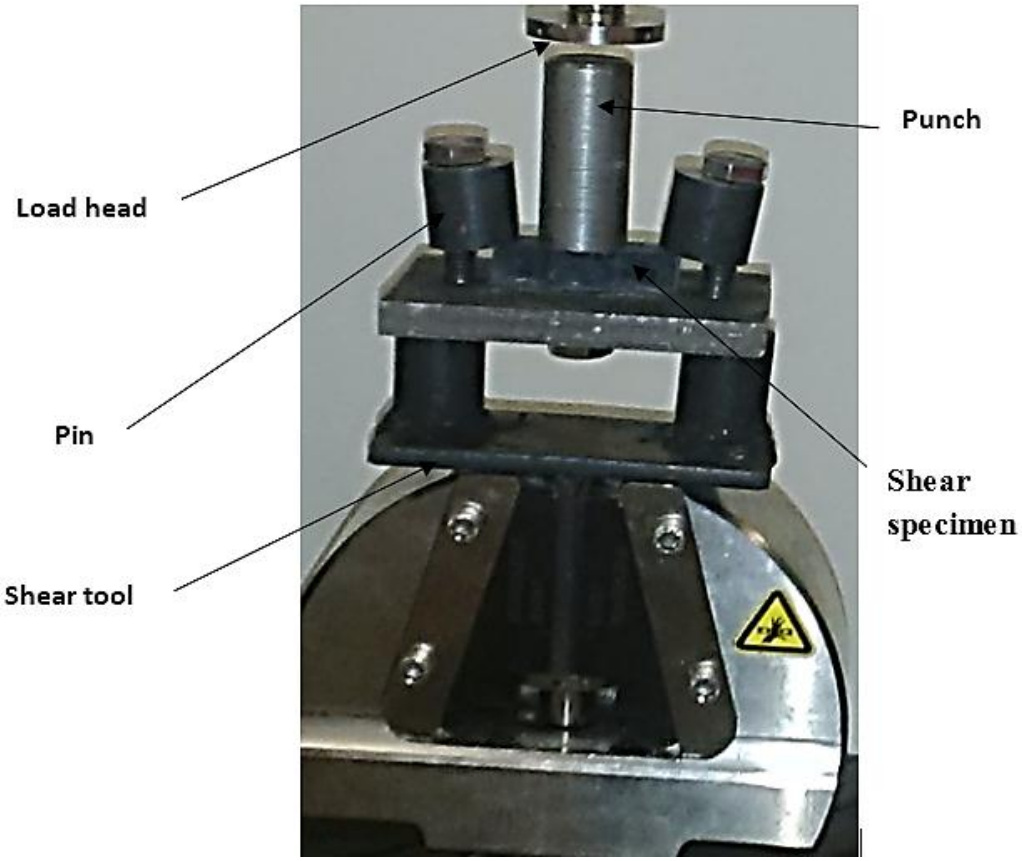

Figure 3.8: Compressive test with shear jig tools on Lloyd testing machine

Each specimen as shown in Figure 3.8 was stressed until it fails. Five specimens were investigated under room temperature at a speed of testing 1.3± 0.3 mm (0.050±0.010 in.)/min. The average values of five specimens were used for graphical illustrations and discussion. Shear strength was calculated using the following equation.

$$\tau = \frac{F}{d \, x \, \pi r^2} \qquad 3.4$$

Where;

τ: Shear strength

F: the maximum load

d: the specimen width

π: pi (22/7)

r: punch radius.

3.7.1.3 Impact

In order to determine fabricated and commercial brake pads impact resistance, charpy tests were conducted at room temperature using a Hounsfield Balance Impact Tester manufactured by Tensometer Ltd., Croydon, England. The Hounsfield Balance Impact Machine has a three-point to charpy apparatus created in ASTM D6110-10 [121]. The dimension of the test specimens geometric were 50 x 10 x 5 mm^3 by length, width, and thickness was cut from the brake pads. As this method permitted variation across the width of the specimen for different material, either brittle or ductile.

The width stated in the specification covers the measurable and should be indicated by the impact values. All the specimens have a notch of 4mm deep in the middle of part opposite the impact part, leaving the impact width to be 6mm by the width area. Five specimens were tested for each formation of the brake pad, and the impact velocity was approximately 6.7 m/s. The average values collected were used to calculate energy absorption using the following equation.

$$IS = \frac{AE}{TW} \qquad 3.5$$

IS: impact strength (kj/m^2)

AE: absorbed energy (Joule)

T: specimen thickness (m)

W: Remaining width at notch (m)

3.7.1.3 Hardness

Barber Colman Barcol impressor hardness tester was used to determine brake pad hardness since it suitable for testing fabricated and individual specimen for production control. Hardness test was conducted according to ASTM D 2583 test standard specification [122]. The hardness test describes the indentation hardness of a material by gauging the depth of the indenter point penetration as shown in Figure 3.9. The Barcol impressor (model GYZJ-934-1) hardness tester commonly used for composite materials was used to measure and determine the hardness of specimens. This

impresser has a hardened steel truncated cone (intender), at an angle of 26^0 with a flat tip of 0.157 mm in diameter. This was fitted into a hollow spindle and held down by a spring-loaded plunger. It also has an indenter leg for balancing on the testing specimen surface.

The Barcol impressor indenter point was placed parallel to the sample plate as shown in Figure 3.9. A uniform downward force was applied by hand until the dial indicator reaches a maximum reading, and the maximum reading was recorded. Fifteen indentation values were randomly taken on samples, and the mean value was taken for graphical illustration.

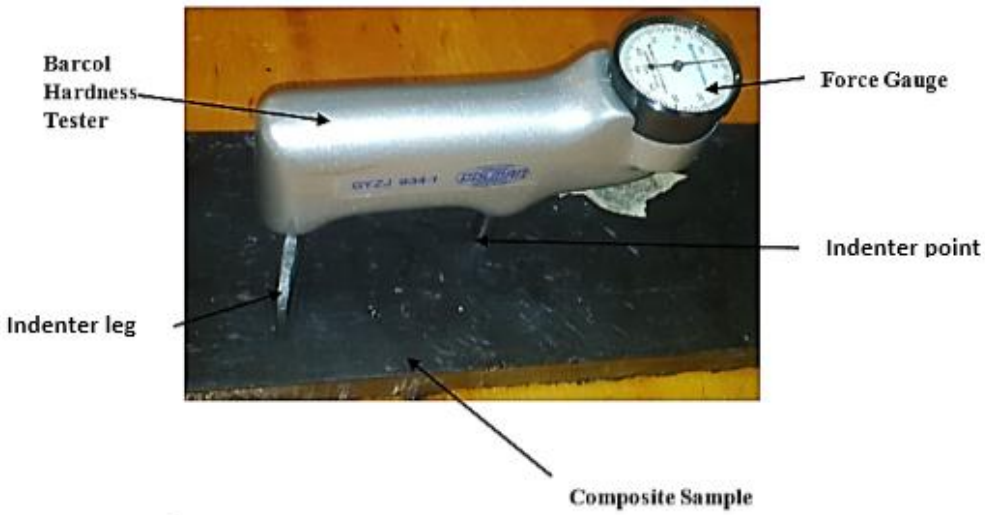

Figure 3.9: Barcol hardness performed on brake pad materials samples.

3.8 ABSORPTION TEST

Brake pad absorption rate normally influences braking performance [4]; therefore, it will be imperative to investigate water and oil absorption of the brake pad specimens. In this regard, the procedure used for determining brake pad absorptions are as follows.

3.8.1 Water Absorption

The water absorption for brake pad was investigated to determine the sample rate of water absorption and the effects of exposure to water or humid condition. The test was conducted according to ASTM D 570-98 standard test specification [123]. The water absorption was determined by weighing the sample (W_1) using a Kern digital electronic

scale with 0.01g accuracy (model D-72336) made in Germany. The samples were immersed in water at an ambient temperature for 24 hours. Afterward, the sample was removed, wiped with a dry napkin and weighed (W_2). Three specimens cut from each batch were tested. The average value of the three samples was used for graphical illustrations and discussion. The percentage of water absorption was calculated using the following equation.

$$P_{wa} = \frac{w_2 - w_1}{w_1} \qquad 3.6$$

Where;

P_{wa}: percentage of water absorption,

w_1: specimen initial weight, and

w_2: specimen final weight

3.8.2 Oil Absorption

The brake pad material sample rate of oil absorption was investigated to determine the sample rate of oil absorption and the effects of exposure to oil. The oil absorption was determined by weighing the sample (W_1) using a Kern digital electronic scale with 0.01g accuracy (model D-72336) made in Germany. The samples were immersed in water at an ambient temperature for 24 hours. Subsequently, the sample was removed, wiped with a dry napkin and weighed (W_2). Three specimen cut from each brake pad were used, and percentage of water absorption was obtained. The average value of five samples was used for graphical illustrations and discussion. The percentage of water absorption was calculated using the following equation.

$$P_{Oa} = \frac{wo_2 - wo_1}{wo_1} \qquad 3.7$$

Where;

P_{Oa} = percentage of oil absorption,

wo_1 = specimen initial weight, and

wo_2 = specimen final weight

3.9 DYNAMOMETER TEST PROCEDURE

Prior to dynamometers investigation, properly cured hybrid nanocomposite was cut to the dimension shown in Figure 3.11 using a band saw. It was later adhered to the back plate using a mixture of the debris collected while cutting and epoxy.

A dynamometer coupled to a Aisin Toyota 5k engine was used to determine brake pads stopping distances, tribological behaviours, heat dissipation and noise level. The Toyota engine (Model: 0031700) has the drive speed of 5000rpm (222.4 km/h), driven power of 45hp, and driven torque of 110 Nm. The dynamometer unit has a rotor of 236mm diameter and brake pad caliper. This setup was used to determine the braking performance of all the brake pads. In order to determine wear rate, brake pads were weighed before and after the testing by using a Kern (model D-72336) digital electronic scale with 0.01g accuracy.

Each pair of the brake pad shown in Figure 3.10 was then positioned in the caliper and mounted adjacent to the rotor as shown in Figure 3.14. The dynamometer connected to the computer was used to measure speed. Pressure gauge and brake master cylinder attached to the brake assembly unit was used to measure braking force. The engine speed was set at 1250rpm (15.5m/s) and the brake was applied after reaching the pre-set speed.

After each test, the caliper was disassembled, brake pads were removed and their final weight was taken. During braking, a non-contact infrared (IR) thermometer (MAJOR TECH- MODEL: MT697) shown in Figure 3.12 was placed at about 20cm away from the tracking edge of the brake pad to measure wheel temperature [57]. The interfacial temperature was measured on the spot of the wheel as shown in Figure 3.13.

Figure 3.10: Hybrid nanocomposite brake pads

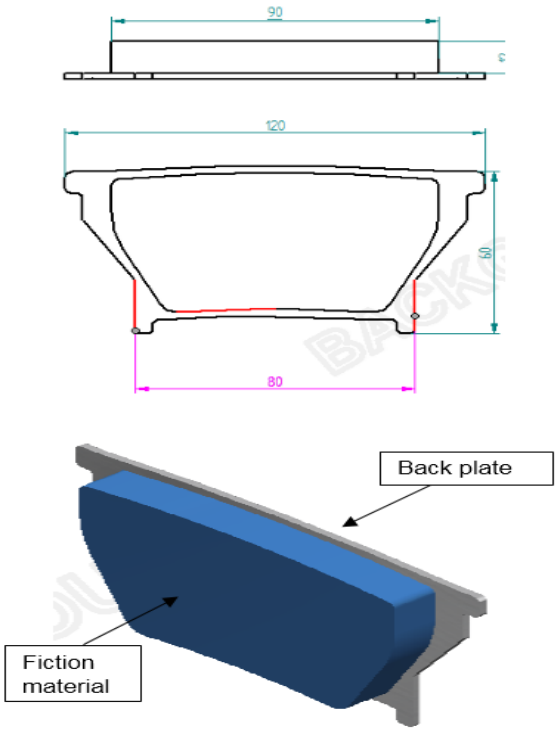

Figure 3.11: Schematic diagram of the fabricated brake pad

Figure 3.12: Non-contact infrared (IR) thermometer (MAJOR TECH- MODEL: MT697) used for measuring counterpart temperature.

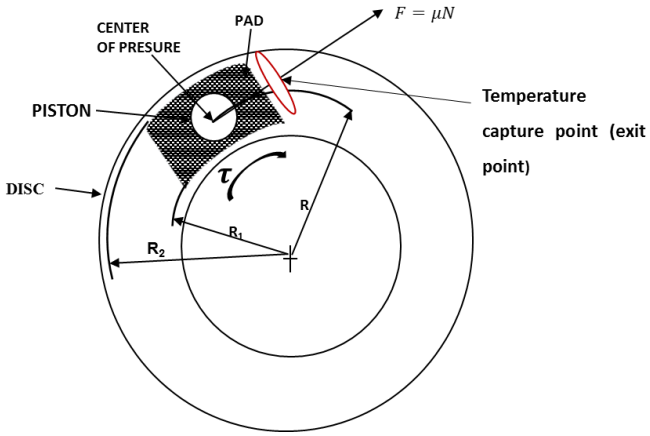

Figure 3.13: Schematic diagram of brake disc and pad.

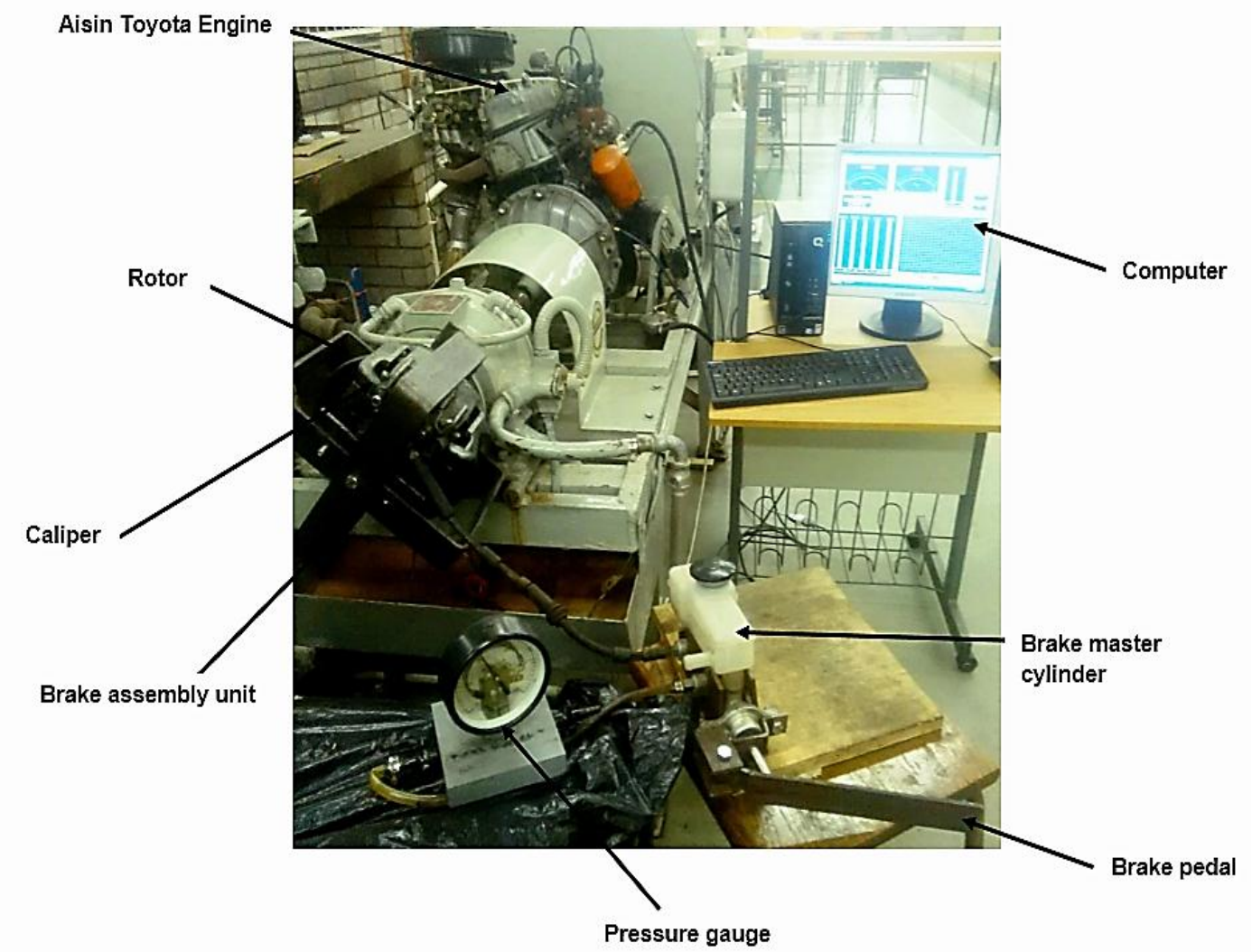

Figure 3.14: Inertia dynamometer used for brake pad testing

Additionally, sound level meter commonly used for quantifying different kinds of noise, especially for industrial and environmental was used to measure brake pad noise level [124]. A digital sound level meter (CL151137) microphone was held in place by, and projected 2cm from, adjacent contact with the brake pad and rotor to measure noise caused during braking. Furthermore, stopping time was also measured when applying brake using a stopwatch. These tests were repeated for the following sliding distances, 18.4m/s, 21.6m/s, 24.7m/s and 27.8m/s to obtain a consistent wear rate and the coefficient of friction. Similarly, the commercial brake pad was evaluated. The data collected from the computer, pressure gauge, stopwatch, and an electronic scale were used to measure and determine the braking force, using equations.

$$BF = PA \qquad (3.8)$$

Where;

BF: braking force (N)

P: Pressure (GPa) and

A: area of the piston (m^2)

Stopping distance was calculated using this equation

$$V_0 = \frac{2S}{t} - v \qquad (3.9)$$

Where;

v: final velocity [m/s]

v_0: starting velocity [m/s]

s: Stopping distance (m) and

t: Stopping time [s]

Brake pad wear rate was measured using this equation

$$wr = \frac{\Delta w}{z} = \frac{\Delta w}{2\pi NDR} \qquad (3.10)$$

Where;

wr: wear rate (g/Nm)

Δw: mass loss (g)

D: diameter of the rotor (m)

z: total sliding distance (m)

R: revolution per minute(s) (min.) and

N: normal load

The coefficient of friction was determined using equation

$$T_B = 2\mu NR \qquad (3.11)$$

$$R = \frac{R_2 + R_1}{2} \qquad (3.12)$$

Where;

T_B: braking torque (N-mm)

μ: coefficient of friction (μ)

N: normal load

R_1: distance between the brake pad inner edges and rotor center (m)

R_2: distance between the brake pad outer edges and rotor center (m), and

R: center of disc rotation (m)

The average values of the results taken were used for graphical illustrations and discussion. In conclusion, all the test procedures from tribological to dynamometer investigation were repeated for the commercial brake pad.

3.10 STRUCTURE AND MORPHOLOGY

3.10.1 Scanning Electron Microscopy (SEM)

Scanning Electron Microscopy (SEM) using Zeiss Environmental SEM (EVO HD 15 model) operating at controlled atmospheric conditions of 20kVat1000 times zooming, was used to examine brake pad samples worn surfaces microstructure after the wear investigation. It was also used to determine the fracture mechanism of brake pad after mechanical tests such as shear and impact strength. Prior to microstructure investigation, the samples were coated with electronic thin gold, and the worn microstructure of the samples was examined to determine its worn mechanisms under sliding [17, 125, 126]

3.11 Summary

This chapter described the method used for the development of the polymer-based hybrid nanocomposite brake pad to validate result reliability and easy comparison to current commercial brake pad (control). The materials used were defined. A description of the various procedures and its applicability in this study were specified.

The next chapter discusses performance properties of hybrid nanocomposite brake pad in comparison with the control.

Chapter Four: Results and Discussion

This chapter presents the results and discussions of this study. The results are based on the tests that were conducted as described in previous chapter. Overall, this chapter is structured into two sections. Section one describes the mechanical properties of the hybrid nanocomposite brake pad. These properties include compressive strength; shear strength; impact strength and hardness. It also documents brake pads thermal stability and material degradation results. In Section two the braking performance, such as stopping distance, heat dissipation, noise level, wear rate and coefficient of friction is reported.

4.1 MECHANICAL PROPERTIES

[127]4.1.1 Compressive properties

The results of compressive test conducted on hybrid nanocomposite (HC), and commercial brake pad (CR) is shown in table 4.1. It was observed that the brake pads HC3 – HC12 exhibited superior compressive strength compared to CR. It can be seen that HC4 had an 80% higher strength than CR.

This improved compressive strength may be attributed to the interconnecting (carbon-carbon) C-C bond of the MWCNTs and NG. The transfer of atom and electron of these carbon based materials, formed a covalent bonding that enhanced the bond between carbon fiber and the epoxy matrix, which in turn improved strength. Similarly, the improved force resistance and load carrying capability of carbon fibers may be the reason for the increased strength shown in table 4.2.

It was observed that HC1, HC2, HC3, HC4, HC7, HC8, HC9, and HC11 exhibited higher modulus values compared to CR; with HC 7 having a 28.7% modulus greater than that of commercial brake pad. This implied that the interconnecting (carbon-carbon) C-C bonding does not only improve the strength but also enhanced the stiffness of the HC brake pads. However, samples HC5, HC6, HC10, and HC12 have moduli values, which were lesser than CR. It is well known that the amounts of additive(s) in the composition of a material influences final properties [6, 126]. The lower modulus obtained from HC5, HC6, HC10 and HC12 as shown in Table 4.5 may be as a result of high-loading of carbon fiber and graphite nanoparticle in these formulations.

Table 4.1: Compressive properties of hybrid nanocomposite and commercial pads:

Hybrid nanocomposite samples	Compressive strength (MPa)	Remarks (%)	Compressive modulus(GPa)	Remarks (%)
CR	918	-	1.917	-
HC1	725.4	-21	2.218	16
HC2	789.8	-14	2.035	6
HC3	1128	23	2.459	28.2
HC4	1656	80	1.948	3
HC5	1077	17	1.73	-9.7
HC6	988	8	1.709	-10.8
HC7	1409	53	2.469	28.7
HC8	1481	61	2.014	5
HC9	1277	39	2.016	5.1
HC10	981	7	1.668	-12.9
HC11	1409	53	2.155	12.4
HC12	1112	21	1.554	-18.9

As illustrated in Figure 4.1, it was observed that each brake pad formulation had different compressive strength. The relationship between the amount and type of constituent influences the strength of the composite and hence determines final properties [4]. Considering this factor, inconsistent compressive strength shown in Figure 4.1, may be attributed to the different amount of additives in the formulation of each brake pad. Although, all the carbon based ingredient selected has good mechanical properties but high-loading of these additives deteriorates final material properties. Therefore, the higher-loading of graphite nanopowder resulted in lesser compressive strength obtained from HC5, HC6. HC10 and HC12 compared to that of HC4. Due to the variance in applied loads, certain resistance is required. In other words, better bonding of brake pad additives influenced the strength.

The compressive strength of 10% carbon fiber filled HC brake pad improved with a corresponding increase in carbon nanotube content. Despite the increase in carbon fiber content for brake pads HC7– HC12, HC4 still exhibited a higher strength. This implied that HC4 had a better force resistance compared to other hybrid nanocomposite and commercial brake pads. Agglomeration caused by high-loading of carbon fiber in HC7– HC12 brake pads may have affected their structural formation. This agglomeration created high localized stresses in the composite that often generate cracking during the test, leading to a premature fracture. The damage that

occurred as a result of the compressive stress, accompanied by failure, were brake pad additives delamination and fracture. Despite the increase in carbon fiber loading in brake pads HC7– HC12, HC4 still had the highest compressive strength. This implied that HC4 had a superior force resistance compared to other hybrid nanocomposite and commercial brake pads. The large amount additives in HC brake pad affected their structural behaviors. The agglomeration of additives created high localized stresses in the matrix created cracking during the compressive test, leading to premature fracture. The damage that occurred as a result of the compressive test, accompanied by failure, were brake pad additives delamination and fracture.

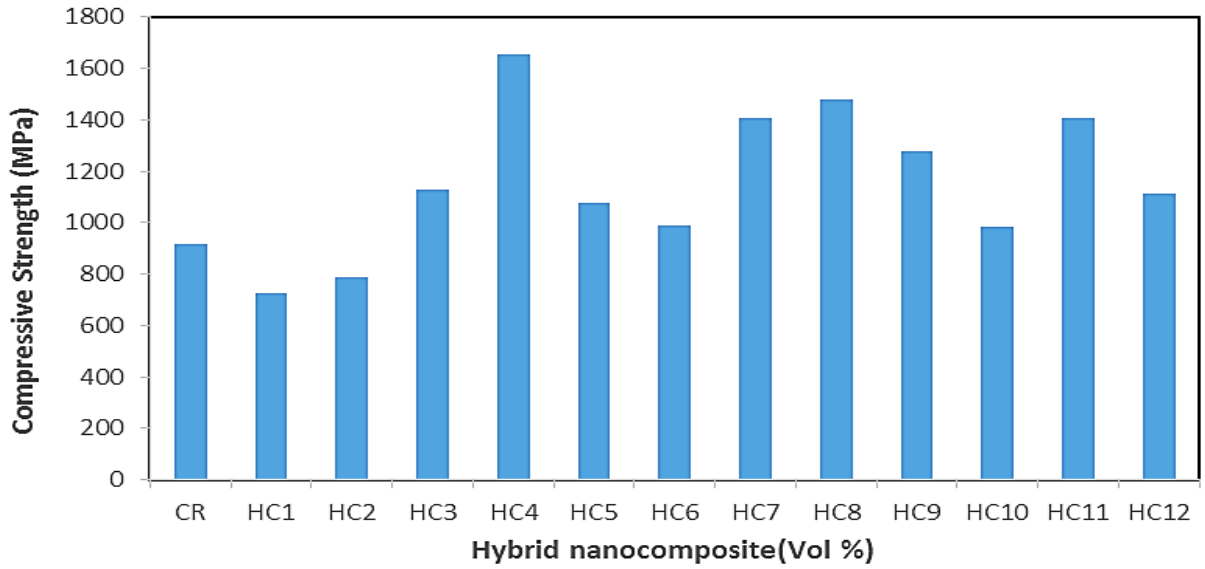

Figure 4.1: Compressive strength of hybrid nanocomposite and commercial brake pads

The compressive modulus obtained from the linear portion of the engineering stress vs strain bars were plotted against the different formulation of HC brake pads and CR were as shown in Figure 4.2. The result indicate that HC1, HC2, HC3, HC4, HC7, HC8, and HC11 brake pads exhibited higher elastic modulus compared to CR. HC13 had a modulus that was about 77% higher than that of CR. This may be attributed to the uniform dispersion of carbon fiber, carbon nanotube, and graphite nanopowder.

This constituent formed a synergistic interconnecting bond with the matrix, acting in concert to produce a more stable structure resulting in a better stiffness.

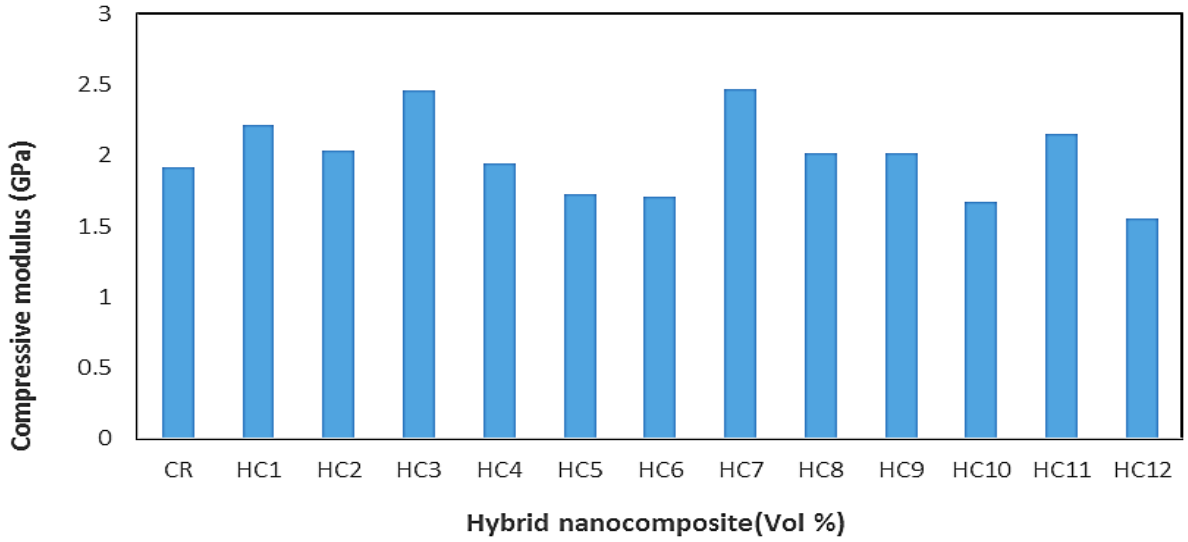

Figure 4.2: Compressive modulus of hybrid nanocomposite and commercial brake pads.

However, the compressive strains of HC2, HC3, HC11, and HC12 lower than that of the commercial pad has observed in Figure 4.2. The brittleness behavior of these set of HC brake pads at additives loading caused quick fracture of the material during the test.

4.1.2 Shear strength

Shear strength values for hybrid nanocomposite and commercial brake pad were measured using a shear tool. Five specimens were tested, average value of the five specimens is shown in Table 4.2. It was observed that all hybrid nanocomposite brake pads had higher shear strength than that of the commercial brake pad (3.706 MPa). Although HC brake pads have improved shear strength than commercial brake pad, both types of brake pad seem to have superior shear strength compared to the standard shear strength (2.10 MPa) for brake pad at room temperature [122, 123]. HC9 with higher shear strength of 17.645 MPa, offered better improvement of 376% compared to the commercial brake pad.

Table 4.2: Shear properties of hybrid nanocomposite and commercial pads

Hybrid nanocomposite samples	Mean Shear strength(MPa)	Remarks (%)
CR	3.706	-
HC1	11.078	198.9
HC2	11.370	206.7
HC3	13.737	270.7
HC4	15.050	306.1
HC5	11.352	206.1
HC6	11.250	203.5
HC7	16.629	348.7
HC8	15.672	322.8
HC9	17.645	376.1
HC10	9.1079	145.7
HC11	11.661	214.6
HC12	11.146	200.7

Figure 4.3 presents a variation of load against displacement for hybrid nanocomposite and commercial pads. It is notable that the brake pad formulation determined the shear strength properties. The increase in strength was observed from HC1 to HC3 by 24 % as loading of carbon nanotube increased from 0.1-0.3 %.vol. The same trend was also observed from HC7 to HC9. This indicated that the addition of carbon nanotube increased interfacial bonding of the material, which resulted in strength improvement [128]. However, increase in graphite nanopowder loading (from 1 to 3 %.vol) reduced the shear strength of some HC brake pads formulation. This may be a result of a large amount of graphite nanopowder, softening the HC brake pad, which in turn reduced resistance to shear stress [66].

It is well-known that the agglomeration of additives causes high-stress concentration on composite material. This often affects material properties, which eventually reduces the strength [67]. The decrease in shear strength HC5, HC6, HC10, HC11, and HC12 brake pad may be attributed to the agglomeration of the high loading of the additives.

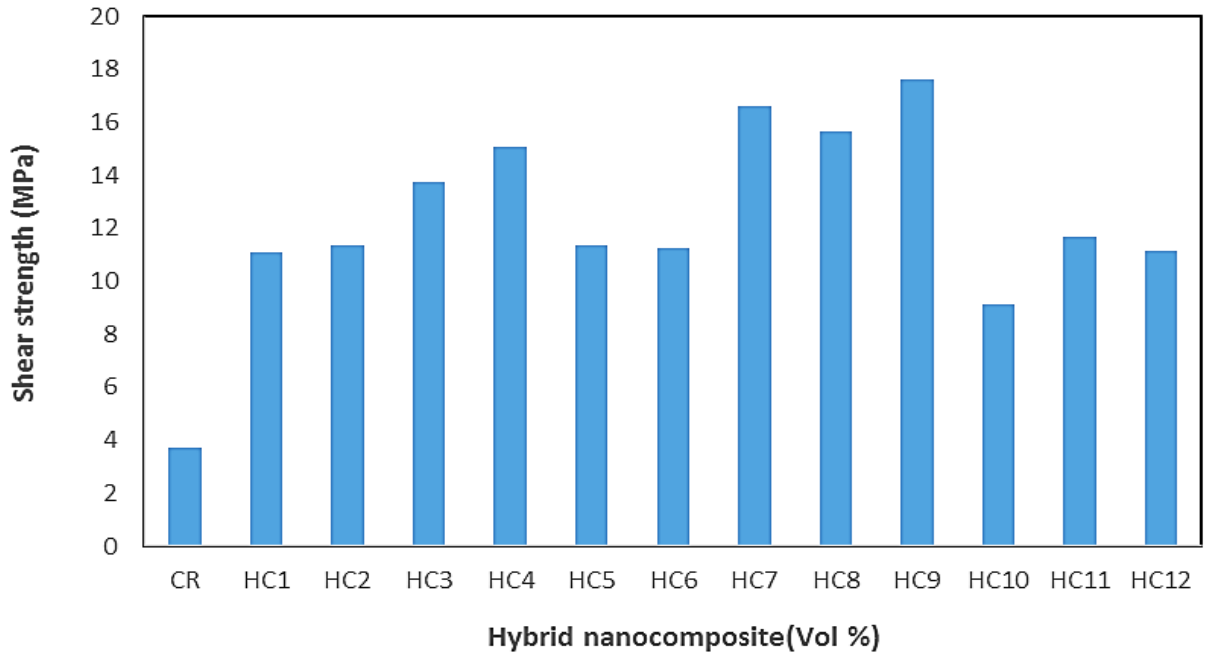

Figure 4.3: Shear strength of hybrid nanocomposite and commercial pads.

To have better understanding of the brake pads failure mode, their fracture surfaces were observed under SEM to analyze the functions of fillers as a related to their shear properties and fracture behaviors. Shear part of hybrid nanocomposite and commercial brake pad specimen were glued together after MTS machine had detected a break and stopped. However, crack was observed on the side that was stressed. The cracked section was separated to analyse shear fractured and to determine brake pad shear mechanisms. A lesser amount of fiber can be seen in figure 4. 3a, this indicated that CR had a lower content of fibers.

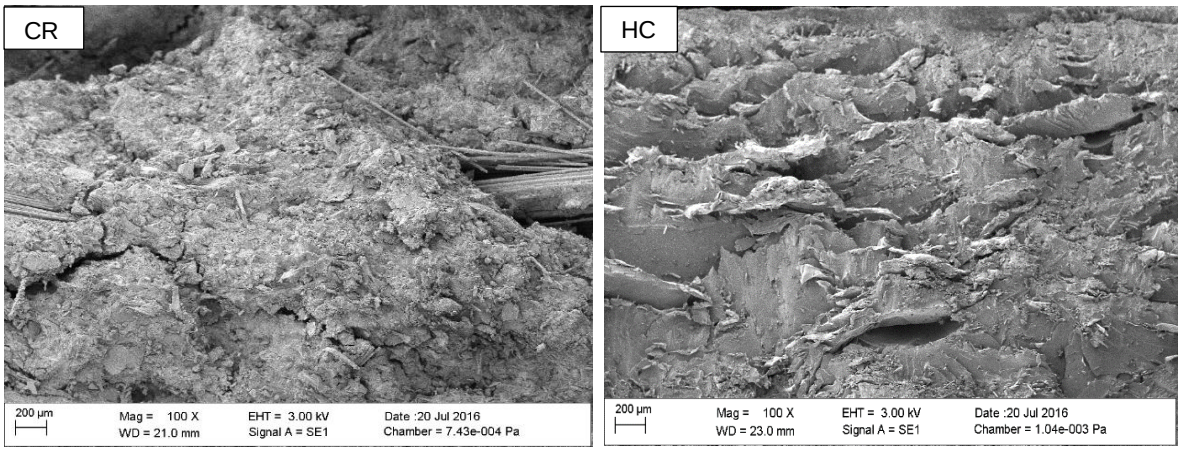

Figure 4.4: SEM micrograph showing shear fracture surface of (a) commercial brake pad (CR) and (b) hybrid nanocomposite (HC) brake pad

Bunch of fibers can also be seen on CR micrograph. This feature indicated inhomogeneous dispersion of the fiber in the matrix/fillers. Additionally, the combination of constituents used for commercial brake pad seemed not uniformly mixed, as fibers were separated from the matrix/additives. Poor connectivity of these constituents may be the cause of brittle fracture and cracks shown on the commercial brake pad shear surface. In this case, the increase in loading resulted in cracks extension, which reduces shear strength. However, this was not occurred in the case of the HC brake pad. It is difficult to identify constituent of HC brake pads shown Figure 4. 4b. This shown a homogeneous dispersion of carbon-based additives. This uniform dispersion enhanced constituent bonding that formed interlocking features shown in Figure 4.4b. This, therefore, created better load carrying mechanism, which in turn reduced additives disintegration and enhance shear strength.

4.1.3 Impact properties

The impact strength of HC brake pads and CR measured on Charpy impact tester was as recorded in Table 4.3. The impact strength of developed and commercial brake pad is illustrated in Figures 4.4. It was noted that the HC brake pad had improved impact resistance than the commercial brake pad except for HC6, HC8, and HC12 that was on the contrary. The decrease in impact strength of HC6, HC8, and HC12 may be as a result of the agglomeration formed by high-loading of graphite nanopowder. The impact resistance of HC brake pads varied with their formulation. HC9 has a higher impact resistance of 49.9 KJ/m^2, which was 184% superior compared to 17.6 KJ/m^2 obtained from commercial brake pad. It clearly shown that HC4 and HC9 exhibited an impact strength that over 100% higher than CR. Moreover, Chand N et al. reported that the standard impact strength for brake pad ranges from 11.5 – 15.4 KJ/m^2. This implied that both types of pads have an improved strength for better shock resistance.

The enhancement in impact strength may be attributed to the interconnecting bond formed by additives, which eventually improved energy -absorbing ability.

Table 4.3: Impact strength of hybrid nanocomposite and commercial pads

Hybrid nanocomposite samples	Impact strength(KJ/m²)	Remarks (%)
CR	17.6	-
HC1	19.6	11.4
HC2	17.7	0.6
HC3	30.4	72
HC4	41.4	135
HC5	34.2	94.3
HC6	8.7	-50
HC7	26.1	48
HC8	12.8	-27
HC9	49.9	184
HC10	28.1	60
HC11	44.5	153
HC12	12.8	-27

HC4 and HC9 exhibited an impact strength that was over 100% higher than commercial brake pad. The significant enhancement in impact strength can be attributed to the interconnecting bond formed by additives.

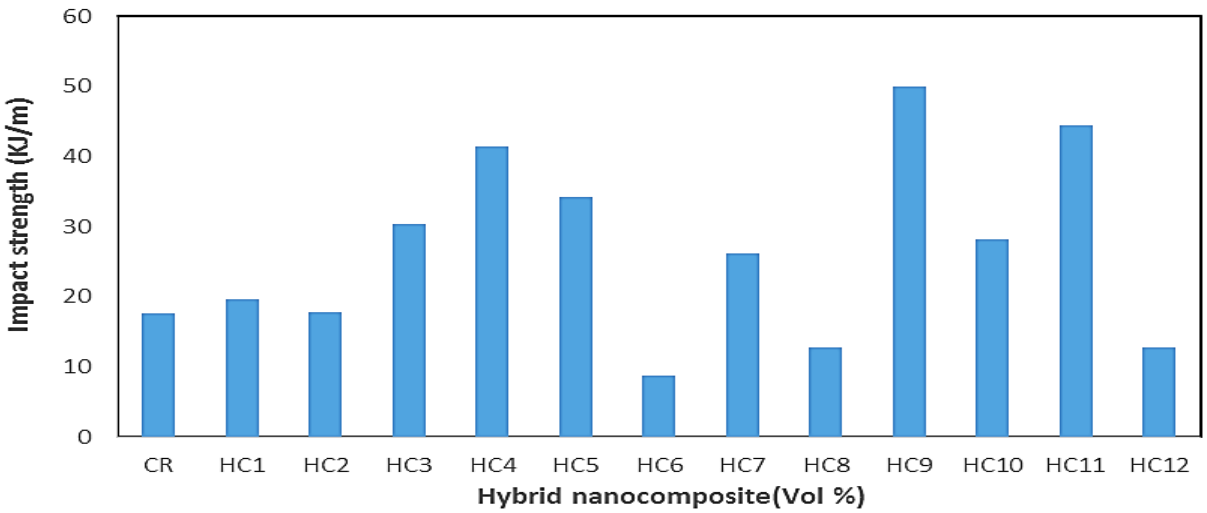

Figure 4.5: Impact fracture resistance of HC and CR

Scanning electron microscopy study was subsequently performed to determine the impact failure mechanism of the brake pad. Figure 4.17 shows the SEM micrograph taken for commercial and hybrid nanocomposite brake pad. The fracture surface of

the commercial brake showed constituent disintegration, porosity, and surface degradation, leaving CR impact surface with cracks. This suggested a brittle failure and in consistent with the impact value recorded in Table 4.4. However, the reverse was the trend for HC brake pads, as the fractured parts are together, with tough fracture surfaces. Similarly, homogenous dispersion of carbon fiber, supporting impact stress resistance was also seen. This enhances HC brake pads inner toughness resulted in better fracture resistance.

Microcracks and surface degradation were observed on HC1, HC8, HC10, and HC12 as shown in Figure 4.6. These may be a result of either fiber-matrix or additives agglomeration at a spot in the matrix, which in turn led to delamination and drop in HCs brake pads strength. When the loading of fiber is increased the fiber-fiber interface decreases, and the matrices between the fibers are often patched and broken off, then the crack grows along the fiber surface. Consequently, this reduced the impact strength as shown in Table 4.4.

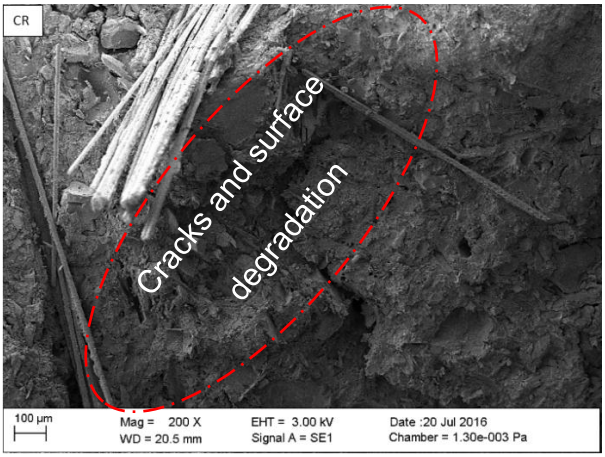
CR
Cracks and surface degradation
100 µm
Mag = 200 X
WD = 20.5 mm
EHT = 3.00 kV
Signal A = SE1
Date :20 Jul 2016
Chamber = 1.30e-003 Pa

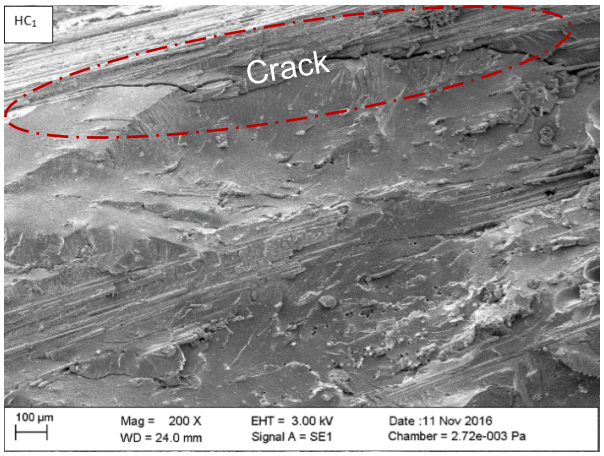
HC1
Crack
100 µm
Mag = 200 X
WD = 24.0 mm
EHT = 3.00 kV
Signal A = SE1
Date :11 Nov 2016
Chamber = 2.72e-003 Pa

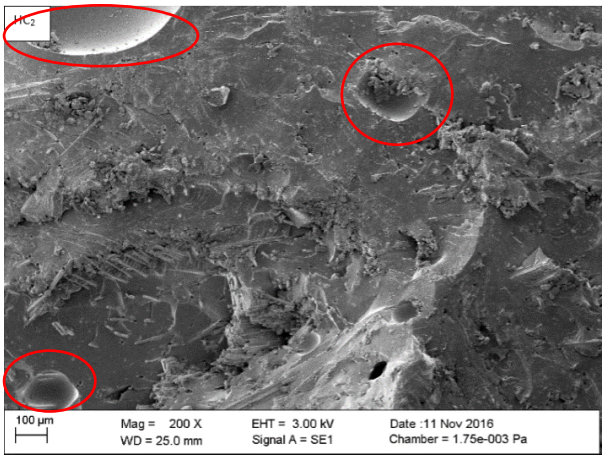
HC2
100 µm
Mag = 200 X
WD = 25.0 mm
EHT = 3.00 kV
Signal A = SE1
Date :11 Nov 2016
Chamber = 1.75e-003 Pa

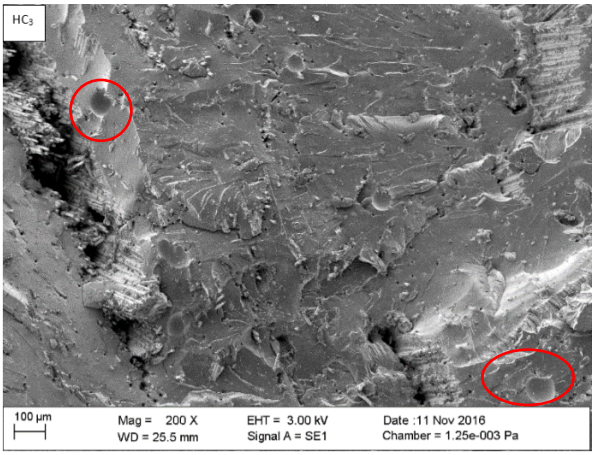
HC3
100 µm
Mag = 200 X
WD = 25.5 mm
EHT = 3.00 kV
Signal A = SE1
Date :11 Nov 2016
Chamber = 1.25e-003 Pa

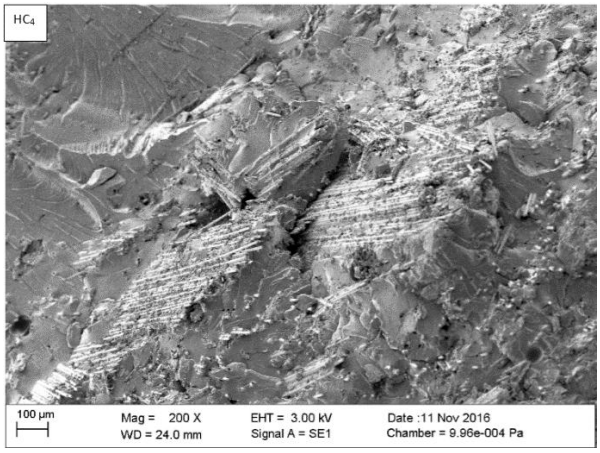
HC4
100 µm
Mag = 200 X
WD = 24.0 mm
EHT = 3.00 kV
Signal A = SE1
Date :11 Nov 2016
Chamber = 9.96e-004 Pa

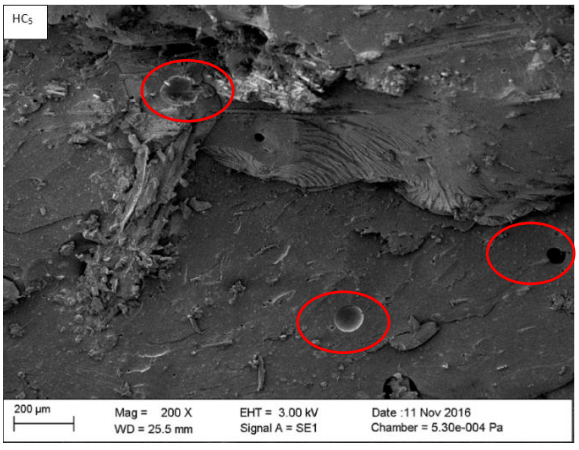
HC5
200 µm
Mag = 200 X
WD = 25.5 mm
EHT = 3.00 kV
Signal A = SE1
Date :11 Nov 2016
Chamber = 5.30e-004 Pa

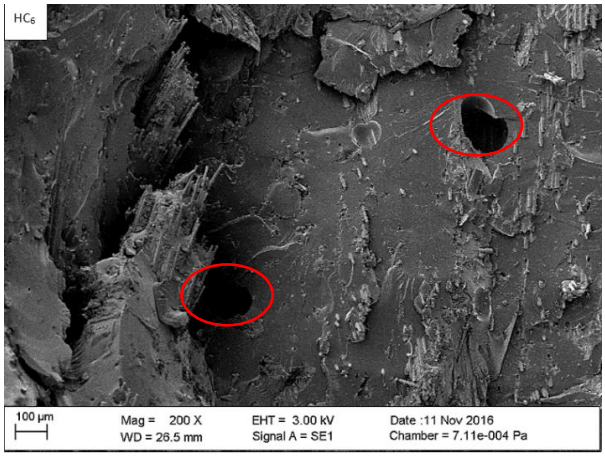
HC6
100 µm
Mag = 200 X
WD = 26.5 mm
EHT = 3.00 kV
Signal A = SE1
Date :11 Nov 2016
Chamber = 7.11e-004 Pa

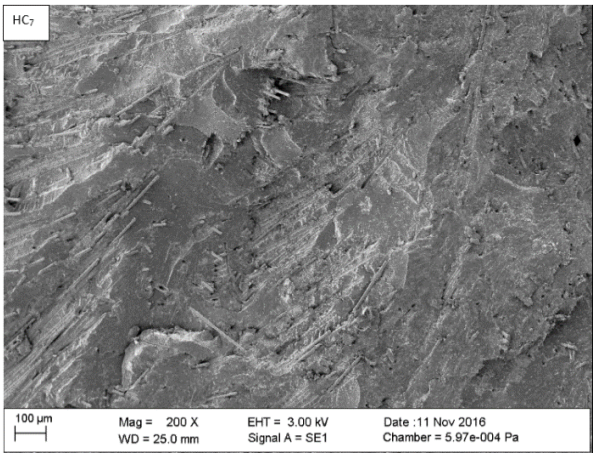
HC7
100 µm
Mag = 200 X
WD = 25.0 mm
EHT = 3.00 kV
Signal A = SE1
Date :11 Nov 2016
Chamber = 5.97e-004 Pa

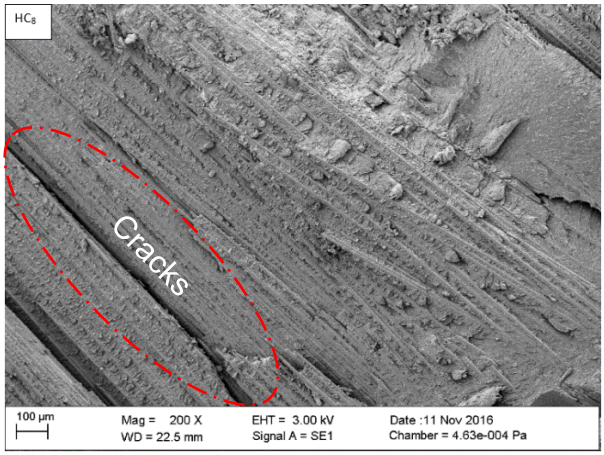
HC8
Cracks
100 µm
Mag = 200 X
WD = 22.5 mm
EHT = 3.00 kV
Signal A = SE1
Date :11 Nov 2016
Chamber = 4.63e-004 Pa

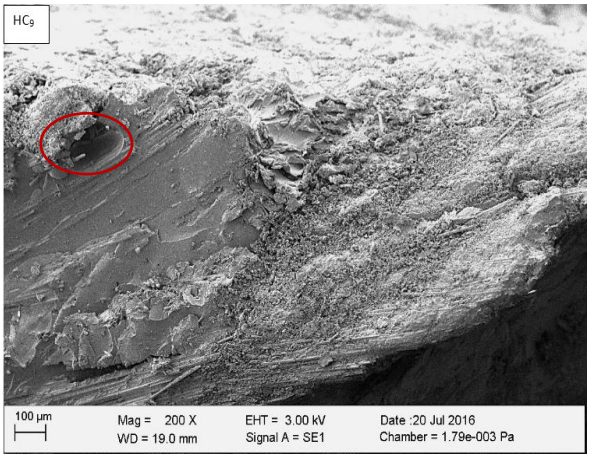
HC9
100 µm
Mag = 200 X
WD = 19.0 mm
EHT = 3.00 kV
Signal A = SE1
Date :20 Jul 2016
Chamber = 1.79e-003 Pa

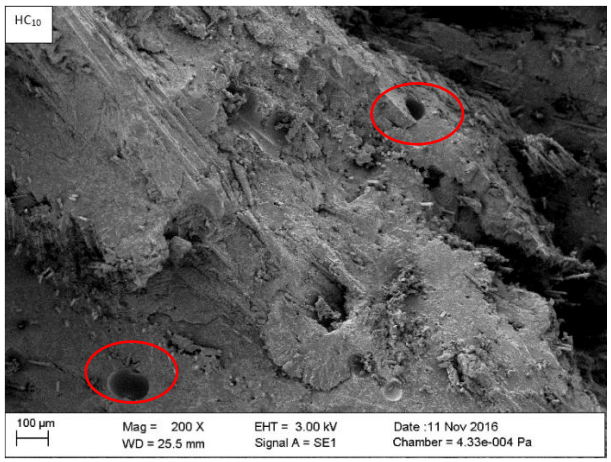
HC10
100 µm
Mag = 200 X
WD = 25.5 mm
EHT = 3.00 kV
Signal A = SE1
Date :11 Nov 2016
Chamber = 4.33e-004 Pa

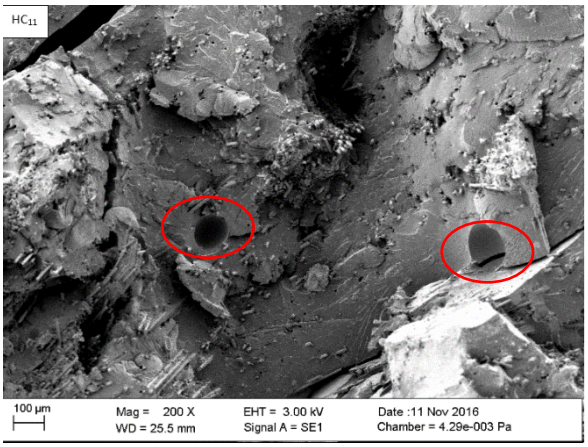
HC11
100 µm
Mag = 200 X
WD = 25.5 mm
EHT = 3.00 kV
Signal A = SE1
Date :11 Nov 2016
Chamber = 4.29e-003 Pa

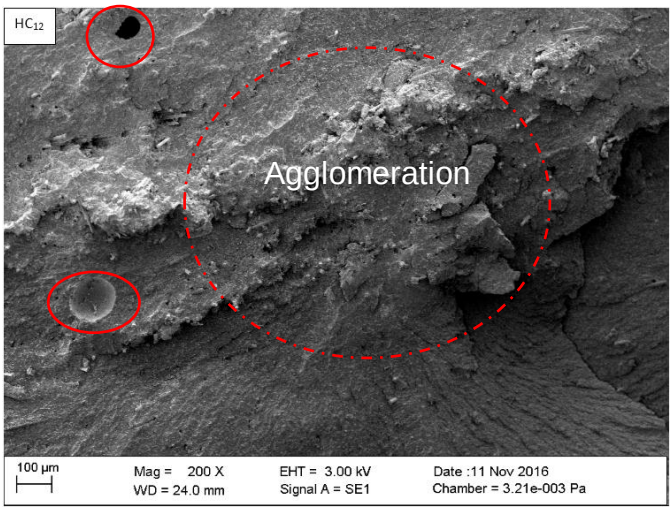

Figure 4.6: SEM micrograph showing impact fracture surfaces of the brake pads. The unlabelled circles in the diagram are indicating porosity.

It can be seen that HC4, HC7, and HC9 shown a relatively and tough fractured surface with a homogeneous mixture of constituents infused together. This structural formation increased interfacial bonding of carbon-carbon constituents, which was in agreement with the superior impact resistance recorded in Table 4.4.

In this regard, the total energy required to break HC brake pad was assumed to be as a result of the interfacial bond existing between the binder and other additives. Therefore, the increase in fracture resistance at which HC pad broke may be attributed to the better load carrying properties of carbon fiber, adhesive qualities of the binder and synergistic functions of the carbon-based constituents.

4.1.4 Hardness properties

The hardness values of the developed and commercial brake pad was as recorded in Table 4.4. The variation of the hardness reported was distinct for each formulation. In this regards, as expected, the different formulation of the brake pads offered different hardness values as shown in Table 4.4. Furthermore, HC7 and commercial brake pad have the same hardness values, which indicated that their surface toughness is equal. The agglomeration of graphite nanopowder in HC10, HC11, and H12 formulation resulted in slight dropping in hardness properties.

This trend is consistent with Rukiye et al [74] study, where high graphite content caused a reduction in brake pad hardness. The hardness value of CR was 37.3 Hv.

This was approximately 10% higher than the hardness values obtained from almost all the nanocomposite brake pad formulations except for HC7, HC8, and HC9.

Table 4.4: Hardness properties of hybrid nanocomposite and commercial pad

Hybrid nanocomposite samples	Hardness	Remarks (%)
CR	37.3	-
HC1	32.3	-13.4
HC2	30.4	-18.5
HC3	34.6	-7.2
HC4	34.9	-6.4
HC5	33.7	-9.6
HC6	35	-6.1
HC7	37.3	-
HC8	39.1	4.8
HC9	41.1	10
HC10	32.2	-13.6
HC11	36.1	-3.2
HC12	37.8	1.3

Loading and homogeneous dispersion of ceramic additive (silicon carbide) in CR resulted in high hardness properties shown in Figure 4.5. However, HC9 and HC12 with a hardness value of 39.1 Hv, 41.1 Hv, and 39.1 Hv respectively are higher compared with the CR hardness value. HC8, HC9, and HC12 superior hardness can be attributed to carbon fiber and carbon nanotube loading. Consequently, HC8, HC9, and HC12 hardness values are worth noticing as they have better surface toughness compared to the commercial brake pad.

It can also be seen that the hardness properties for both the HC and CR brake pads were statistically comparable.

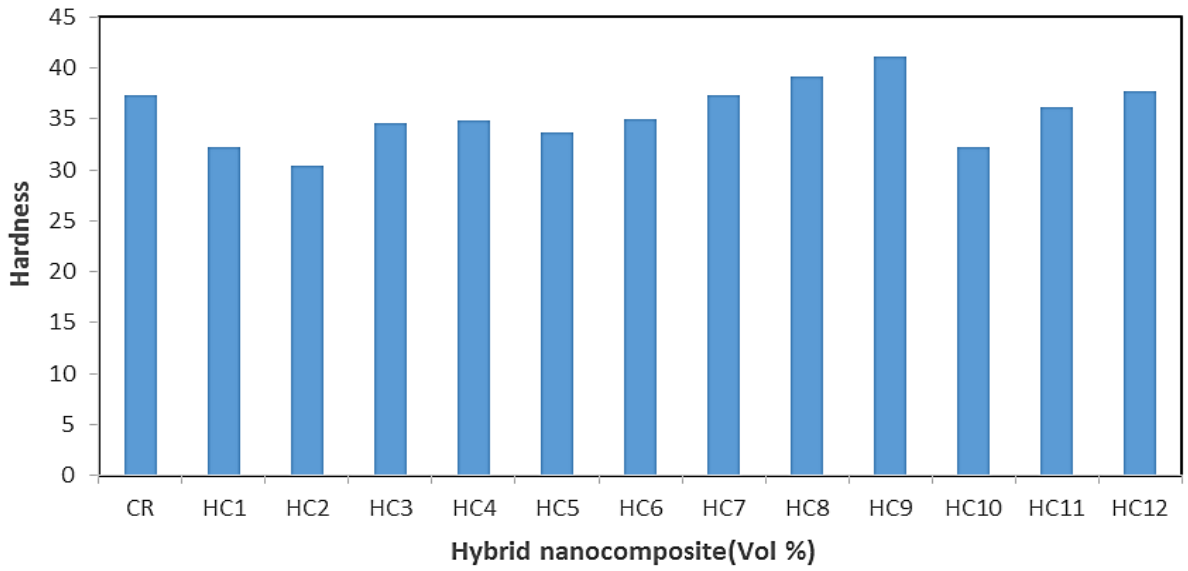

Figure 4.7: Hardness properties of hybrid nanocomposite and commercial pads

As insignificant different in hardness of HC brake pad with the same loading of carbon fiber suggested a consistent processing of the HC brake pad. However, some brake pads can be materially tougher than others when measuring their surface hardness. This resulted in the variation of HC brake pads hardness values. This trend is in line with previous studies, where formulation and processing consistency determined hardness [129].

4.2 THERMAL PROPERTIES

4.2.1 Thermo-gravimetric analysis (TGA)

Brake pads thermal stability, and degradation studied using thermogravimetric analysis (TGA) procedure was as shown in Figure 4.5. It was observed that the CR had better thermal stability and degradation temperature than the HC brake pad. This performance may be attributed to the inherent thermal properties of ceramic and metallic fillers in CR formulation. Figure 4.5, also shown that the weight loss raised with a corresponding increase in temperature.

As seen from the figure, the decomposition temperatures varied with a different formulation. This indicated that the graphite nanoparticle loading has an effect on the decomposition temperature of HC brake pads. It is well clear that HC brake pad with 3 vol. % amount of graphite nanopowder exhibited better degradation than those with 1 vol. %. However, carbon nanotube loading showed a positive effect on HC brake

pads with 10 vol.% of carbon fiber and 1 vol.% of graphite nanopowder as thermal stability improved with a corresponding increase in carbon nanotube content.

The first weight loss up to 100^0C correspond to the heat of vaporization of water in the sample. The second weight loss at about, 330^0C was due to thermal depolymerization of hemicellulose and the cleavage of glucosidic linkages of cellulose [130]. The third weight loss at about, 450^0C is due to the further breakage of the decomposed product of stage II leading to the formation of tar through levoglucosan [131]. It was found that the thermal decomposition of cured materials was independent of cure temperature.

The Tg of the TGA which was the temperature at which the mass was volatilized provides a good idea of the thermal stability. It shows a shift of the weight loss toward higher temperature for the HC brake pad. The TGA curves demonstrated that the incorporation of carbon-carbon additives in the resin-matrix gave significant improvement to the thermal stability of the material, however, CR had a superior thermal stability.

At temperatures higher than 450°C by the cross-over between degradation curves, an increase in the thermal stability was observed HC11 and HC12 with a larger amount of carbon-carbon additives becoming so predominant in the thermal stability. This enhancement in the thermal stability can be attributed carbon-based additives thermal properties, which hindered the diffusion of volatile decomposition product from the matrix. This agreed with Krump et al and Duquesne et al [127, 128] report where volatile degradation products adsorbed from the surface of the material improved thermal stability.

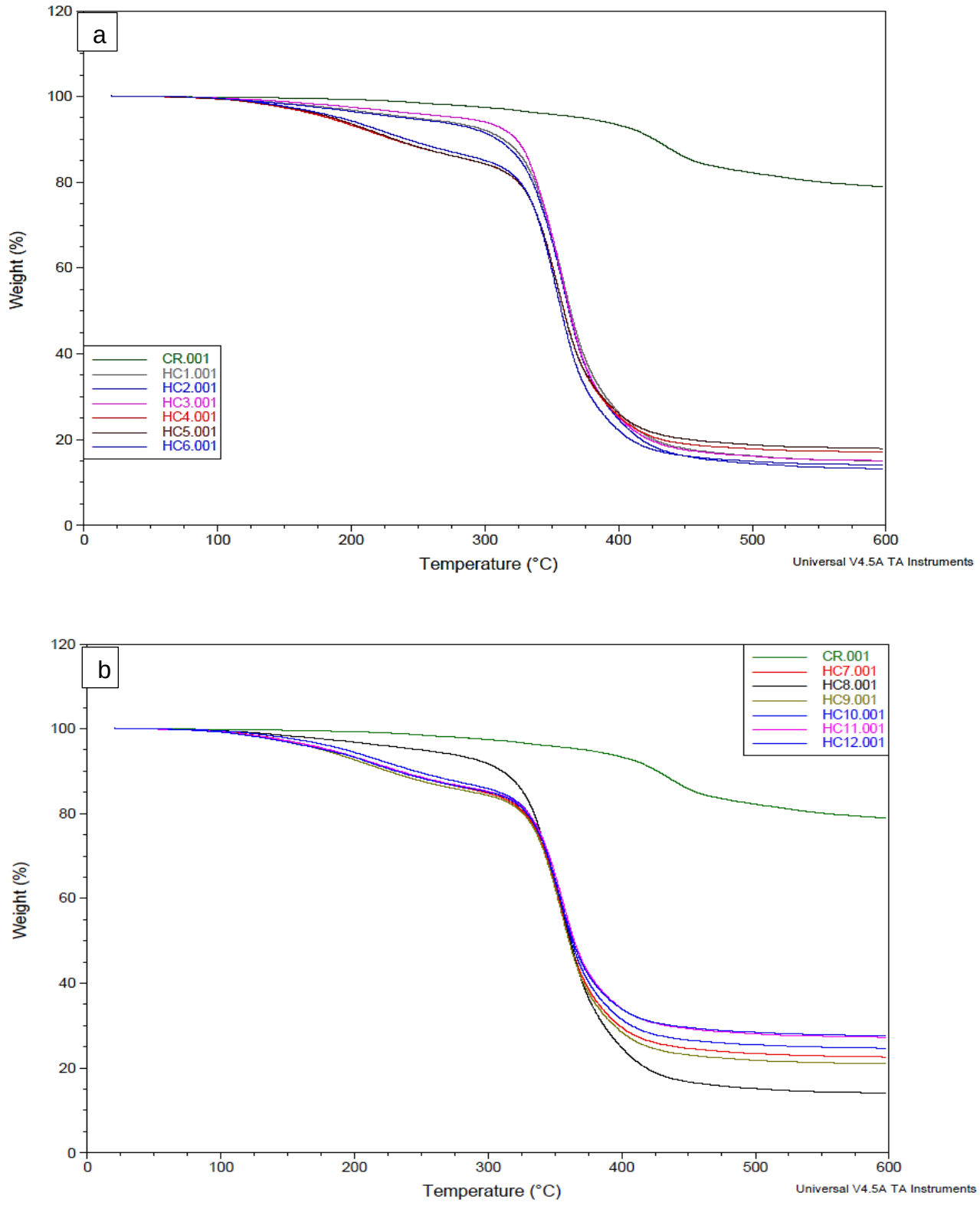

Figure 4.8: Hybrid nanocomposite and commercial brake pad TGA thermogram curve. (a) Hybrid nanocomposite with 10 vol.% of carbon fiber and (b) hybrid nanocomposite with 20 vol.% of carbon fiber.

Thermal degradations taken from 100% to final weight loss were as recorded in table 4.5. This was obtained at three different Tg (%) for HC brake pads and CR.

Table 4.5: Thermal degradation parameter of commercial and developed brake pad

Material		Weight loss (°C) T_g			Average T_g (°C)
		T_{100} (°C)	T_{310} (°C)	T_{410} (°C)	
Hybrid nanocomposite	CR	0.17	2.18	7.62	3.32
	HC_1	0.36	9.36	76.85	28.86
	HC_2	1.52	10.28	78.46	30.08
	HC_3	0.34	7.16	77.66	28.39
	HC_4	0.61	16.95	77.08	31.55
	HC_5	0.56	16.86	76.30	31.24
	HC_6	0.69	16.31	73.74	30.24
	HC_7	0.63	16.33	72.45	29.80
	HC_8	0.47	9.98	78.30	29.58
	HC_9	0.69	16.75	73.74	30.39
	HC_{10}	0.49	15.21	70.51	28.74
	HC_{11}	0.76	15.77	67.91	28.15
	HC_{12}	0.84	15.86	67.86	28.19

From Table 4.5; it can be clearly seen that the thermal stabilities of the HC brake pads are lesser than that of CR. The thermal stability of the HC brake pads can be related to organic nature of the constituents used.

4.2.2 Differential Scanning Calorimetry (DSC)

The thermal analysis of brake pads evaluated by power compensation DSC is as seen in Figure 4.8. Heat flow versus temperature curve regarding different brake pad formulations was as illustrated. The slope of the thermogram curves for brake pad was determined with respect to the heating rate.

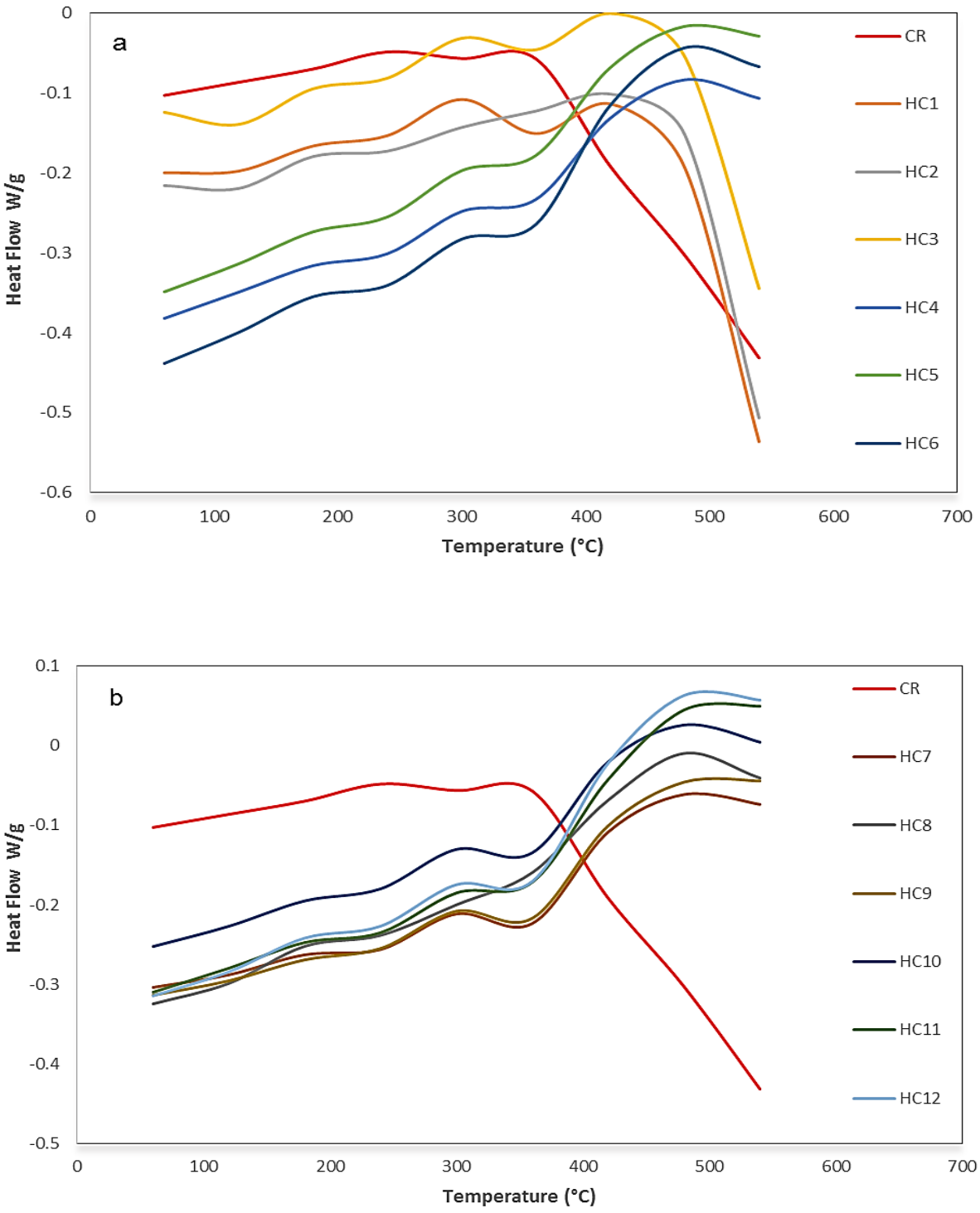

Figure 4.9: DSC thermogram curve showing Heat flow vs. Temperature for (a) 10 vol. % of carbon fiber reinforced HC brake pads and (b) 20 vol. % of carbon fiber reinforced HC brake pads

The baseline of the slopes of the DSC on the differences between the heat capacity of the samples and the references evidenced that the HC brake pad has low heat build-up rate during the heating process. This implied that carbon-based additive in HCs reduced the accumulation of heat under the loading conditions. The thermograph for HCs showed a broader peak as compared with CR, indicating the uniform mixing HC brake pads components.

The degradation temperature for HCs was as a function of formulation and significantly higher (bout 50%) to that of CR. The degradation temperature obtained from HC4 to HC12 was 535˚C, however, that of HC1 to HC3 were lower by 35%. This thermal performance may be attributed to the amount and uniform dispassion of carbon-based additives.

4.3 ABSORPTION PROPERTIES

4.3.1 Water absorption

Water absorption rate of the brake pad is as shown in Table 4.6. and illustrated in Figure 4.9. It can be seen that both brake pads exhibited low water absorption rate ranging from 0.01-0.36%. This trend was lesser than the water absoption rate value of the brake pad (5.03) reported by Dagwa *et al.* and 5-9% reported by Mayowa *et al.* [3, 94]. However, Figure 4.9 clearly show that the HC brake pads exhibited lower moisture absorption rate (0.1-0.33) than that of the commercial brake pad (0.36). The brake pad samples HC3 and HC6 exhibited water absorption rate of 0.012 % and 0.01 % respectively. These water absorption rates were about 100% lesser than that of the commercial brake pad.

This significant reduction can be as a result of the carbon-carbon component hydrophobic nature, and the interconnecting bond formed by the additives. It may also result from the closer packing of the carbon-carbon additives, resulting in a stronger binding, which barely allows water penetration [3]. The higher rate of moisture in the commercial may result from the poor compatibility of friction ingredient and porosity.

Table 4.6: Water absorption rate of commercial and developed brake pad

Hybrid nanocomposite samples	Water absorption (%)	Remarks (%)
CR	0.36	-
HC1	0.048	87
HC2	0.14	61
HC3	0.0129	96
HC4	0.128	64
HC5	0.15	58
HC6	0.01	97
HC7	0.11	69
HC8	0.22	39
HC9	0.11	69
HC10	0.136	62
HC11	0.13	64
HC12	0.33	8.3

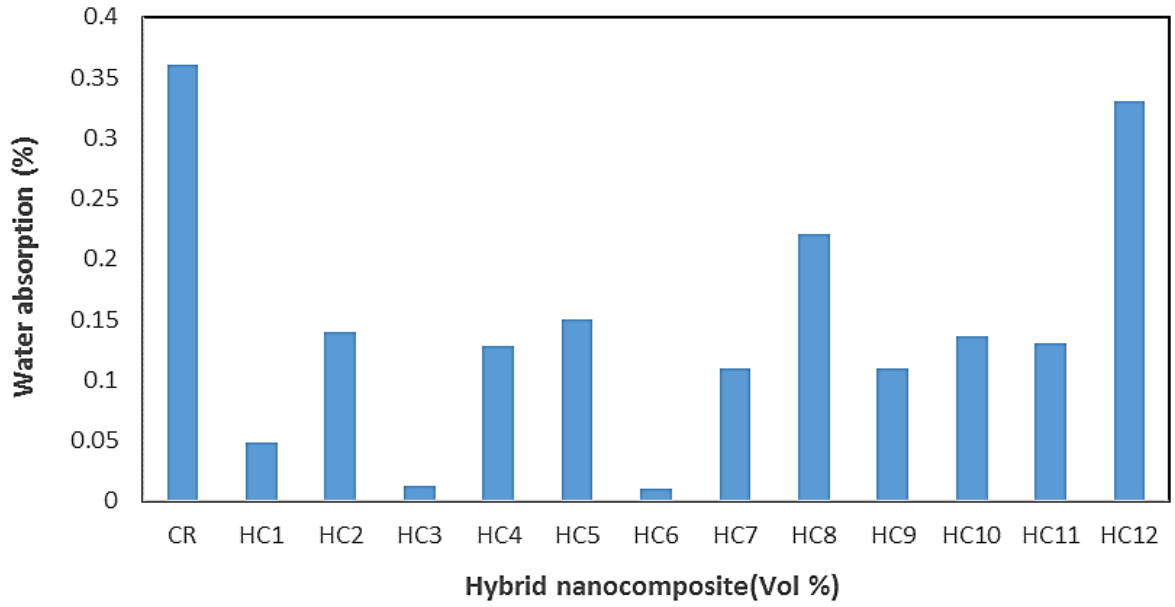

Figure 4.10: Graph showing water absorption rate of hybrid nanocomposite and commercial brake pad.

The water absorption rates for HC brake pads, including the commercial pad compared well with the standard values of 0-4% for commercial brake pads [17].

According to Kim *et al.* [15], water absorption increases brake pad weight and thickness, which eventually reduces mechanical properties of the brake pad such as hardness and compressibility. This suggested that low moisture absorption rate of hybrid nanocomposite brake pad prevents variability of performance phenomena such as the coefficient of friction, which correspond with the coefficient of friction reported in Figure 4.13.

4.3.2 Oil absorption rate

The rate of oil absorption for HC brake pads alongside CR was presented in Table 4.7. It shows that the oil absorption rate varied with brake pad formulations. Both pads exhibited lesser absorption than 2.34% reported by Mayowa .A. *et al.* They also compared well with 0.44% reported by Dagwa *et al.* [3, 94]. However, most of the HC brake pads absorb lesser oil than CR under the same condition. HC1 has a lower oil absorption rate of 0.01 %, which was 98% better than to 0.5 % obtained from CR.

Table 4.7: Oil absorption rate of commercial and developed brake pad.

Hybrid nanocomposite samples	Oil absorption (%)	Remarks (%)
CR	0.5	-
HC1	0.01	98
HC2	0.3	40
HC3	0.15	70
HC4	0.19	62
HC5	0.6	-20
HC6	0.1	80
HC7	0.25	50
HC8	0.9	-80
HC9	0.27	46
HC10	0.33	34
HC11	0.62	-24
HC12	0.68	-34

This low absorption rate can be attributed to closer interfacial bonding of carbon-based material. However, the amount of oil absorbed by hybrid nanocomposite pads HC5, HC8, HC11, and HC12 were higher than commercial brake pad.

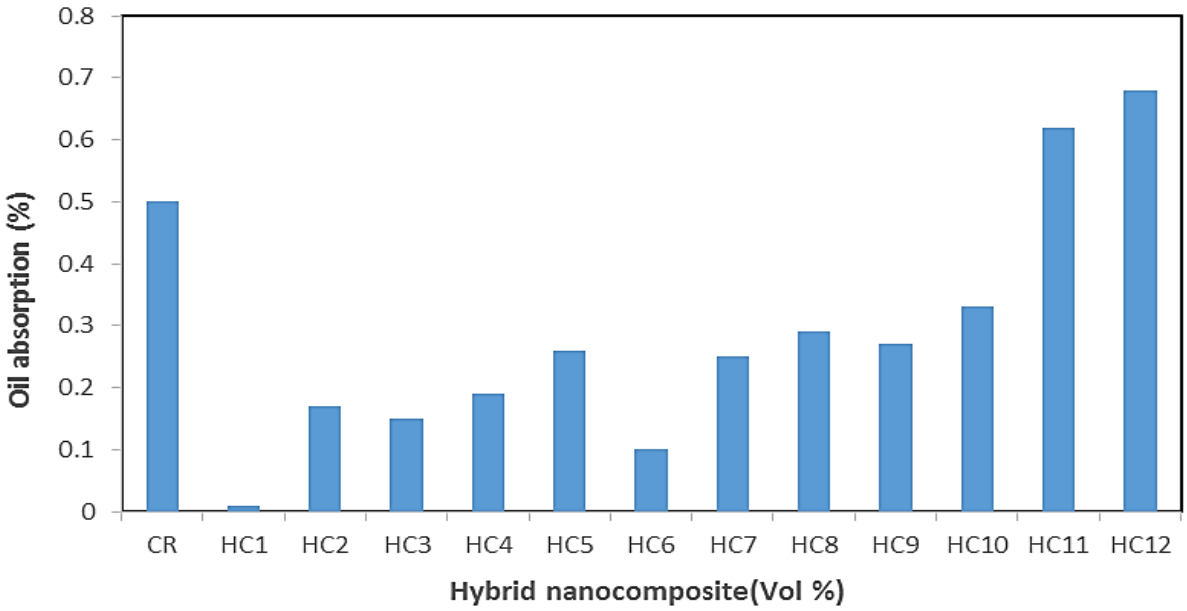

Figure 4.11: Graph showing oil absorption rate for hybrid nanocomposite and commercial brake pad.

The probable reason behind the increase in oil absorption may be due to the high loading of carbon fiber and graphite nanopowder. The increase in carbon-fiber concentration reduced the matrix between fibers interface. This generated pore holes that allowed the fluid flow. It is well known that graphite has a porosity that ranges from 0.7 – 53 %[132]. Therefore, an increase in oil absorption of hybrid nanocomposite pads can also be ascribed to graphite nanopowder loading.

4.4 BRAKING PERFORMANCE

The braking performance of HC and CR brake pads such as wear resistance, the coefficient of friction, noise level, interfacial temperatures and stopping distance measured using a dynamometer was reported in this section. This performance characterization was conducted under constant braking force of 1.38 KN and calculated as per equation 3.1. The brake pads wear rates and coefficient of friction measured at five different speeds was as recorded in Table 4.8.

Table 4.8: Brake pads wear rates and coefficient of friction

Hybrid nanocomposite samples	Wear rate (g/Nm) at different speed (m/s)					Coefficient of friction (μ) at different speed(m/s)				
	15.5	18.4	21.6	24.7	27.8	15.5	18.4	21.6	24.7	27.8
CR	1.07E-6	2.94E-7	2.92E-7	2.20E-7	3.59E-7	0.387	0.389	0.404	0.418	0.429
HC1	1.29E-7	9.52E-8	8.81E-7	7.04E-7	4.79E-7	0.378	0.380	0.395	0.409	0.419
HC2	1.43E-7	1.07E-7	7.40E-8	7.59E-8	5.83E-8	0.380	0.382	0.397	0.411	0.422
HC3	9.03E-8	1.11E-6	8.81E-7	7.51E-7	5.90E-7	0.380	0.382	0.397	0.411	0.422
HC4	7.19E-8	6.74E-8	5.78E-8	3.70E-7	3.27E-7	0.378	0.380	0.395	0.409	0.419
HC5	1.67E-7	1.07E-7	9.25E-8	7.23E-8	1.19E-6	0.378	0.380	0.395	0.409	0.419
HC6	8.99E-9	3.95E-8	4.47E-8	3.91E-8	3.27E-8	0.383	0.385	0.399	0.414	0.424
HC7	6.90E-8	5.58E-8	8.14E-7	1.10E-6	8.85E-7	0.378	0.380	0.395	0.409	0.419
HC8	2.15E-7	1.54E-7	1.17E-7	2.02E-6	1.68E-6	0.378	0.380	0.395	0.409	0.419
HC9	1.07E-7	7.71E-8	5.55E-8	5.64E-7	4.79E-7	0.383	0.385	0.399	0.414	0.424
HC10	5.11E-7	2.94E-7	2.31E-7	3.32E-6	2.12E-6	0.386	0.388	0.403	0.417	0.428
HC11	7.77E-6	5.39E-6	3.47E-6	2.69E-6	5.20E-6	0.383	0.385	0.399	0.414	0.424
HC12	2.85E-7	2.31E-7	3.96E-6	6.07E-6	3.59E-6	0.387	0.389	0.404	0.418	0.429

4.4.1 Wear rate

Figure 4.11 shows the variation of wear rate for HC and CR brake pads at five consecutive speeds. The relationship between brake pad formulations and wear rates was measured as a function of speed. It can be seen that the wear rate of CR reduced with a corresponding increase in the speed. This may probably due to the toughness and better thermal resistance of additives incorporated in CR. For HC brake pads, a random wear rate was observed for an increase in speed. It was also observed that the wear rates of HC1, HC2, H3, H7, HC8, HC9, and H10 were not responded to

increase in speed. These HCs brake pads exhibited a low wear rate of about 88.1%, 81.4%, 85.4%, 73.23%, 71.2%, 66.86 and 75.4%, respectively compared to CR.

This better wear resistant may be attributed to the quality of binder and homogenous distribution of carbon fiber in the matrix. Furthermore, the synergistic effect formed through carbon-based additives and the adhesion property of the epoxy resin offered superior components bonding that resists abrasion. This study is consistent with the result reported by Li *et al*. and Wang *et al*. [133, 134] in which incorporation of the fiber shown lesser wear rate.

As the speed increases, the relationship of wear rate and speed on HC4, HC5, HC6, HC11 and HC12 became noticeable. This set of HC brake pads exhibited a random wear rate with a corresponding increase in speed. This behavior may be due to slow build-up of thermal stress generated as sliding distance increases. It was further observed that HC1, HC2, H3 with of 10 wt. % carbon fiber and 1 wt. % of graphite nanopowder exhibited low wear rate than others, including the commercial brake pad.

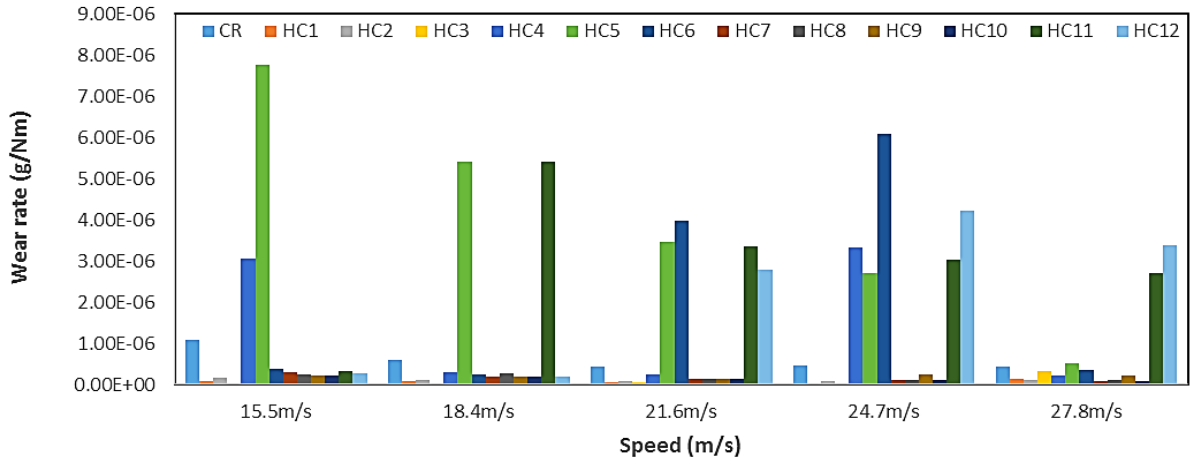

Figure 4.12: Bar charts showing wear rate of hybrid nanocomposite and commercial brake pad

This may be attributed to the homogenous dispersion of carbon fiber and the nanoparticle potential, resulted in effective wear resistance. This trend concurred with Friedrich *et al*., report where 10 wt. % of carbon fiber incorporation showed better wear resistance. It is well known that the addition of carbon nanotubes (CNTs) often enhanced composite mechanical and thermal properties. In this regard, the lower wear

rate exhibited by hybrid nanocomposite brake pad may be attributed to the synergistic functions of SCF, GN and MWCNTs, acting in concert to produce a coiled and more stabled structure resulting in high-strength, stiffness, improved heat absorption and tougher [39, 80, 127].

It has been reported that increase in speed increases rotor and brake pads contact [17, 135]. Consequently, the increase in wear rate of HC4, HC5, HC6, HC11, and HC12 may be due to the increase in contact between the brake pad and rotor as speed increases. This increase the frictional heat and impacted thermal inductive stress on the brake pad, leading to additives disintegration, which eventually caused the increase in wear rate.

4.4.2 Coefficient of friction (CoF)

The relationships of speed and coefficient of friction for brake pads were as reported in Table 4.8. The coefficient of friction as illustrated in Figure 4.12 varied with brake pads different formulation. This fictional output can be attributed to the loading of abrasive filler and friction modifier in the brake pad material formulations [4, 38].

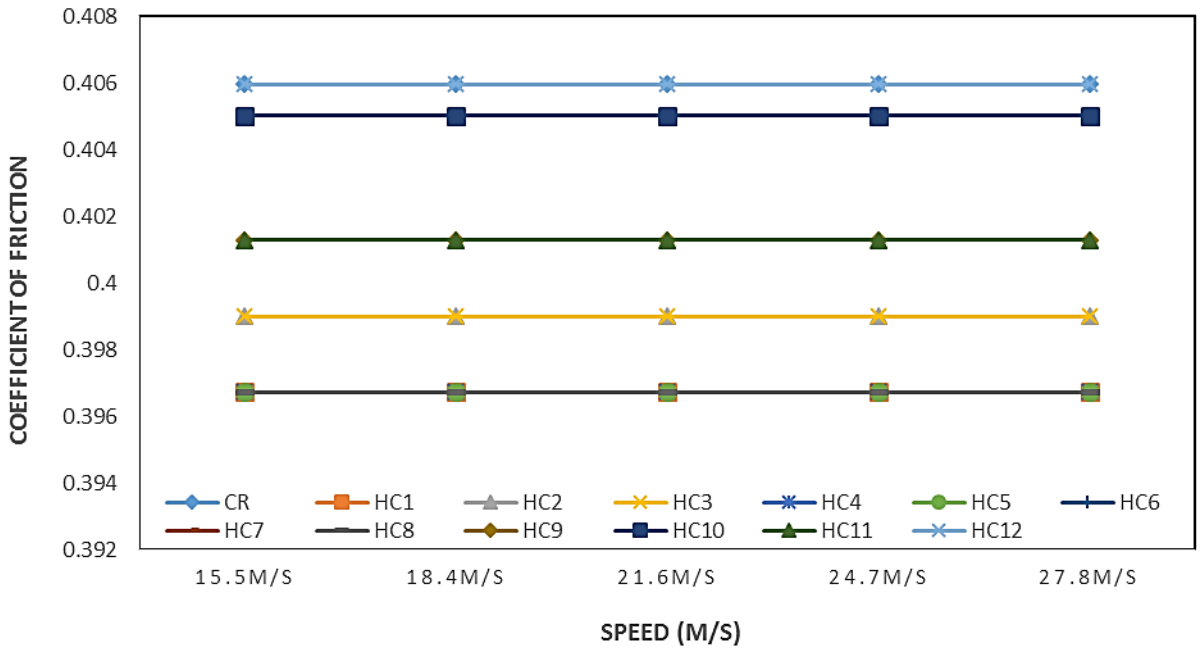

Figure 4.13: Variation of the coefficient of friction with speed**.**

Fig 4.13 show that the hybrid nanocomposite brake pad together with commercial brake pad maintains a constant coefficient of friction as the speed changes from 15.5 m/s to 27.8 m/s. This trend corresponds with Jang *et al*. [37] report where a stable

coefficient of friction was observed for different formulation of the brake pads. It was also observed that the coefficient of friction obtained for HCs and CR varied from 0.396 - 0.406. These values are within the SAE J661 CODE (0.35-0.6) standard value recommended for vehicle brake pads [6].

It was futher observed that the increase in carbon fiber loading, increased the “bite," which in turn increased HCs coefficient of friction [4, 21, 38]. Hybrid nanocomposite brake pad HC12 offered the same coefficient of friction as commercial brake pad (0.406). Similarly, the firm transferring ability of graphite may be the reason for the HC12 stable coefficient of friction. An uninterrupted increase in the coefficient of friction has been linked with the addition of metal chips. These metal chips/particles also increased the brake pad coefficient of friction while in contact with the cast iron wheel [136]. Consequently, the stable coefficient of HCs resulted from non-inclusion of metallic fiber. HCs stable coefficient of friction can also be attributed to the carbon-carbon additives lubricating synergistic structure and heat resistant ability. This frictional behaviour reduced brake pad adhesion to the counterpart and bulk interfacial temperature.

4.4.3 Stopping distance

Figure 4.13, shows the variation of the stopping distance as a function of the speed. It was observed that the stopping distance increased as speed increased from 15.5 to 27.8 m/s for the commercial brake pad. It was also noticed that all HC brake pads offered shorter stopping distance compared to CR irrespective of speed variation. It was observed that the HC brake pad exhibited a reduced stopping distance by more 90% compared to stopping distance value obtained from commercial brake pad while speed increased by 79%.

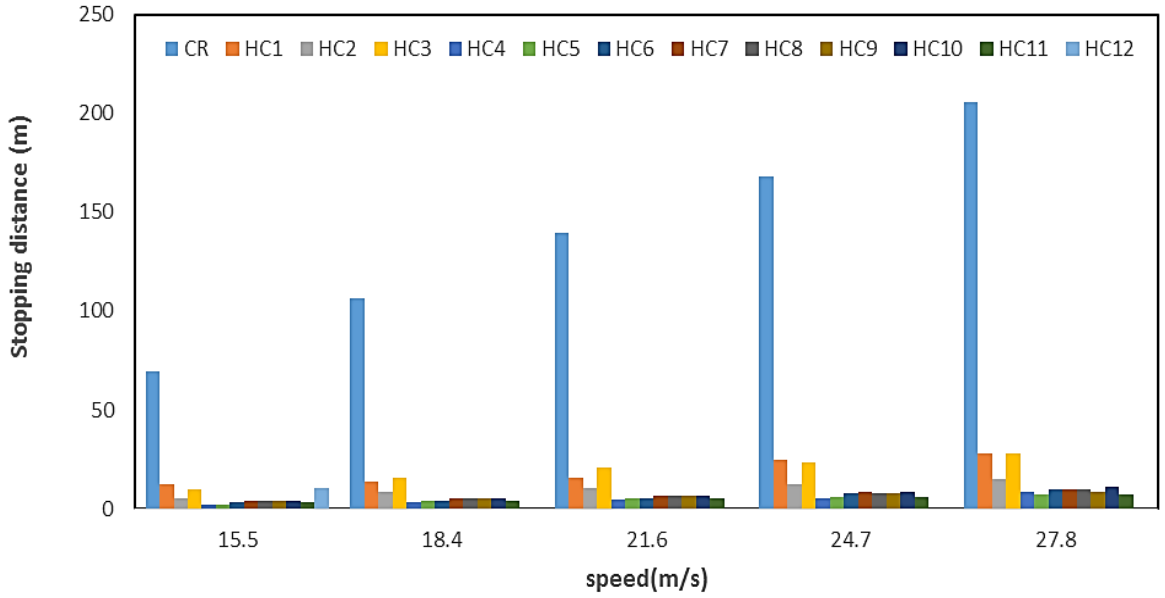

Figure 4.14: Stopping distance of hybrid nanocomposite and commercial brake pad

It has been reported that the inclusion of fiber helps in controlling fade and also increase braking effectiveness [4, 6]. Therefore, the shorter stopping distance obtained for hybrid nanocomposite brake pad may be as a result of the carbon-fiber inclusion. Furthermore, brake pad with a combination of carbon-based additives has affirmed to have better thermal properties that often increase the brake pad ability to absorb heat generated by friction. This ultimately helps in retaining the braking efficiency observed in Figure 4.14 [137, 138].

4.4.4 Interfacial temperature

The interfacial temperatures obtained for HC and CR pads were as illustrated in Figure 4.14. It was observed that the temperature generated between the pad, and the rotor increased as speed rises. The interfacial temperature obtained from HC brake pad increased from 31-93^{0}C comparatively lower than the temperature ranging from 120-300 ^{0}C obtained from CR.

The low interfacial temperature obtained from HC brake pad as shown in Figure 4.14, could be attributed to the carbon-carbon additive formulation. The heat resistance of the binder (epoxy resin) may also be another reason for low heat build-up, resulting in a low temperature at the interface. It has been affirmed by Savage *et al* and Manocha *et al* [137, 138], that more than one carbon-based additives in a material may form a better thermal synergy which absorbs heat and stabilizes temperature.

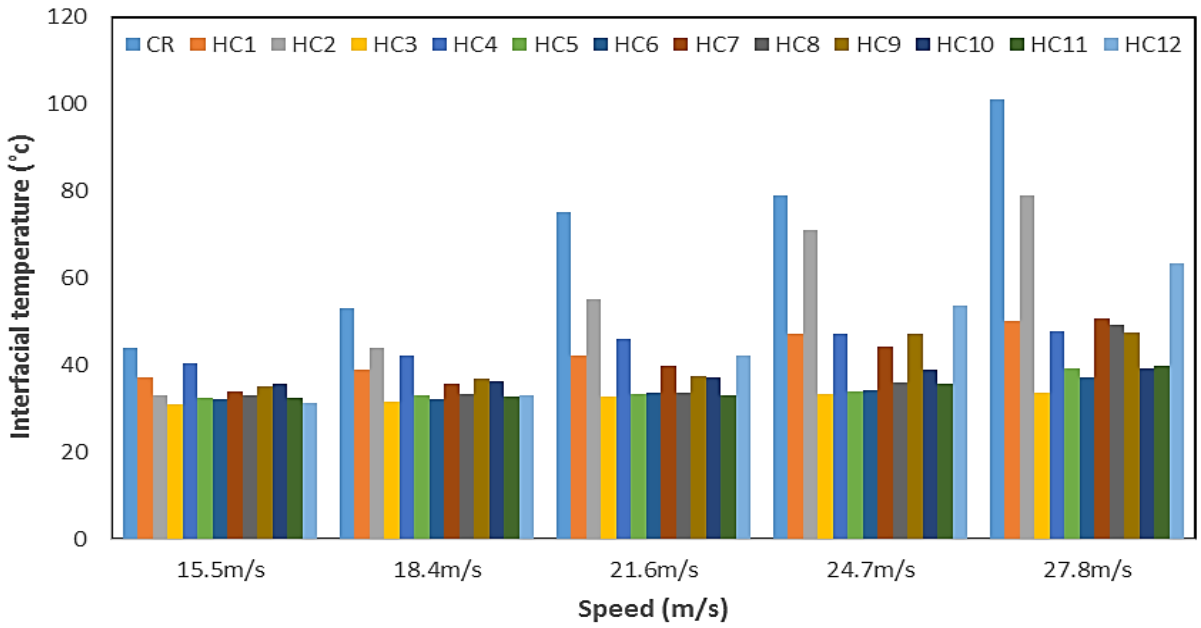

Figure 4.15: Interfacial temperature of HCs and CR brake pads.

The synergistic thermal function formed by carbon nanotubes, carbon fiber, and graphite resulted in the reduction in HC brake pads interfacial temperature. It was observed that the commercial pad interfacial temperature increased by 214% as speed increased by 79%. However, for the hybrid nanocomposite pad, a reversed trend was seen. HC offered an average interfacial temperature which was 71% lower and better than the value obtained from commercial brake pad. This indicated that the thermal efficiency of the carbon-based additives in HC brake pad enhanced its stopping performance.

4.4.5 Brake pad noise level

Figure 4.15 presents the average noise level generated by the brake pad during braking. Machine noise level was surprisingly reduced while engaging the brakes. The friction hampering between different surfaces, such as joints and connections of the dynamometer resulted in excessive machine noise levels [139].

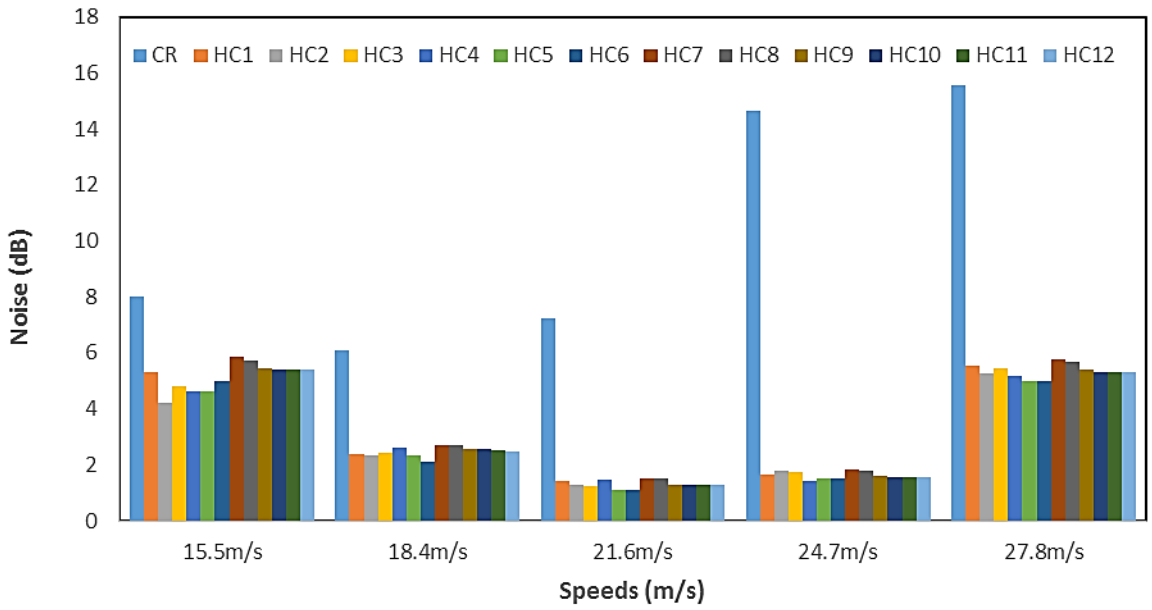

Figure 4.16: Bar charts showing hybrid nanocomposite and commercial brake pad noise levels.

The reduction in noise level during braking may be due to the low vibration from the machine. It was clear that the noise levels linearly increased as speed increased. However, a distinctive noise level was observed for a different formulation. This trend corresponds with the result reported by Ikpambese *et al* [17]. The brake pad reduced machine noise level by data varied from 1.1-15.55 dB. Reduction in dynamometer noise level obtained by CR ranged from 6.1-15.55 dB, while that of the composite brake pad varied from 1.1-5.86. This indicated that the HC brake pad exhibited a noise level that was about 55% lower than CR. This performance may be attributed to the non-inclusion of aggressive particles in the formulation. This result agreed with Kim *et al*.[77], report, where non-inclusion of hard and abrasive particles reduced friction-induced vibration that often leads to excessive noise.

Figure 4.16 shows the SEM micrographs of brake pad worn surfaces magnified at 500X to determine the braking performance mechanism of the brake pads. Figure 4.16(CR) show the worn surface of commercial brake pad, rough debris formed plateaus, and inconsistent surface textures were observed. The plateaus formed may be as a result of the high content of tough abrasive material and broken fibres, which control abrasion and also increased the coefficient of friction. The hard inclusion and broken fibers became more visible on the CR worn surface after the matrix had worn

off. This indicated that these two constituents serve as the main load-carrying component of commercial brake pad. However, the primary plateaus formed by these additives scratched the rotor and increased the noise level. Comparing brake pads worn surfaces; a uniform dispersion of fiber, crack, smooth self-sustaining layers and surface degradation was seen on HC brake pad worn surfaces.

The worn surface of HC brake pad shown a structural formation of carbon fibers infused in the matrix. The synergistic of carbon-based bond and good adhesive properties of epoxy formed a coiled (tough) structure, which in turn serve as the main load-carrying component. A smooth self-sustaining layer observed on the HC1 worn surface was the reason its stable coefficient of friction and low wear rate. It is well known that this kind of layer controls frictions and abrasion. This abrasion behaviour may be attributed to the lower wear rate and coefficient of friction exhibited by HC1 shown in Figure 4.11 and 4.12 respectively.

In Figure 4.16 HC2, HC3, HC4, HC5, HC6, HC7, HC9, HC10, and HC12, a relatively smooth surface was observed due to a restriction of epoxy matrix cracking caused by the incorporation of short carbon fiber. Uniform distribution and better carbon fibers-matrix interaction were also observed. The matrix and broken fibers of HC2, HC3, HC4, HC5, and HC6 formed relatively smooth plateaus on the worn surfaces. However, an obvious crack was observed on the HC2 worn surface. This may be as a result of the braking compressive stress and the brake pad toughness.

The smooth surface observed on worn surfaces of HC brake pads and non-inclusion of hard materials accounted for low noise level observed in Figure 4.15. This surface smoothness also helped in keeping the rotor and the brake pad contact. This behaviour can be linked to shorter stopping distance observed in Figure 4.11. It may also be the reason for a low wear rate, and the stable coefficient of friction observed in Figure 4.11 and 4.12 respectively.

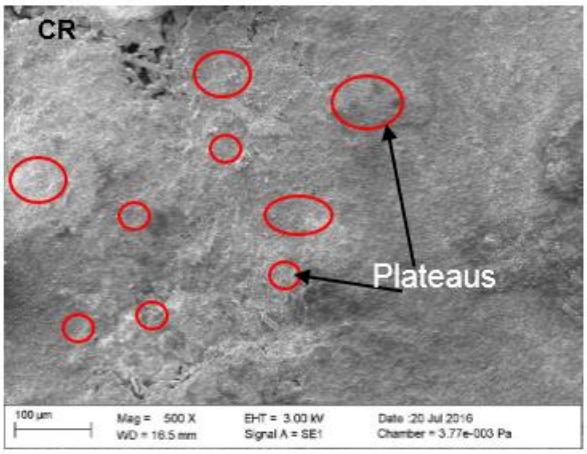
CR
Plateaus
100 µm
Mag = 500 X
WD = 16.5 mm
EHT = 3.00 kV
Signal A = SE1
Date :20 Jul 2016
Chamber = 3.77e-003 Pa

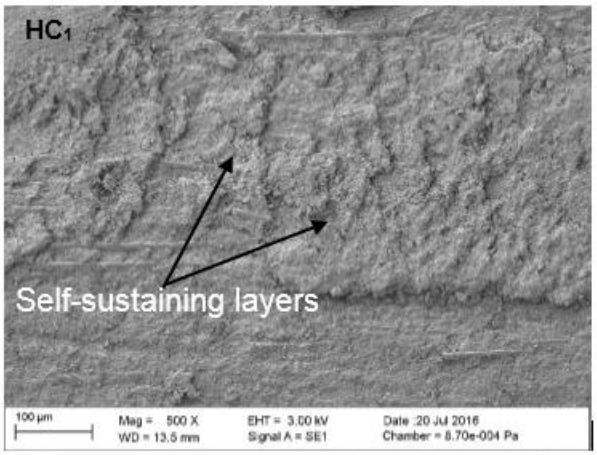
HC1
Self-sustaining layers
100 µm
Mag = 500 X
WD = 13.5 mm
EHT = 3.00 kV
Signal A = SE1
Date :20 Jul 2016
Chamber = 8.70e-004 Pa

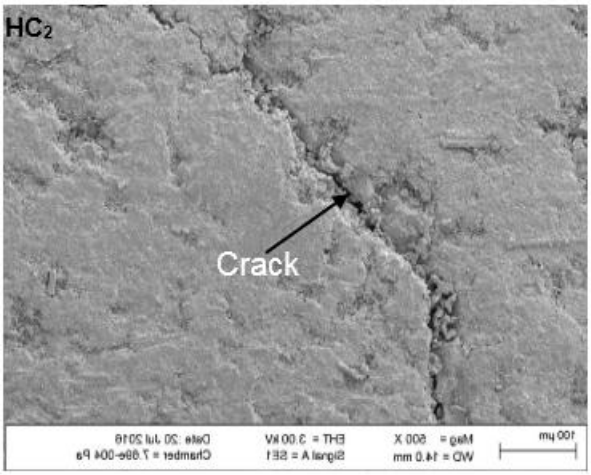
HC2
Crack

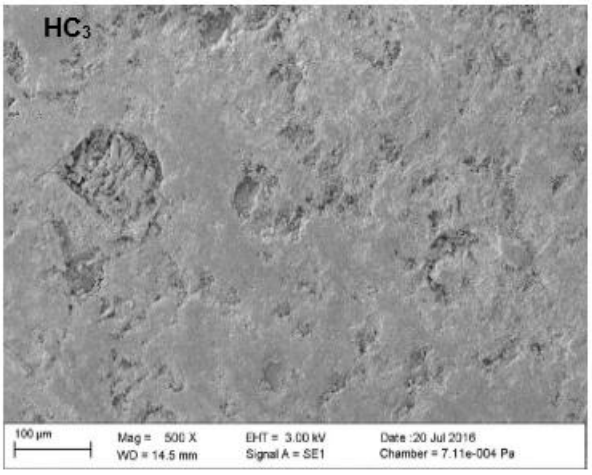
HC3
100 µm
Mag = 500 X
WD = 14.5 mm
EHT = 3.00 kV
Signal A = SE1
Date :20 Jul 2016
Chamber = 7.11e-004 Pa

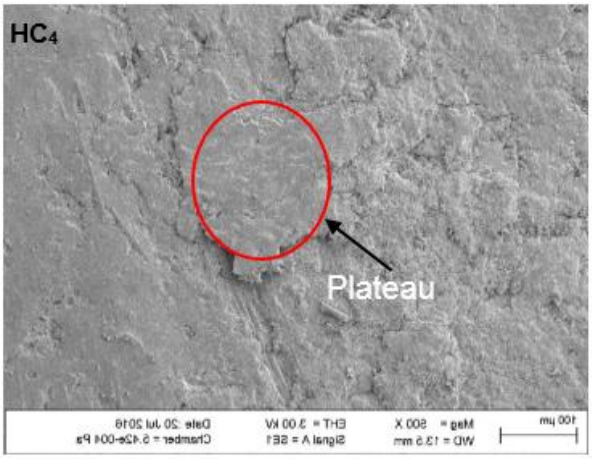
HC4
Plateau

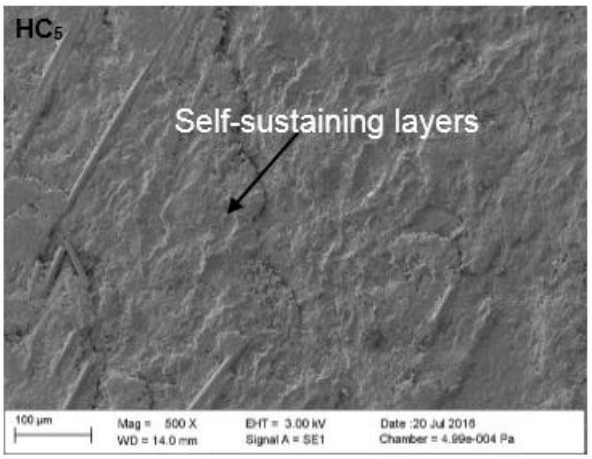
HC5
Self-sustaining layers
100 µm
Mag = 500 X
WD = 14.0 mm
EHT = 3.00 kV
Signal A = SE1
Date :20 Jul 2016
Chamber = 4.99e-004 Pa

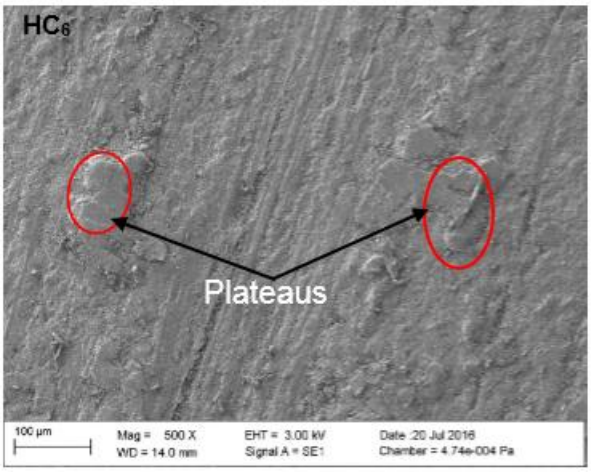
HC6
Plateaus
100 µm
Mag = 500 X
WD = 14.0 mm
EHT = 3.00 kV
Signal A = SE1
Date :20 Jul 2016
Chamber = 4.74e-004 Pa

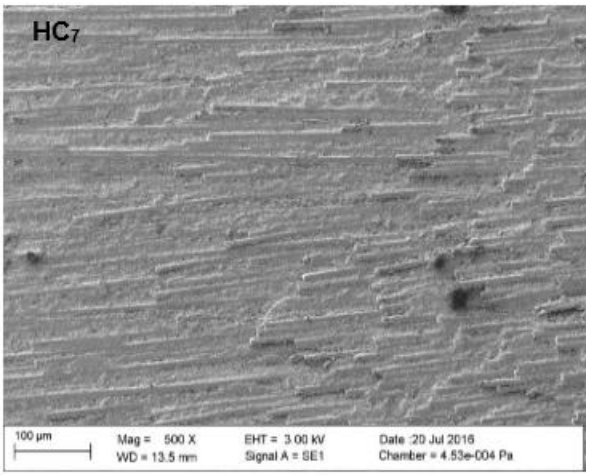
HC7
100 µm
Mag = 500 X
WD = 13.5 mm
EHT = 3.00 kV
Signal A = SE1
Date :20 Jul 2016
Chamber = 4.53e-004 Pa

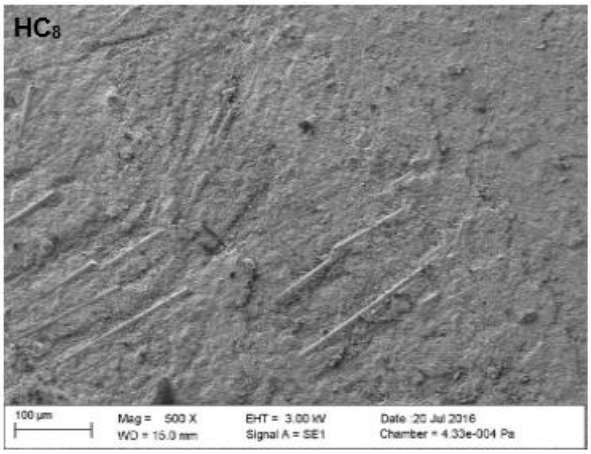
HC8
100 µm
Mag = 500 X
WD = 15.0 mm
EHT = 3.00 kV
Signal A = SE1
Date :20 Jul 2016
Chamber = 4.33e-004 Pa

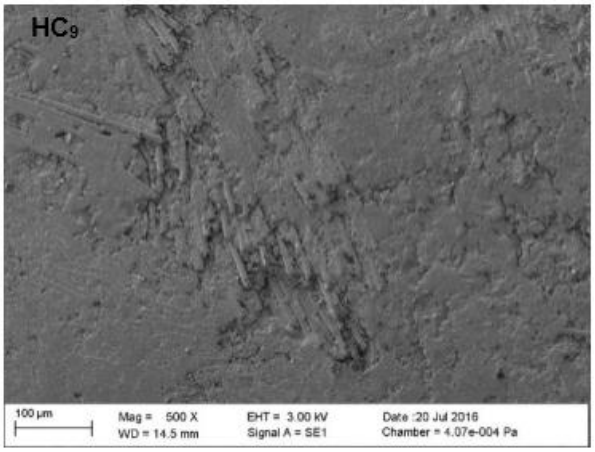
HC9
100 µm
Mag = 500 X
WD = 14.5 mm
EHT = 3.00 kV
Signal A = SE1
Date :20 Jul 2016
Chamber = 4.07e-004 Pa

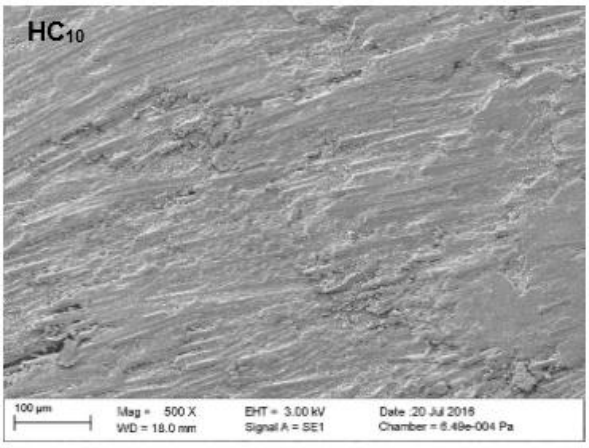
HC10
100 µm
Mag = 500 X
WD = 18.0 mm
EHT = 3.00 kV
Signal A = SE1
Date :20 Jul 2016
Chamber = 6.49e-004 Pa

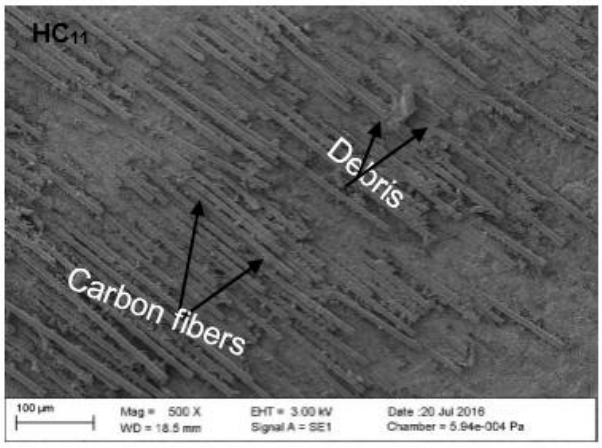
HC11
Debris
Carbon fibers
100 µm
Mag = 500 X
WD = 18.5 mm
EHT = 3.00 kV
Signal A = SE1
Date :20 Jul 2016
Chamber = 5.94e-004 Pa

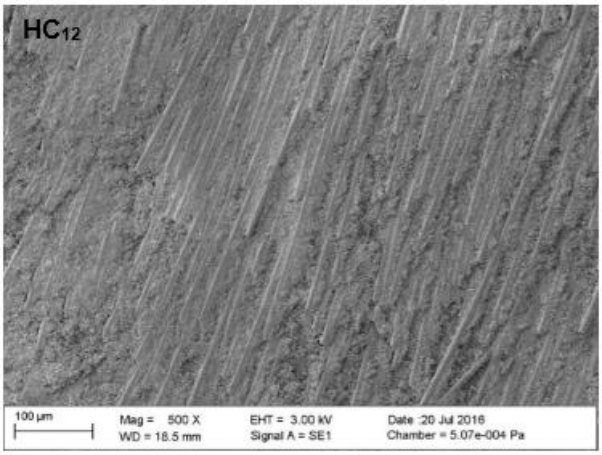

Figure 4.17: SEM micrograph of brake pads worn surfaces.

Comparing the worn surfaces of HCs brake pad materials containing a large amount of carbon fiber, a smooth structure was observed for the case of HC7, HC8, HC9, and HC10. Excellent adhesion of carbon fiber within the epoxy matrix due to addition of carbon nanotube may be one of the reasons for decreasing in wear rate as well as the increase in the coefficient of friction. The smooth structure observed for this set of brake pads was the reason for their better tribological performance. For HC11 and HC12, exposures of carbon and scanty debris were observed on the worn surfaces this was probably due to the limited amount of the epoxy matrix at the interfaces. This may be due to high-loading of carbon fiber and graphite nanopowder. This resulted in fillers agglomeration. The agglomeration of filler materials increased the surface roughness, which often impact friction and wear behaviours of the nanocomposite material. The surface roughness in this case increased the asperities slope angle, which in turn increased coefficient of friction and wear rate.

Chapter Five- Conclusions and Recommendations

The aim of this study was to develop a polymer-based hybrid nanocomposite material for brake pad application. In an attempt to address the challenges of the braking system highlighted in chapter one, a combination of carbon fiber, carbon nanotubes, graphite nanopowder and epoxy resin was used to manufacture brake pad. Although all the reinforcements are carbon based material, they evidently perform different function. Multi-wall carbon nanotubes was used to improve the thermal conductivity, mechanical and tribological properties. Graphite nanopowder was used as an internal lubricator, which controls wear and friction of the brake pad. The addition of short carbon fiber improved mechanical strength, thermal stability, creep and wear resistance of the brake pad.

It is well known that material or combination of materials for brake pads should possess certain properties before it could be considered for brake pad application. These include but not limited to thermal stability, mechanical strength, shorter stopping distance, a stable coefficient of friction and low wear rate. In this regard, the developed material was subjected to several characterization techniques to determine its suitability for brake pad application. These include mechanical, dynamometer, fluid absorption rate and thermal investigation.

The hybrid nanocomposite brake pad exhibited an 80% higher compressive strength than CR. This higher compressive strength was attributed to the interconnecting (carbon-carbon) C-C bond of the MWCNTs and NG that formed covalent bonding between carbon fiber and the epoxy matrix. The shear strength for CR (3.9 MPa) was higher than the standard shear strength recommended for the brake pad by RS 124 specifications. However, all HC brake pads showed a 100% higher shear strength when compared to CR brake pad. The impact strength for CR was 17.6 KJ/m^2 while that of the HC brake pads varied with the formulation. HC4 and HC9 exhibited an impact strength that was 100% higher than CR.

CR exhibited a hardness (37.3) that was slightly higher when compared to hardness obtained from almost all the HC brake pad except for HC8, HC9, and HC12 which exhibited a 4.8%, 10% and 1.3% harder. The homogeneous dispersion of ceramic additive (silicon carbide) in commercial pad resulted in the improved hardness

property. In addition, increase in carbon fiber loading increased the hardness of HC7, HC8, and HC9 brake pads.

Thermal stability and degradation temperature hybrid nanocomposite material varied with a corresponding increase in temperature. CR had a better thermal stability and weight loss than HCs. This thermal behavior was attributed to the inherent thermal properties of ceramic and metallic fillers in commercial pad formulation. However, HCs final weight loss was after 450˚C, which was above the brake pad normal working (300 -400ºC). This was directly attributed to the addition of the carbon-based additives.

HCs and CR exhibited low water absorption rate ranging from 0.01-0.36%, which was better when compared to absorption value reported in the literature [3, 94]. However, HCs exhibited lower moisture absorption rate (0.1-0.33) than that of the commercial brake pad (0.36). HC3 and HC6 exhibited water absorption rate of 0.012 % and 0.01 % respectively, which were about 100% lower than to that of the CR. This performance was attributed to hydrophobic nature and compatibility of the carbon-carbon components, and the interconnecting bond formed by the additives.

The rate of oil absorption for HCs and CR varied with different formulations. Most of the hybrid nanocomposite brake pads absorb lesser oil than commercial brake pad under the same conditions. Significantly, HC1 had a lower oil absorption rate of 0.01 %, which was 98% better that obtained with commercial brake pad. This was attributed to lower porosity and closer interfacial bonding of carbon-based materials.

Results from braking performance investigation show that the coefficient of friction for both pads was insensitive to increasing in speed. The coefficient of friction for both types of brake pad ranged from 0.396 - 0.413, which were within the SAE J661 CODE F (0.35-0.45) standard value recommended for vehicle brake pad. HC offered a 90% shorter stopping distance, lower wear rate, 71% lower interfacial temperature and 55% lower noise level than CR. It was concluded the increase in content and uniform distribution of carbon fiber resulted in stopping distance reduction and the increase in the coefficient of friction. The synergistic effect of carbon-carbon additives and quality of binder resulted in HC wear rate and interfacial temperature reduction, and non-inclusion of metallic fiber resulted in lower noise level. All indications suggest that hybrid nanocomposite material may be used for efficient brake pad application.

5.1 Recommendations

The completion of this research brought forth certain limitation and consequently, provides opportunities for future research. The drawback such as longer curing time will affect mass production. Therefore, this study recommends fast curing resin. Thermal stability and degradation of hybrid nanocomposite brake pad are another potential area for further research. Improvement in this area will help future researchers in more efficient brake pad production. This material was tested under room temperature. In this regard, investigation of these material properties at an elevated and sub ambient temperature may also be explored in the future.

REFERENCES

[1] J.-P. Rodrigue and T. Notteboom. (1998-2016, 31/10/2016). *Transportation and Economic Development*. Available: https://people.hofstra.edu/geotrans/eng/ch7en/conc7en/ch7c1en.html

[2] Wikipedia. (2016). *Railway brake*. Available: https://en.wikipedia.org/wiki/Railway_brake

[3] M. Afolabi, O. Abubakre, S. Lawal, and A. Raji, "Experimental Investigation of Palm Kernel Shell and Cow Bone Reinforced Polymer Composites for Brake Pad Production," *International Journal of Chemistry and Materials Research,* vol. 3, pp. 27-40, 2015.

[4] Imaekhai Lawrence and U. A. Paul, "Critical evaluation/reassessment of (abfm) automotive brake friction materials," *Standard Research Journal.,* 2013.

[5] M. Kumar, B. K. Satapathy, A. Patnaik, D. K. Kolluri, and B. S. Tomar, "Hybrid composite friction materials reinforced with combination of potassium titanate whiskers and aramid fibre: Assessment of fade and recovery performance," *Tribology International,* vol. 44, pp. 359-367, 2011.

[6] P. J. Blau, "Compositions, functions, and testing of friction brake materials and their additives," Oak Ridge National Lab., TN (US)2001.

[7] K. W. Liew and U. Nirmal, "Frictional performance evaluation of newly designed brake pad materials," *Materials & Design,* vol. 48, pp. 25-33, 6// 2013.

[8] B. Electromechanical. (2007). *Automobile History*. Available: http://www.motorera.com/history/hist07.htm

[9] T. m. center. (2016). *Mesothelioma in South Africa*. Available: http://www.asbestos.com/mesothelioma/south-africa/

[10] N. C. INSTITUTE. (2009). *Asbestos Exposure and cancer risk*. Available: http://www.cancer.gov/about-cancer/causes-prevention/risk/substances/asbestos/asbestos-fact-sheet

[11] Wikipedia. (2016). *List of rail accidents (2010–present)*. Available: https://en.wikipedia.org/wiki/List_of_rail_accidents_(2010%E2%80%93present)

[12] T. live. (2015). *Prasa 'stifled' train crash investigation*. Available: http://www.timeslive.co.za/thetimes/2016/03/15/Prasa-stifled-train-crash-investigation

[13] I. reporter. (2010). *Crash costs Rovos Rail R15m*. Available: http://www.iol.co.za/news/south-africa/crash-costs-rovos-rail-r15m-481511

[14] C. Cruceanu, "Train Braking," *Reliability and Safety in Railway, InTech,* pp. 29-74, 2012.

[15] S. W. Kim, S. J. Lee, B. K. Park, and S. K. Rhee, "A Comprehensive Study of Humidity Effects on Friction, Pad Wear, Disc Wear, DTV, Brake Noise and Physical Properties of Pads," 2011.

[16] S. Nagesh, C. Siddaraju, S. Prakash, and M. Ramesh, "Characterization of Brake Pads by Variation in Composition of Friction Materials," *Procedia Materials Science,* vol. 5, pp. 295-302, 2014.

[17] K. K. Ikpambese, D. T. Gundu, and L. T. Tuleun, "Evaluation of palm kernel fibers (PKFs) for production of asbestos-free automotive brake pads," *Journal of King Saud University - Engineering Sciences,* 2014.

[18] Tire rack. (2015). *Why Ceramic Brake Pads ?* Available: http://www.tirerack.com/brakes/tech/techpage.jsp?techid=88

[19] M. Rivera, "Brake Pad Comparisons – Which Material Is Best?," ed, 2014.

[20] H. Jang, J. S. Lee, and J. W. Fash, "Compositional effects of the brake friction material on creep groan phenomena," *Wear,* vol. 251, pp. 1477-1483, 10// 2001.

[21] K. J. BUTNOR, T. A. SPORN, and V. L. ROGGLI, "Exposure to brake dust and malignant mesothelioma: a study of 10 cases with mineral fiber analyses," *Annals of Occupational Hygiene,* vol. 47, pp. 325-330, 2003.

[22] Greg Monforton. (2014). *History of brake pads*. Available: http://www.gregmonforton.com/evolution-brake-systems.html,
[23] A. f. T. S. D. Registry. (2008). *Asbestor*. Available: http://www.atsdr.cdc.gov/asbestos/asbestos/health_effects/
[24] B. MacDowell. (2015). *Brake pad*. Available: http://www.dimensionsinfo.com/brake-pads-dimensions
[25] Jamie page deaton. (1998-2015). *How Brake Pads Work*. Available: http://auto.howstuffworks.com/auto-parts/brakes/brake-parts/brake-pads1.htm
[26] eBay. (1995-2015). *Metallic vs. Ceramic Brake Pads*. Available: http://www.ebay.co.uk/gds/Metallic-vs-Ceramic-Brake-Pads-/10000000178258842/g.html
[27] e. Hartman. (2012). *Ceramic Brake Pads Vs. Semi-Metallic*. Available: http://www.ehow.com/about_5632707_ceramic-pads-vs_-semi-metallic.html
[28] Steve Smith. (1999-2015). *How Do I Know a Ceramic or Semi-Metallic*. Available: http://www.ehow.com/how_6572126_do-ceramic-semi_metallic_.html
[29] sixity. (2011). *Which Brake Pads to Choose? Organic Sintered or Ceramic*. Available: http://www.ebay.co.uk/gds/Which-Brake-Pads-to-Choose-Organic-Sintered-or-Ceramic-/10000000020322378/g.html
[30] Diffen. *Ceramic Brake Pad vs Metallic Brake Pad*. Available: http://www.diffen.com/difference/Ceramic_Brake_Pad_vs_Metallic_Brake_Pad
[31] G. V. I. A. F. Beloivan, I. D. Radomysel'skii, N. I. Shcherban', "The mechanical properties of sintered metal-glass materials," *Soviet Powder Metallurgy and Metal Ceramics,* vol. Volume 5, Issue 5 , pp 380-385 1966.
[32] B. H. t. J. Wheels. (2012). *Sintered compound brake pad noise ?* Available: http://forums.mtbr.com/brake-time/sintered-compound-brake-pad-noise-806612.html
[33] M. Asif, K. Chandra, and P. Misra, "Development of iron based brake friction material by hot powder preform forging technique used for medium to heavy duty applications," *Journal of Minerals and Materials Characterization and Engineering,* vol. 10, p. 231, 2011.
[34] S. J. Kim and H. Jang, "Friction and wear of friction materials containing two different phenolic resins reinforced with aramid pulp," *Tribology International,* vol. 33, pp. 477-484, 7// 2000.
[35] J. Bijwe, Nidhi, N. Majumdar, and B. K. Satapathy, "Influence of modified phenolic resins on the fade and recovery behavior of friction materials," *Wear,* vol. 259, pp. 1068-1078, 7// 2005.
[36] H. J. Hwang, S. L. Jung, K. H. Cho, Y. J. Kim, and H. Jang, "Tribological performance of brake friction materials containing carbon nanotubes," *Wear,* vol. 268, pp. 519-525, 2/4/ 2010.
[37] H. Jang, K. Ko, S. J. Kim, R. H. Basch, and J. W. Fash, "The effect of metal fibers on the friction performance of automotive brake friction materials," *Wear,* vol. 256, pp. 406-414, 2// 2004.
[38] K.-J. Lee, M.-H. Hsu, H.-Z. Cheng, J. S.-C. Jang, S.-W. Lin, C.-C. Lee*, et al.*, "Tribological and mechanical behavior of carbon nanotube containing brake lining materials prepared through sol–gel catalyst dispersion and CVD process," *Journal of Alloys and Compounds,* vol. 483, pp. 389-393, 8/26/ 2009.
[39] M. H. Cho, S. J. Kim, D. Kim, and H. Jang, "Effects of ingredients on tribological characteristics of a brake lining: an experimental case study," *Wear,* vol. 258, pp. 1682-1687, 6// 2005.
[40] Wikipedia. (2014). *Brake pad*. Available: http://en.wikipedia.org/wiki/Brake_pad
[41] M. Maleque, S. Dyuti, and M. Rahman, "Material selection method in design of automotive brake disc," 2010.
[42] G. Nicholson, "Facts about friction," *Gedoran America, Winchester,* 1995.
[43] H. Jang and S. J. Kim, "The effects of antimony trisulfide (Sb2S3) and zirconium silicate (ZrSiO4) in the automotive brake friction material on friction characteristics," *Wear,* vol. 239, pp. 229-236, 4// 2000.
[44] F. E. Kennedy, A. C. Balbahadur, and D. S. Lashmore, "The friction and wear of Cu-based silicon carbide particulate metaal matrix composites for brake applications," *Wear,* vol. 203–204, pp. 715-721, 3// 1997.

[45] Wikipedia. (2016). *Asbestos*. Available: https://en.wikipedia.org/wiki/Asbestos
[46] G. Yi and F. Yan, "Mechanical and tribological properties of phenolic resin-based friction composites filled with several inorganic fillers," *Wear,* vol. 262, pp. 121-129, 1/4/ 2007.
[47] S. Sharma, J. B. and, and M. Kumar, "Comparison Between Nano- and Micro-Sized Copper Particles as Fillers in NAO Friction Materials," *Nanomaterials and Nanotechnology,* vol. 3, 2013.
[48] D. C. and and G. W. Stachowiak, "Review of Automotive brake friction materia,s," 2004.
[49] W. Österle and I. Urban, "Friction layers and friction films on PMC brake pads," *Wear,* vol. 257, pp. 215-226, 2004.
[50] M. M. Farag, *Materials and process selection for engineering design*: CRC Press, 2013.
[51] D.-q. Cheng, X.-t. Wang, J. Zhu, D.-h. Qiu, X.-w. Cheng, and Q.-f. Guan, "Friction and wear behavior of carbon fiber reinforced brake materials," *Frontiers of Materials Science in China,* vol. 3, pp. 56-60, 2009.
[52] P. Cai, Y. Wang, T. Wang, and Q. Wang, "Effect of resins on thermal, mechanical and tribological properties of friction materials," *Tribology International,* vol. 87, pp. 1-10, 7// 2015.
[53] D. G. Solomon and M. N. Berhan, "Characterization of Friction Material Formulations for Brake Pads," in *World Congress on Engineering*, 2007, pp. 2-4.
[54] S. Ho, J. C. Lin, and C.-P. Ju, "Effect of fiber addition on mechanical and tribological properties of a copper/phenolic-based friction material," *Wear,* vol. 258, pp. 861-869, 2005.
[55] J. Gerlici, T. Lack, and J. Harušinec, "Rail vehicles wheels and brake blocks wear laboratory test stand utilization," *Prace Naukowe Politechniki Warszawskiej. Transport,* pp. 21--32, 2014.
[56] R. Abhik, V. Umasankar, and M. A. Xavior, "Evaluation of properties for Al-SiC reinforced metal matrix composite for brake pads," *Procedia Engineering,* vol. 97, pp. 941-950, 2014.
[57] K. W. Liew and U. Nirmal, "Frictional performance evaluation of newly designed brake pad materials," *Materials & Design,* vol. 48, pp. 25-33, 6// 2013.
[58] Ahmet Akkus and M. Yeğin, "Research on Wear Rate and Mechanical Properties of Brake Sabots (Shoes) Used in Railway Rolling Stocks," *International Journal of Applied Science and Technology,* vol. 4, 2014.
[59] M. Kumar and J. Bijwe, "NAO friction materials with various metal powders: Tribological evaluation on full-scale inertia dynamometer," *Wear,* vol. 269, pp. 826-837, 10/28/ 2010.
[60] S. J. Kim, M. H. Cho, D. S. Lim, and H. Jang, "Synergistic effects of aramid pulp and potassium titanate whiskers in the automotive friction material," *Wear,* vol. 251, pp. 1484-1491, 10// 2001.
[61] B. K. Satapathy and J. Bijwe, "Performance of friction materials based on variation in nature of organic fibres: Part I. Fade and recovery behaviour," *Wear,* vol. 257, pp. 573-584, 9// 2004.
[62] M. H. Cho, J. Ju, S. J. Kim, and H. Jang, "{Abhik, 2014 #2;Jang, 2000 #7;Lee, 2013 #6;Maleque, 2010 #3;Österle, 2004 #4;Varrica, 2013 #5}Tribological properties of solid lubricants (graphite, Sb2S3, MoS2) for automotive brake friction materials," *Wear,* vol. 260, pp. 855-860, 4/7/ 2006.
[63] S. J. Kim, M. Hyung Cho, K. Hyung Cho, and H. Jang, "Complementary effects of solid lubricants in the automotive brake lining," *Tribology International,* vol. 40, pp. 15-20, 1// 2007.
[64] P. Deshmukh, M. Lovell, W. G. Sawyer, and A. Mobley, "On the friction and wear performance of boric acid lubricant combinations in extended duration operations," *Wear,* vol. 260, pp. 1295-1304, 6/30/ 2006.
[65] L. Han, L. Huang, J. Zhang, and Y. Lu, "Optimization of ceramic friction materials," *Composites Science and Technology,* vol. 66, pp. 2895-2906, 12/1/ 2006.
[66] R. Ertan and N. Yavuz, "The effects of graphite, coke and ZnS on the tribological and surface characteristics of automotive brake friction materials," *Industrial Lubrication and Tribology,* vol. 63, pp. 245-253, 2011.

[67] K. Friedrich, Z. Zhang, and A. K. Schlarb, "Effects of various fillers on the sliding wear of polymer composites," *Composites Science and Technology,* vol. 65, pp. 2329-2343, 12// 2005.
[68] M. Eriksson, F. Bergman, and S. Jacobson, "On the nature of tribological contact in automotive brakes," *Wear,* vol. 252, pp. 26-36, 1// 2002.
[69] A. M. Martinez and J. Echeberria, "Towards a better understanding of the reaction between metal powders and the solid lubricant Sb2S3 in a low-metallic brake pad at high temperature," *Wear,* vol. 348–349, pp. 27-42, 2/15/ 2016.
[70] M. H. a. Cho, J. a. Ju, S. J. a. Kim, and H. Jang, "Tribological properties of solid lubricants (graphite, Sb2S3, MoS2) for automotive brake friction materials," *Wear,* vol. 260, 2005.
[71] S. Watanabe, J. Noshiro, and S. Miyake, "Tribological characteristics of WS2/MoS2 solid lubricating multilayer films," *Surface and Coatings Technology,* vol. 183, pp. 347-351, 5/24/ 2004.
[72] D. Varrica, F. Bardelli, G. Dongarrà, and E. Tamburo, "Speciation of Sb in airborne particulate matter, vehicle brake linings, and brake pad wear residues," *Atmospheric Environment,* vol. 64, pp. 18-24, 1// 2013.
[73] W. K. Lee, T. H. Rhee, H. S. Kim, and H. Jang, "Effects of antimony trisulfide (Sb2S3) on sliding friction of automotive brake friction materials," *Metals and Materials International,* vol. 19, pp. 1101-1107, 2013.
[74] R. Ertan and N. Yavuz, "The effect of graphite, coke and zinc on the tribological and surface characteristic of automobile brake friction materials," *Industrial Lubrication and Tribology,* 2011.
[75] Y. Ma, G. S. Martynková, M. Valášková, V. Matějka, and Y. Lu, "Effects of ZrSiO4 in non-metallic brake friction materials on friction performance," *Tribology International,* vol. 41, pp. 166-174, 3// 2008.
[76] H. Jang and S. J. Kim, "Polymer Tribology," in *Imperial College Press*, 2009.
[77] S. S. Kim, H. J. Hwang, M. W. Shin, and H. Jang, "Friction and vibration of automotive brake pads containing different abrasive particles," *Wear,* vol. 271, pp. 1194-1202, 7/18/ 2011.
[78] M. Kumar and J. Bijwe, "Role of different metallic fillers in non-asbestos organic (NAO) friction composites for controlling sensitivity of coefficient of friction to load and speed," *Tribology International,* vol. 43, pp. 965-974, 5// 2010.
[79] V. M. Kryachek, "Friction Composites: Traditions and New Solutions (Review). Part 2. Composite Materials," *Powder Metallurgy and Metal Ceramics,* vol. 44, pp. 5-16, 2005.
[80] D.-S. Lim, J.-W. An, and H. J. Lee, "Effect of carbon nanotube addition on the tribological behavior of carbon/carbon composites," *Wear,* vol. 252, pp. 512-517, 3// 2002.
[81] T. Liu, I. Y. Phang, L. Shen, S. Y. Chow, and W.-D. Zhang, "Morphology and mechanical properties of multiwalled carbon nanotubes reinforced nylon-6 composites," *Macromolecules,* vol. 37, pp. 7214-7222, 2004.
[82] T. Liu, W. Wood, B. Li, B. Lively, and W.-H. Zhong, "Effect of reinforcement on wear debris of carbon nanofiber/high density polyethylene composites: Morphological study and quantitative analysis," *Wear,* vol. 294–295, pp. 326-335, 7/30/ 2012.
[83] Z. Shen, S. Bateman, D. Wu, P. McMahon, M. Dellolio, and J. Gotama, "The effects of carbon nanotubes on mechanical and thermal properties of woven glass fibre reinforced polyamide-6 nanocomposites," *Composites Science and Technology,* vol. 69, pp. 239-244, 2009.
[84] B. K. Satapathy and J. Bijwe, "Performance of friction materials based on variation in nature of organic fibres: Part II. Optimisation by balancing and ranking using multiple criteria decision model (MCDM)," *Wear,* vol. 257, pp. 585-589, 9// 2004.
[85] H. Hwang, S. Jung, K. Cho, Y. Kim, and H. Jang, "Tribological performance of brake friction materials containing carbon nanotubes," *Wear,* vol. 268, pp. 519-525, 2010.
[86] K. W. Hee and P. Filip, "Performance of ceramic enhanced phenolic matrix brake lining materials for automotive brake linings," *Wear,* vol. 259, pp. 1088-1096, 7// 2005.

[87] Y. C. Kim, M. H. Cho, S. J. Kim, and H. Jang, "The effect of phenolic resin, potassium titanate, and CNSL on the tribological properties of brake friction materials," *Wear,* vol. 264, pp. 204-210, 2/4/ 2008.
[88] D. Chan and G. Stachowiak, "Review of automotive brake friction materials," *Proceedings of the Institution of Mechanical Engineers, Part D: Journal of Automobile Engineering,* vol. 218, pp. 953-966, 2004.
[89] U. N. K.W. Liew, "Frictional performance evaluation of newly designed brake pad materials," 2013.
[90] Klaus Friedrich, Zhong Zhang, and A. K. Schlard, "Effect of various fillers on sliding wear of polymer composites," 2005.
[91] G. Zhao, I. Hussainova, M. Antonov, Q. Wang, T. Wang, and D.-L. Yung, "Effect of temperature on sliding and erosive wear of fiber reinforced polyimide hybrids," *Tribology International,* vol. 82, pp. 525-533, 2015.
[92] G. Zhang, B. Wetzel, B. Jim, and W. Oesterle, "Impact of counterface topography on the formation mechanisms of nanostructured tribofilm of PEEK hybrid nanocomposites," *Tribology International,* vol. 83, pp. 156-165, 2015.
[93] J. Li and Y. Xia, "The reinforcement effect of carbon fiber on the friction and wear properties of carbon fiber reinforced PA6 composites," *Fibers and Polymers,* vol. 10, pp. 519-525, 2009.
[94] I. M. Dagwa and A. Ibhadode, "Some physical and mechanical properties of asbestos–free experimental brake pad," *Journal of Raw Materials Research,* vol. 3, 2015.
[95] U. Idris, V. Aigbodion, I. Abubakar, and C. Nwoye, "Eco-friendly asbestos free brake-pad: Using banana peels," *Journal of King Saud University-Engineering Sciences,* 2013.
[96] A. R. Curtis, W. M. Palin, G. J. P. Fleming, A. C. C. Shortall, and P. M. Marquis, "The mechanical properties of nanofilled resin-based composites: The impact of dry and wet cyclic pre-loading on bi-axial flexure strength," *Dental Materials,* vol. 25, pp. 188-197, 2// 2009.
[97] J. A. Ajayi and O. A. Adeleke, "Failure analysis of railway brake blocks," *Engineering Failure Analysis,* vol. 4, pp. 205-213, 9// 1997.
[98] A. Q. Glossary. (2004). *Fitness for purpose*. Available: http://www.qualityresearchinternational.com/glossary/fitnessforpurpose.htm
[99] H. Bush, D. Rowson, and S. Warren, "The application of neutron activation analysis to the measurement of the wear of a friction material," *Wear,* vol. 20, pp. 211-225, 1972.
[100] S. K. Rhee, M. G. Jacko, and P. H. S. Tsang, "The role of friction film in friction, wear and noise of automotive brakes," *Wear,* vol. 146, pp. 89-97, 5/30/ 1991.
[101] E. Materials. (2014). *UTM - Components, Tests and Uses* Available: http://www.aboutcivil.org/universal-testing-machine-tools-components-applications.html
[102] AMETEKTEST. (2015). *Measuring Up to Your Standards!* Available: http://www.ametektest.com/
[103] L. Instruments. (2012). *Materials testing machines* Available: http://www.lloyd-instruments.com/?referrer=AZOMDOTCOM
[104] B. Wielage, T. Lampke, G. Marx, K. Nestler, and D. Starke, "Thermogravimetric and differential scanning calorimetric analysis of natural fibres and polypropylene," *Thermochimica Acta,* vol. 337, pp. 169-177, 10/11/ 1999.
[105] LINSEIS. (2012). *Simultaneous Thermal Analysis - Thermogravimetry / Calorimetry*. Available: http://www.linseis.com/en/
[106] P. N. Patil, S. K. Rath, S. K. Sharma, K. Sudarshan, P. Maheshwari, M. Patri*, et al.*, "Free volumes and structural relaxations in diglycidyl ether of bisphenol-A based epoxy–polyether amine networks," *Soft Matter,* vol. 9, pp. 3589-3599, 2013.
[107] K. Yang, M. Gu, Y. Guo, X. Pan, and G. Mu, "Effects of carbon nanotube functionalization on the mechanical and thermal properties of epoxy composites," *Carbon,* vol. 47, pp. 1723-1737, 2009.

[108] S.-Y. Yang, W.-N. Lin, Y.-L. Huang, H.-W. Tien, J.-Y. Wang, C.-C. M. Ma*, et al.*, "Synergetic effects of graphene platelets and carbon nanotubes on the mechanical and thermal properties of epoxy composites," *Carbon,* vol. 49, pp. 793-803, 3// 2011.
[109] F. H. Gojny and K. Schulte, "Functionalisation effect on the thermo-mechanical behaviour of multi-wall carbon nanotube/epoxy-composites," *Composites Science and Technology,* vol. 64, pp. 2303-2308, 11// 2004.
[110] F. H. Gojny, M. H. G. Wichmann, U. Köpke, B. Fiedler, and K. Schulte, "Carbon nanotube-reinforced epoxy-composites: enhanced stiffness and fracture toughness at low nanotube content," *Composites Science and Technology,* vol. 64, pp. 2363-2371, 11// 2004.
[111] Izvleček, "Titanium and/or titanium alloy sintered friction material," United States Patent and Trademark Office Patent, 1999.
[112] A. Yasmin, J.-J. Luo, and I. M. Daniel, "Processing of expanded graphite reinforced polymer nanocomposites," *Composites Science and Technology,* vol. 66, pp. 1182-1189, 7// 2006.
[113] R. Sengupta, M. Bhattacharya, S. Bandyopadhyay, and A. K. Bhowmick, "A review on the mechanical and electrical properties of graphite and modified graphite reinforced polymer composites," *Progress in Polymer Science,* vol. 36, pp. 638-670, 5// 2011.
[114] J. L. Delgado, M. a. A. Herranz, and N. Martin, "The nano-forms of carbon," *Journal of Materials Chemistry,* vol. 18, pp. 1417-1426, 2008.
[115] M. d. P. L. López, J. L. V. Palomino, M. L. S. Silva, and A. R. Izquierdo, *Optimization of the Synthesis Procedures of Graphene and Graphite Oxide*, 2016.
[116] Z. Zhang, C. Bredit, F. Haupert, and K. Friedric, "Enhancement of the wear resistance of epoxy: short fibre, graphite, PTFE and nano-TiO2 " pp. 1385-1392, 2005.
[117] N. W. Khun, H. Zhang, L. H. Lim, C. Y. Yue, X. Hu, and J. Yang, "Tribological properties of short carbon fibers reinforced epoxy composites," *Friction,* vol. 2, pp. 226-239, 2014.
[118] m. eduteam. *Materials Chemistry*. Available: http://web.mit.edu/3.082/www/team2_f01/chemistry.html
[119] American Society for Testing and Materials, "Standard Test Method for Rigid Plastics," vol. D 695-2a, ed, 2006.
[120] American Society for Testing and Materials, "Standard Test Method for Shear Strenght of Plastics by Punch Tool," vol. D-732-02, ed, 2006.
[121] American Society for Testing and Materials, "Standard Test Method for Determining the Charpy Impact Resistance of Notched Specimens of Plastics1," ed, 2004.
[122] American Society for Testing and Materials, "Standard Test Method for Indentation Hardness of Rigid Plastics by Means of a Barcol Impressor," vol. D 2583 – 95, ed, 2001.
[123] American Society for Testing and Materials, "Standard Test Method for Water Absorption of Plastics1," vol. D 570 – 98, ed, 1998.
[124] J. R. Foster, D. A. Hall, A. Q. Summerfield, A. R. Palmer, and R. W. Bowtell, "Sound-Level Measurements and Calculations of Safe Noise Dosage During EPI at 3 T," *Journal of Magnetic Resonance Imaging,* vol. 12, pp. 157-163, 2000.
[125] S. S. Pesetskii, S. P. Bogdanovich, and N. K. Myshkin, "Tribological behavior of nanocomposites produced by the dispersion of nanofillers in polymer melts," *Journal of Friction and Wear,* vol. 28, pp. 457-475, 2007.
[126] F.-h. Su, Z.-z. Zhang, and W.-m. Liu, "Mechanical and tribological properties of carbon fabric composites filled with several nano-particulates," *Wear,* vol. 260, pp. 861-868, 4/7/ 2006.
[127] O. J. Gbadeyan, K. Kanny, and T. P. Mohan, "Influence of the multi-walled carbon nanotube and short carbon fibre composition on tribological properties of epoxy composites," *Tribology - Materials, Surfaces & Interfaces,* pp. 1-7, 2017.
[128] A. A. Koval'chuk, V. G. Shevchenko, A. N. Shchegolikhin, P. M. Nedorezova, A. N. Klyamkina, and A. M. Aladyshev, "Effect of carbon nanotube functionalization on the structural and mechanical properties of polypropylene/MWCNT composites," *Macromolecules,* vol. 41, pp. 7536-7542, 2008.

[129] S. International. (2015). *Hardness of Brake Lining(STABILIZED Aug 2015)*. Available: http://standards.sae.org/j2654_201508/
[130] T. Nguyen, E. Zavarin, and E. M. Barrall, "Thermal Analysis of lignocellulosic materials: Part I. Unmodified materials," *Journal of Macromolecular Science—Reviews in Macromolecular Chemistry,* vol. 20, pp. 1-65, 1981.
[131] M. Tang and R. Bacon, "Carbonization of cellulose fibers—I. Low temperature pyrolysis," *Carbon,* vol. 2, pp. 211-220, 1964.
[132] A. MATERIALS. (2000-2016). *Graphite (C) - Classifications, Properties and Applications of Graphite*. Available: http://www.azom.com/article.aspx?ArticleID=1630
[133] D.-X. Li, Y.-L. You, X. Deng, W.-J. Li, and Y. Xie, "Tribological properties of solid lubricants filled glass fiber reinforced polyamide 6 composites," *Materials & Design,* vol. 46, pp. 809-815, 2013.
[134] J. Wang, M. Gu, B. Songhao, and S. Ge, "Investigation of the influence of MoS2 filler on the tribological properties of carbon fiber reinforced nylon 1010 composites," *Wear,* vol. 255, pp. 774-779, 8// 2003.
[135] A. Ibhadode and I. Dagwa, "Development of asbestos-free friction lining material from palm kernel shell," *Journal of the Brazilian Society of Mechanical Sciences and Engineering,* vol. 30, pp. 166-173, 2008.
[136] N. S. M. El-Tayeb and K. W. Liew, "On the dry and wet sliding performance of potentially new frictional brake pad materials for automotive industry," *Wear,* vol. 266, pp. 275-287, 1/5/ 2009.
[137] G. Savage, "Applications of Carbon-carbon Composites," in *Carbon-Carbon Composites*, ed: Springer, 1993, pp. 323-359.
[138] L. M. Manocha, "High performance carbon-carbon composites," *Sadhana,* vol. 28, pp. 349-358, 2003.
[139] A. Akay, "Acoustics of friction," *The Journal of the Acoustical Society of America,* vol. 111, pp. 1525-1548, 2002.